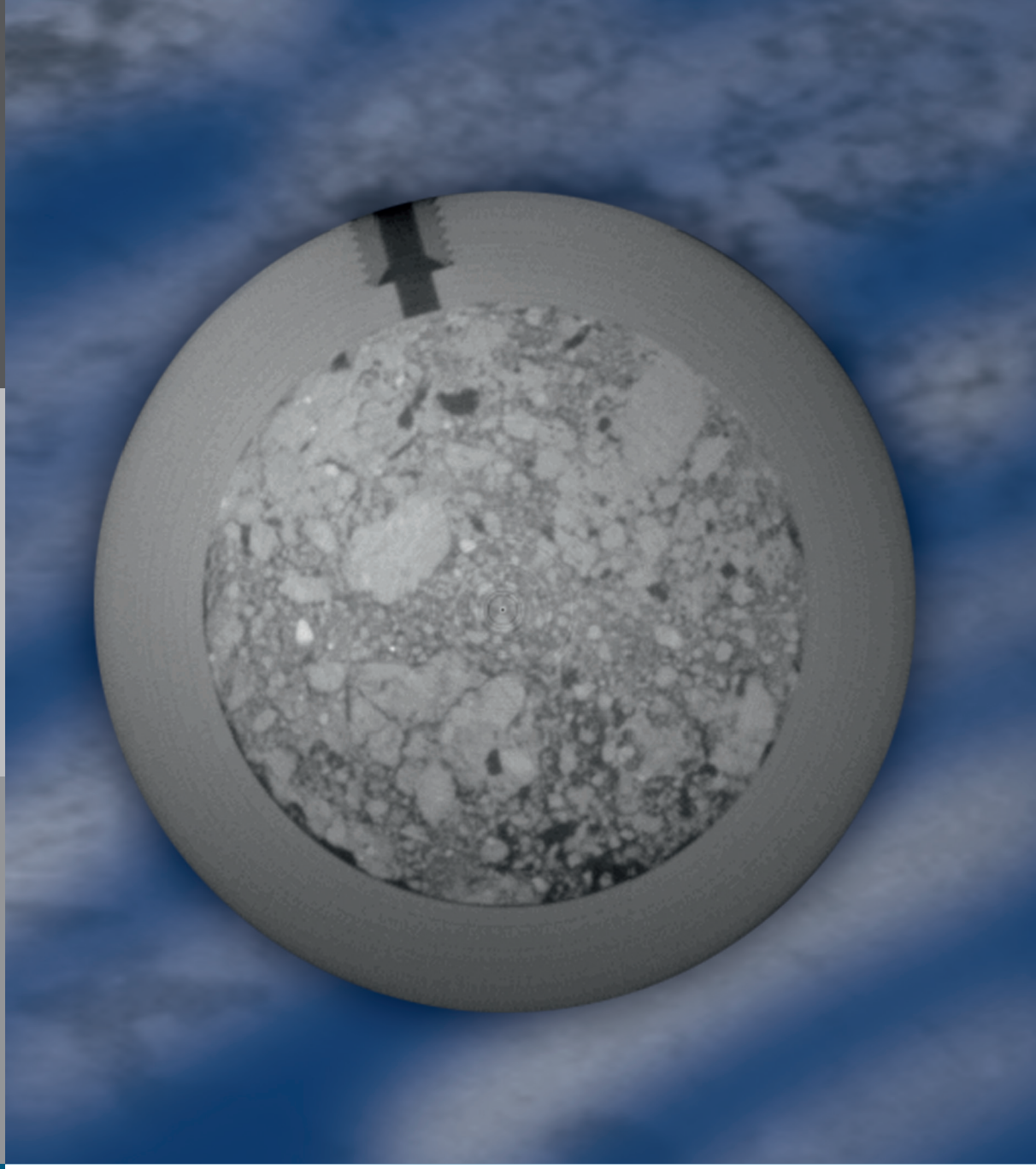

Experiments and numerical studies on transport of sulfadiazine in soil columns

Myriam Unold

Mitglied der Helmholtz-Gemeinschaft

JÜLICH
FORSCHUNGSZENTRUM

Schriften des Forschungszentrums Jülich
Reihe Energie & Umwelt / Energy & Environment Band / Volume 81

Forschungszentrum Jülich GmbH
Institute of Chemistry and Dynamics of the Geosphere (ICG)
Agrosphere (ICG-4)

Experiments and numerical studies on transport of sulfadiazine in soil columns

Myriam Unold

Schriften des Forschungszentrums Jülich
Reihe Energie & Umwelt / Energy & Environment Band / Volume 81

ISSN 1866-1793 ISBN 978-3-89336-663-7

Bibliographic information published by the Deutsche Nationalbibliothek.
The Deutsche Nationalbibliothek lists this publication in the Deutsche Nationalbibliografie; detailed bibliographic data are available in the Internet at http://dnb.d-nb.de.

Publisher and Distributor:	Forschungszentrum Jülich GmbH Zentralbibliothek 52425 Jülich Phone +49 (0) 24 61 61-53 68 · Fax +49 (0) 24 61 61-61 03 e-mail: zb-publikation@fz-juelich.de Internet: http://www.fz-juelich.de/zb
Cover Design:	Grafische Medien, Forschungszentrum Jülich GmbH
Printer:	Grafische Medien, Forschungszentrum Jülich GmbH
Copyright:	Forschungszentrum Jülich 2010

Schriften des Forschungszentrums Jülich
Reihe Energie & Umwelt / Energy & Environment Band / Volume 81

D 5 (Diss., Bonn, Univ., 2010)

ISSN 1866-1793
ISBN 978-3-89336-663-7

The complete volume ist freely available on the Internet on the Jülicher Open Access Server (JUWEL) at http://www.fz-juelich.de/zb/juwel

Acknowledgements

First of all I want to thank my promotor Prof. Harry Vereecken, head of the ICG-4, Agrosphere, Forschungszentrum Jülich GmbH, Dr. Thomas Pütz and Dr. Joost Groeneweg, head of the project "Veterinary pharmaceuticals in soils", for the chance to conduct this thesis at the Agrosphere Institute which included amongst others the possibility to stay in the USA for three month. Furthermore I thank Prof. Wulf Amelung (University of Bonn) for being my co-promotor. I express my gratitude to the German Research Foundation for funding this thesis in the frame of the research group "Veterinary medicines in soils – Basic Research for Risk analysis" and I thank the members of the research group for many inspiring discussions and information. I am especially grateful to Dr. Marc Lamshöft (University of Dortmund) for his support in the analysis of metabolites. I also thank Bayer HealthCare for providing the ^{14}C-labeled sulfadiazine and BayerCropScience AG for the performance of the feeding experiment.

I appreciate the staff of the ICG-4 for the pleasant working atmosphere, especially numerous people who greatly contributed to the performance of the experiments and the evaluation of data. A special thank goes to my direct mentor Dr. Roy Kasteel for his excellent advice and support during the last years. For adapting the Hydrus-1D code to my experiments, the corrections of the second manuscript and the kind hospitality I thank Prof. Jirka Šimůnek and also his working group at the University of California, Riverside. For building the experimental setup for the soil column experiments and their quick help in all kind of technical questions I express my gratitude to Ansgar Weuthen and Jürgen Höltkemeier. I am also very grateful to Thorsten Büttner and Rainer Harms for their efforts during sampling in the field. The performance of the transport experiments in the laboratory would have been impossible without the splendid help of Thorsten Büttner, Kavita Mayekar, Stefan Masjosthuisman and Maja Stiefelhagen. For conducting the HPLC-measurements and his patience in detecting and quantifying metabolites I am very grateful to Stephan Köppchen. For advice in questions regarding laboratory issues I thank also Odilia Esser, Werner Mittelstädt, Anke Langen, Herbert Philipp, Anne Berns, Ulrike Langen and Martina Krause. For answering all questions regarding programming and the Hydrus1D-code I am much obliged to Horst Hardelauf. I thank Roy Kasteel, Joost Groeneweg and Harry Vereecken for reading drafts of the manuscript. For their company and friendship during my stay in Jülich I thank my fellow PhD-students, especially my roommates Jana and Katrin as well as our neighbours Christoph and John. Finally, special thanks to my family, friends and Ansgar for their love, support and understanding.

Summary

Veterinary antibiotics like sulfadiazine (SDZ) are used in large amounts worldwide. Excreted as parent compounds or in the form of metabolites they reach agricultural soils mainly via spreading of manure or sewage sludge and may be transported to the groundwater. Recently, antibiotics have been detected in several environmental compartments leading to an increasing concern about their hazardous effects. To asses the leaching potential of SDZ from soils into groundwater, knowledge on its transport processes in soils is necessary. Also the transport of its metabolites as well as possible transformation processes have to be considered.

In this work transport experiments at the column scale were performed. Therefore, SDZ and pig manure were used to analyze the governing processes that affect the transport of SDZ in disturbed and undisturbed soil columns of a loamy sand and a silty loam. For this purpose the Hydrus model (Šimůnek et al., 2008) has been adapted and applied to the observed BTCs and resident concentrations.

The occurrence of transformation products in the outflow of repacked soil columns of both soils was investigated in experiments with a SDZ-solution. For the prediction of the ^{14}C-distribution in the repacked soil columns, empirical approaches to describe irreversible sorption were tested. Furthermore the influence of flow rate and concentration/applied mass on SDZ transport was investigated and the respective experiments were simultaneously described with a common set of parameters. In transport experiments with pig manure, the effect of pig manure on the transport of SDZ as well as the transport behavior of the main metabolites of SDZ present in pig manure, N-Ac-SDZ and 4-OH-SDZ, were investigated.

Without considering a known photo-degradation product transformation was very low in both investigated soils. In soil columns where most of the ^{14}C was found near the soil surface, the prediction of the ^{14}C-concentration profiles was improved by applying two empirical models other than first-order to predict irreversible sorption. The application of SDZ at a higher flow rate led to higher eluted masses and concentrations compared to experiments conducted at a lower flow rate. The simultaneous fitting process with a three site attachment/detachment model revealed that although the same sorption mechanisms seem to occur in all experiments, their characteristic time scales were different, especially under transient flow conditions. As the main difference between experiments with manure and SDZ-solution an accumulation of ^{14}C in the upper soil layer was found in the experiments with manure. The modeling process revealed a high mobility of both SDZ and its transformation products. While the transformation of N-Ac-SDZ into SDZ was fast and no extended tailing of N-Ac-SDZ was observed, the transport behavior of 4-OH-SDZ was similar to SDZ.

Kurzfassung

In der Tiermedizin angewandte Antibiotika wie Sulfadiazin (SDZ) werden weltweit in großen Mengen eingesetzt. Nachdem sie als Ausgangssubstanz oder in der Form von Metaboliten ausgeschieden werden, gelangen sie hauptsächlich durch das Ausbringen von Gülle oder Klärschlamm in landwirtschaftliche Böden von wo aus sie ins Grundwasser transportiert werden können. In den letzten Jahren wurden Antibiotika in verschiedenen Umweltmedien nachgewiesen was aufgrund ihrer schädlichen Auswirkungen zu einer steigenden Besorgnis geführt hat. Um das Potential einer möglichen Auswaschung von SDZ ins Grundwasser einschätzen zu können, sind Kenntnisse über die Transportprozesse in Böden entscheidend. Auch der Transport der Metabolite sowie mögliche Transformationsprozesse müssen berücksichtigt werden.

In dieser Dissertation wurden Transportexperimente auf der Skala von Bodensäulen durchgeführt. Anhand von SDZ-Lösungen und SDZ-haltiger Schweinegülle wurden Prozesse untersucht, die den Transport von SDZ in gestörten und ungestörten Bodensäulen eines lehmigen Sandes und eines schluffigen Lehms beeinflussen. Dazu wurde das Model Hydrus (Šimůnek et al., 2008) verändert und zur Modellierung der gemessenen Durchbruchskurven und Profilkonzentrationen genutzt.

Das Auftreten von Transformationsprodukten im Ausfluss von gepackten Bodensäulen beider Böden wurde in Experimenten mit einer SDZ-Lösung untersucht. Zur Vorhersage der ^{14}C-Konzentrationen in den Bodenprofilen wurden empirische Ansätze zur Beschreibung der irreversiblen Sorption getestet. Zusätzlich wurde der Einfluss von Fließrate und Konzentration/applizierter Masse auf den Transport von SDZ untersucht. Während des Modellierungsprozesses wurden die entsprechenden Experimente mit einem gemeinsamen Parametersatz beschrieben. In Transportexperimenten mit Schweinegülle wurden der Einfluss von Schweinegülle auf den Transport von SDZ sowie das Verhalten der in der Schweingülle vorhandenen Hauptmetabolite, N-Ac-SDZ und 4-OH-SDZ, untersucht.

Ohne Berücksichtigung eines bekannten Phototransformationsproduktes war die Transformation von SDZ in beiden Böden sehr gering. In den Bodensäulen wurde die größte Menge an ^{14}C nahe der Oberfläche gefunden. Die Beschreibung dieses Musters konnte durch die Anwendung zweier empirischer Modelle zur Beschreibung der irreversiblen Sorption verbessert werden. Die Applikation von SDZ bei einer höheren Fließrate führte, im Vergleich zu Experimenten, die bei einer geringen Fließrate durchgeführt wurden, zu höheren eluierten Mengen. Die simultane Modellierung mit einem dreiseitigen attachment/detachment Model zeigte, dass die charakteristischen Zeitskalen in den Experimenten verschieden sind, obwohl in allen Experimenten dieselben

Sorptionsmechanismen stattzufinden scheinen. Dies gilt insbesondere im Vergleich zwischen Experimenten mit konstanten und transienten Fließbedingungen. Der Hauptunterschied zwischen Experimenten mit SDZ-Lösung und Gülle war eine Anreicherung von ^{14}C in der obersten Schicht der Bodensäulen in den Experimenten mit Gülle. Die Ergebnisse der Modellierung ergaben eine hohe Mobilität für SDZ und die Transformationsprodukte. Während die Transformation von N-Ac-SDZ zu SDZ schnell verlief und die Durchbruchskurven von N-Ac-SDZ kein ausgeprägtes Tailing aufwiesen, war das Transportverhalten von 4-OH-SDZ dem von SDZ ähnlich.

Contents

List of Tables

Page

List of Figures

Page

Abbreviations

An-SDZ	4-(2-iminopyrimidin-1(2H)-yl)aniline
BTC	Breakthrough curve
CDE	Convection–Dispersion equation
^{14}C	Sum of SDZ and the transformation products
HPLC	High performance liquid chromatography
LSC	Liquid scintillation counting
N-Ac-SDZ	N^4-acetyl-N^1-2-pyrimidinylsulfanilamide
4-OH-SDZ	N^1-2-(4-Hydroxypyrimidinyl)sulfanilamide
RA	Radioactivity
SDZ	Sulfadiazine

Symbols

C	solute concentration in the liquid phase [ML^{-3}]
C_k	solute concentration in the liquid phase [ML^{-3}] of solute k
C_{org}	content of organic carbon
CEC	cation exchange capacity [chargeM^{-1}]
D	hydrodynamic dispersion coefficient [L^2T^{-1}]
f	fraction of sorption sites in equilibrium [-]
i,j	indizes for counting
k	1. counter of solutes (Chapter 3, 4) 2. exponent or factor to enlarge the exponent in the exponential function (Chapter 2)
K_f	Freundlich soil water distribution coefficient [$M_{solute}^{1-m} L^{3m} M_{soil}^{-1}$]
L	Length [cm]
m	Freundlich exponent [-]
n	number of data points
r	difference between data and model outcome
S	solute concentration in the solid phase [MM^{-1}]
S_k	solute concentration in the solid phase [MM^{-1}] of solute k
pH	negative decadic logarithm of the hydronium ion concentration
pK_a	acidity constant
t	time [T]
T	time [h]
V	Volume [L^3]
w	weighting factor for the data points for a group of data
z	depth [L]
α	kinetic mass transfer coefficient [T^{-1}]
β	irreversible rate coefficient (Chapter 2)
β_i	attachment rate to sorption site i [T^{-1}]
γ_i	detachment rate from sorption site i [T^{-1}]
λ	dispersivity [L]
ρ	soil bulk density [ML^{-3}]

θ	volumetric water content [L^3L^{-3}]
v	pore water velocity [LT^{-1}]
$\mu_{(k)}$	first order rate coefficient for irreversible sorption from liquid phase [T^{-1}] (of solute k)
$\mu_{(k)}'$	first order rate coefficient for transformation from liquid phase [T^{-1}] (of solute k)
ϕ	sum of squared weighed deviations between data and modeling results

1 Introduction

1.1 Antibiotics in the environment

The frequent use of antibiotics in human and veterinary medicine in the last decades lead to their widespread dispersion in the environment (Thiele-Bruhn, 2003). Hence, in the last years antibiotics were detected in surface waters (Pailler et al., 2008; Tamtam et al., 2009, Christian et al., 2003; Managaki, 2007), groundwaters (Focazio, 2008; Hamscher, 2005; Sacher, 2001) and soils (Boxall, 2004; Hamscher, 2005; Höper, 2002). The major concern of the occurrence of antibiotics in the environment is the development and spreading of resistant pathogens (Kemper 2008), especially since these chemicals can reach the food chain via drinking water (Batt et al., 2006; Ye et al., 2007) or the root uptake by plants (Dolliver et al., 2007). In human therapy effects of increasing antibiotic resistance to older antibiotics are clearly visible and cause the search for new and more effective drugs. Contributions to this problem via diffuse pathways like agricultural input must be considered (Rooklidge 2004). Another point of concern is the influence of antibiotics on microbial populations, especially since this kind of pharmaceuticals was explicitly designed to affect bacteria. Influences on microbial process and community structures in soils were demonstrated (Hammesfahr et al., 2008; Kotzerke et al., 2008; Zielezny et al., 2006).

Veterinary antibiotics reach soils mainly through the application of manure or sewage sludge on agricultural fields (Jørgensen and Halling-Sørensen, 2000). Thus to asses their environmental fate knowledge on governing sorption, transport and degradation processes in soils are essential.

One group of antibiotics are the sulfonamides to which the target substance of this thesis, sulfadiazine, belongs to. This group of synthetic antibiotics was discovered in the early 1930s and represents the first group of broad spectra antibiotics (Nobel Lectures, 1965). Sulfonamides affect the growth of bacteria based on the competitive inhibition of the folic acid synthesis in bacterial cells (Löscher et al., 1994) and are still among the most used antibiotics in European countries with contributions between 11 and 21% (Kools et al., 2008). Recently, this group was classified as relevant to the environment (Bergmann et al., 2008). In the last decades a lot of information on the behavior of SDZ of soils was ascertained. In short, a lower sorption coefficient compared to other classes of antibiotics

indicates good water solubility and a higher mobility (Thiele-Bruhn et al., 2004). Sorption proved to be characterized as a nonlinear (Thiele-Bruhn et al., 2004) non-equilibrium process with sorption coefficients increasing with time (Förster et al., 2009, Wehrhan et al., 2009) which may be explained by diffusion processes into the intra-particle pore systems or organic matter. Also sorption hysteresis was reported (Sukul et al., 2008a, Wehrhan et al., 2009) as well as true irreversible sorption via covalent bonding to organic substances (Bialk et al., 2008). In transport experiments, sorption hysteresis became visible in incomplete breakthroughs where parts of the substance were retained in the uppermost soil layers (Kreuzig et al., 2005; Unold et al., 2009a,b; Wehrhan et al., 2007). Measured breakthrough curves (BTCs) showed extended tailings which can be explained by slow kinetic processes or non-linear sorption behavior. Furthermore, the pH value (Kahle and Stamm, 2007a; Kurwadkar et al., 2007) as well as the amount and composition of organic material (Kahle and Stamm, 2007b; Thiele-Bruhn et al., 2004) affected sorption of SDZ. Several studies indicated that transformation of sulfonamides in soils occurs (Burkhardt & Stamm 2007; Unold et al., 2009a,b; Wehrhan, 2006).

However, the influence of many factors is still unknown. With the help of the experiments conducted in this thesis knowledge on the transport behavior of SDZ in soils was supplemented.

1.2 Objectives and Experimental approach

The overall objective of this thesis was to improve the understanding of SDZ transport in soils by means of soil column experiments with two different agricultural soils and modeling of the resulting BTCs and concentration profiles. Specific aims were:

- To investigate the occurrence of transformation products in the outflow of the soil columns to which SDZ was applied in a solution
- To test if empirical approaches for modeling irreversible sorption can improve the description of the ^{14}C concentration profiles
- To study the influence of flow rate and concentration/applied mass on SDZ transport
- To describe experiments with different flow rates and applied SDZ concentrations simultaneously with a common set of parameters

1.3 Objectives and Experimental approach

- To determine the effect of pig manure on SDZ transport
- To study the transport of the main SDZ metabolites in pig manure

In order to get a basic knowledge on the transport of a compound in soils, experiments in the laboratory are suitable because boundary conditions can be defined and controlled. In general sorption parameters of a compound can be characterized by batch or soil column experiments. Compared to batch experiments, soil column experiments have the advantage that they are closer to reality, where transport processes are also influenced by water flow. The effect of water flow can be determined and excluded from the estimation of sorption parameters by conducting transport experiments with a conservative tracer like chloride, for which no sorption is considered.

This thesis was performed within the frame of the research group: Veterinary medicines in Soils – Basic Research for Risk Analysis. In the research group a feeding experiment with ^{14}C-labeled SDZ was performed where ^{14}C-SDZ was applied to fattening pigs. The collection of the manure allowed the investigation of SDZ fate under most realistic conditions since manure is the most important pathway for veterinary antibiotics into soils. The usage of a ^{14}C- labeled compound allowed the detection of SDZ and its transformation products in solutions and soil, independent of the sorption processes or matrix effects.

SDZ was applied in solution and together with pig-manure. The application of SDZ in solution enabled the investigation of substance specific sorption and transformation processes under different boundary conditions without interfering influences like organic particles, ion intensities and transformation products which occur in the presence of slurry. Experiments with SDZ containing manure were closer to reality and provided also insights into the transport of the main SDZ metabolites.

1.3 Thesis outline

The results of the thesis are presented in three chapters (2-4), corresponding to published or submitted publications to international peer-reviewed journals. Some information on the sorption and transport behavior of SDZ that was ascertained in the last decades is presented in the introductions of chapters 2, 3 and 4. Since all these chapters deal with SDZ transport, repetitions could not be avoided.

In the experiments presented in chapter 2, a SDZ-solution was applied to repacked soil columns of the two soils. BTCs of SDZ and the transformation products An-SDZ and 4-OH-SDZ were measured, as well as vertical ^{14}C-distributions in the soil columns. Both, the BTCs and the concentration profiles were described using a model with one kinetic reversible and one irreversible kinetic sorption site. Two empirical approaches for modeling irreversible sorption were tested in order to improve the description of the ^{14}C concentration profiles.

In chapter 3, SDZ transport in dependence of flow rate and applied input concentration was studied using five undisturbed soil columns of the loamy sand. Measured BTCs and concentration profiles of different experiments were modeled with common parameter sets using an attachment/detachment based model approach.

For the experiments described in chapter 4 either a SDZ-solution or pig manure were blended into repacked and undisturbed soil columns. A comparison of the measured BTCs and concentration profiles revealed the effect of pig manure on SDZ transport. Additionally the transport of the main transformation products of SDZ present in pig manure, N-Ac-SDZ and 4-OH-SDZ, was studied.

Finally in chapter 5 the individual results are synthesized and the general conclusions are presented. Detailed information on the investigated solutes, soils, chemicals and instruments is given in the Appendix.

2 Transport and transformation of sulfadiazine in soil columns packed with a silty loam and a loamy sand[1]

2.1 Objectives

The objectives of the experiments presented in chapter two were to investigate the occurrence of transformation products in the outflow of the soil columns and to test if empirical approaches for modeling irreversible sorption can improve the description of the ^{14}C concentration profiles.

2.2 Introduction

The chemical group of sulfonamides to which our target substance sulfadiazine (SDZ) belongs to is among the most used antibiotics in European countries with contributions between 11 and 24% (Kools et al., 2008). Like other veterinary pharmaceuticals, sulfonamides reach agricultural soils mainly through the use of manure or directly through grazing livestock (Jørgensen and Halling-Sørensen, 2000). Evidence that sulfonamides released to soils can possibly reach the food-chain is given by the detection of surface water contamination (Christian et al., 2003), by transport through soil (Hamscher et al., 2005) or surface runoff (Davis et al., 2006) and uptake by plants (Dolliver et al., 2007). Besides possible adverse effects on microorganisms, the major risk of introducing antibiotics into the environment is the development and spreading of resistant pathogens (Heuer and Smalla, 2007; Kemper, 2008; Mazel and Davies, 1998).

To asses the leaching potential of SDZ, it is important to understand its sorption and transport behavior. Thiele-Bruhn et al. (2004) found a nonlinear sorption behavior which was best described by the Freundlich equation. Compared to other classes of antibiotics, SDZ has a low adsorption coefficient indicating good water solubility and therefore a higher mobility (Thiele-Bruhn et al., 2004). Having two pK_a values, SDZ sorption is likely to be pH-dependent, as was shown for other sulfonamides (Gao and Pedersen, 2005; Kahle

* adapted from: Unold, M., R. Kasteel, J. Groeneweg and H. Vereecken (2009). Transport and Transformation of the veterinary antibiotic sulfadiazine in soil columns. Journal of Contaminant Hydrology 103. 38-47.[1]

and Stamm, 2007; Kurwadkar et al., 2007). SDZ was characterized by a fast dissipation after application to soil, since it could not be detected in soil samples treated with SDZ-contaminated manure (Martinez-Carballo et al., 2007). This fast dissipation is not necessarily equivalent to a fast transformation or biodegradation, since in other studies SDZ showed a low mineralisation rate (Kreuzig et al., 2003) and a strong tendency to form non-extractable residues in the upper soil layer (Kreuzig and Höltge, 2005). Examples of non-extractable residues are covalent bondings between sulfonamides and soil organic matter (Bialk et al., 2007). In field studies surface runoff and leaching were two important transport pathways for the fate of SDZ (Burkhardt and Stamm, 2007; Kreuzig et al., 2005). For soil columns Wehrhan et al. (2007) showed an influence of the applied concentration and application time on the shape of ^{14}C-SDZ breakthrough curves and ^{14}C-distributions in soil columns.

Transformation or biodegradation of SDZ in soils is not well understood yet. In pig manure N-acetyl-SDZ and 4-hydroxy-SDZ were found as the main metabolism products (Lamshöft et al., 2007), whereas Woolley and Sigel (1979) detected N-acetyl-SDZ and N-glucuronide-SDZ as the main metabolism products for rats. Results from Wehrhan (2006) and Burkhardt & Stamm (2007) indicated that transformation occurred also in soils. Wehrhan (2006) detected N-acetyl-SDZ, 4-hydroxy-SDZ and an additional unknown product in batch and soil column studies without manure. Burkhardt & Stamm (2007) found the acetylated form of sulfadimidine in soil extracts but not in manure. Transformation products like 4-hydroxy-SDZ can still be active against micro-organisms (Nouws et al., 1989) or they can be re-transformed again into SDZ like N-acetyl-SDZ (Berger et al., 1986). Therefore, the fate of the transformation products in the environment has to be considered, too.

For the transport of reactive solutes in soils, various model concepts are available considering different sorption and degradation processes. The transport of organic compounds was described with models that include multiple sorption regions to account for the heterogeneity of soil materials and sorption properties (Brusseau and Rao, 1989). Sorption of the antibiotic tetracycline on silica, for example, was successfully described with a two-site model containing one irreversible and one reversible sorption site (Turku et al., 2007). Wehrhan et al. (2007) showed that kinetic models based on the Freundlich sorption isotherm which included two reversible and one irreversible sorption site can describe ^{14}C-BTCs of SDZ, but not the ^{14}C-distributions in the soil column profiles. In two

out of three experiments the ^{14}C-concentrations in the soil profiles decreased with depth and were remarkably higher in the uppermost layer, a pattern which could not be described by assuming a first order process. Most mass of ^{14}C which was not eluted out of the soil column after the leaching experiment resided in the irreversible sorption site. It was not possible to distinguish between "bound residues", i.e. no desorption, and very slow desorption processes in her experiments, due to the limited duration of the leaching experiment.

Irreversible sorption, which can be considered as no desorption or a very slow desorption compared to the characteristic time scale of the experiment, is often described with a first-order degradation process (e.g. Baek et al., 2003), although other model concepts have also been applied (Pignatello and Xing, 1996). Kan et al. (1998) used a Langmuirian-type equation to calculate the amount of irreversibly sorbed hydrocarbons and Wilson et al. (2004) used a reversible sorption site, from which irreversible sorption occurred consecutively.

The objectives of this study were a) the detection of possible transformation products in the outflow of the soil columns in order to get information on the persistence of SDZ in soils and b) to model the transport of SDZ with a special emphasis on the ^{14}C-distribution in the soil column profiles which is assumed to be dominated by irreversible sorption. With an improved chemical analysis we were able to distinguish between SDZ and its transformation products in the outflow of the soil columns. Breakthrough curves of ^{14}C-SDZ and ^{14}C-SDZ concentration profiles were fitted with a convective-dispersive transport model with two reversible and one irreversible sorption site. One of the reversible sorption sites is in equilibrium with the concentration in the liquid phase and one exhibits kinetic sorption. We tested two empirical approaches to calculate irreversible sorption, which were different from first-order kinetics.

2.3 Materials & Methods

2.3.1 Experimental set-up

We studied the transport of SDZ in two repacked soil columns near water saturation. No replicates were run. The experimental design of this study corresponded to application scenario B of Wehrhan et al. (2007). The soil materials were collected from the upper

30 cm of two fields with representative soil types for agricultural land use in Germany: a silt loam (Orthic Luvisol, soil M) from a field near Jülich-Merzenhausen (Germany) and a loamy sand (Gleyic Cambisol, soil K) from a field near Kaldenkirchen (Germany). Selected soil properties are shown in Table 2.1. Both soils were sieved to < 2 mm and air-dried. We additionally ground the silt loam, since small aggregates led to asymmetrical breakthrough curves (BTCs) of the conservative tracer chloride which we used to characterize the water flow pathways in the soil columns. Stainless steel columns with an inner diameter of 8.5 cm and a height of 10 cm were used for the experiments. During the packing procedure, layers of about 1 cm thickness were filled into the columns and compacted by a weak pressing with a pestle. Since the air-dried loamy sand was highly water-repellent, this soil was slightly wetted before packing. A thin layer of coarse quartz sand on the top of the column prevented splashing of soil material. The soil columns were slowly saturated from the bottom with tap water for 3 to 4 days. The soil columns were mounted on a porous ceramic plate (high flow, air-entry point > 1 bar). No suction was applied to the system.

Table 2.1: Selected physical and chemical properties of the Kaldenkirchen soil (K) and the Merzenhausen soil (M)

	Unit	Soil K	Soil M
Clay (<0.002 mm)[a]	[% mass]	4.9	15.4
Silt (0.002-0.064 mm)[a]	[% mass]	26.7	78.7
Sand (0.064-2.000 mm)[a]	[% mass]	68.5	5.9
pH (0.01 M $CaCl_2$)[b]		5.9	6.2
C_{org} [a,c]	[% mass]	1.07	1.24
CEC[d]	[$cmol_c kg^{-1}$]	7.8	11.4

[a] Data were measured at the "Institut für Nutzpflanzenwissenschaften und Ressourcenschutz" at the University of Bonn.
[b] average pH-values in the soil columns after the experiments.
[c] C_{org} is the concentration of total organic matter content.
[d] Data for CEC were taken from Förster et al. (2008).

In order to establish steady state flow conditions, the soil columns were irrigated with a 0.01 M $CaCl_2$-solution at a constant rate of approximately 0.25 cm h^{-1} for a few days using an irrigation device with 12 needles. The device was placed on the top of the column. The influent solution was supplied by a flexible-tube pump and the irrigation rate was controlled by weighing the water loss from the fluent storage. The outflow was collected in test tubes of a fraction collector.

2.3 Materials & Methods

We used chloride as a non-reactive tracer to characterize the water flow pathways in the soil columns since it is also present in the background solution and the measurement with an electrical conductivity sensor was unspecific. For measuring the chloride BTCs, the 0.01 M $CaCl_2$-solution was replaced by a 0.05 M $CaCl_2$-solution for one hour. For determining the SDZ-BTCs, the 0.01 M $CaCl_2$-solution was replaced by a solution of 0.57 mg SDZ L^{-1} (in 0.01 M $CaCl_2$) for 68 hours. Since the outflow samples were uncovered during their storage in the fraction sampler, the measured concentrations were corrected for evaporation losses, which were on average 2.2 x 10^{-6} L h^{-1}. After the leaching experiments were finished, the soil columns were cut into slices of 0.5 or 1 cm thickness, in order to detect the ^{14}C-concentrations in the soil column profile.

2.3.2 Analytics of sulfadiazine and transformation products

Sulfadiazine (IUPAC: 4-amino-N-pyrimidin-2-yl-benzenesulfonamide) was provided by Bayer HealthCare AG (Wuppertal, Germany) as a powder with a purity of 99% and a specific radioactivity of 8.88 MBq mg^{-1}. Some physico-chemical properties of SDZ are listed in Table 2.2.

Table 2.2: Selected physicochemical properties of sulfadiazine

Formula	$C_{10}H_{10}N_4O_2S$
Molar weight	250.28 g mol^{-1}
Water solubility	13 to 77 mg L^{-1}
pK_{a1}, pK_{a2}	1.57±0.1/6.50± 0.3
Octanol/water distribution coefficient	0.76
Henry's Law constant	1.60 x 10^{-5} Pa m^3 mol^{-1}

Data were taken from Wehrhan et al. (2007).

The chemical structure is shown in Fig 2.1a. The application solution was prepared by adding the adequate amount of stock solution (9.6 mg SDZ powder dissolved in 20 mL acetonitrile) to a 0.01 M $CaCl_2$ solution. The total amount of radioactivity in the outflow samples was measured with Liquid Scintillation Counting (LSC) with a counting time of 15 minutes. Hence, three aliquots of 1 mL of each liquid sample were mixed with 10 mL scintillation cocktail (Insta-Gel Plus). The detection limit was 0.4 Bq which corresponds to

0.045 ng mass equivalents of SDZ. The samples were corrected for background radiation by an additional measurement of a blank.

SDZ and the main transformation products were separated by the use of Radio-HPLC. The HPLC-system included an reversed-phase column (Phenomenex Synergi Fusion RP 80, 250 mm x 4.6 mm) which was eluted with a mixture of water (490 mL) and methanol (10 mL), buffered with 0.5 mL of a 25% phosphoric acid solution. The injection volume was 0.25 mL for each sample. A gradient with an increased amount of methanol was used for peak separation, starting with 100% water for 6 minutes. The methanol fraction increased linearly to 27% till minute 23, then to 37% in the next three minutes and to 47% in the following two minutes. The methanol part reached its maximum with 57% after 30 minutes. With this protocol, we were able to distinguish four peaks in the chromatograms, of which three were identified as SDZ, 4-hydroxy-SDZ (N1-2-(4-hydroxypyrimidinyl)benzenesulfanilamide) and 4-(2-iminopyrimidin-1(2H)-yl)aniline. We identified SDZ and 4-hydroxy-SDZ according to their retention times which we know from a SDZ-standard and previous experiments. 4-(2-iminopyrimidin-1(2H)-yl)aniline was identified by the Institute of Environmental Research at the University of Dortmund, Germany. In the experiments of Lamshöft et al. (2007), who used another HPLC-separation method, the SDZ-transformation products 5-hydroxy-SDZ and N-formyl-SDZ have similar retention times as SDZ. Therefore we may also not be able to detect them with our HPLC-setup. But in other studies (Lamshöft et al., (2007), Sukul et al., (2008b)) they only appeared in traces and so their possible co-elution would not change our results significantly. These studies do not mention possible co-eluting compounds in the peaks of 4-(2-iminopyrimidin-1(2H)-yl)aniline and 4-hydroxy-SDZ. The chemical structures of these compounds are shown in Figure 2.1.

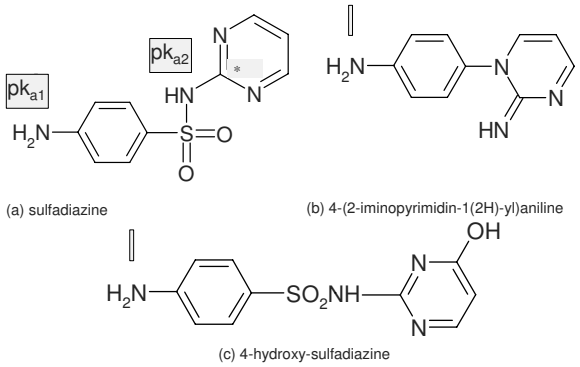

Figure 2.1. Chemical structure of (a) SDZ, the ^{14}C-labeling with a specific radioactivity of 8.88 MBq mg^{-1} is marked by a star and the ionisable moieties (Sakurai & Ishimitsu 1980) at the two pk_a values are marked by rectangles, (b) 4-(2-iminopyrimidin-1(2H)-yl)aniline and (c) 4-hydroxy-SDZ.

Using HPLC the detection limit for SDZ and its transformation products is about 3 µg L^{-1} mass equivalents of SDZ. For the transformation products this concentration was only found in the samples with the highest ^{14}C-concentrations. In order to detect SDZ and the transformation products also in samples at lower concentrations, we changed the measurement procedure. The outflow of the HPLC was collected according to the retention times of SDZ and the transformation products, and also in-between these time frames. We used a standard for sulfadiazine to fix the retention time for the SDZ-peak. No standards were available for 4-hydroxy-SDZ, 4-(2-iminopyrimidin-1(2H)-yl)aniline and an additional unknown product, which was only detected in soil M. Therefore, these compounds were identified by setting their retention times in relation to the retention time of the known peak.

The correction of the background radioactivity was performed by collecting the outflow of the HPLC-column at the beginning and the end of each HPLC-run and subtracting the averaged background radioactivity from the radioactivity in the peaks. In some samples, which were collected outside of the retention times of the peaks, the radioactivity was higher than the background signal, but this radioactivity could not be associated to an own peak. Additionally, the sum of radioactivity in the collected outflow varied between 95% and 105% of the total radioactivity measured in aliquots of the respective samples. Therefore, we performed the following correction to compare the

concentration (C_i) of compound *i*, with the total measured ^{14}C-concentration ($^{14}C_{total}$) in an aliquot of the respective sample:

$$C_i = \frac{(RA_{i_{uncorrected}} - RA_{background})}{\Sigma RA_{j_{corrected}}} * {}^{14}C_{total} \qquad (2.1)$$

where $RA_{i,\text{uncorrected}}$ is the radioactivity in the peak before subtracting the background radioactivity $RA_{background}$ and $RA_{jcorrected}$ is the background corrected radioactivity of compound j in the respective sample. With this procedure, the sum of the transformation products adds up to 100% radioactivity. With the help of the specific radioactivity of SDZ the transformation products can be quantified in mass equivalents of SDZ according to the calculated parts. A transformation product was quantified, when the measured radioactivity was higher than 1.2 Bq, which is three times the detection limit of the LSC. Otherwise its contribution was set to zero. With this method the transformation products could be identified down to a concentration of 0.5 µg L^{-1} mass equivalents of SDZ. The method was validated by determining the correlation between the total radioactivity in one diluted outflow sample of each soil and the radioactivity measured in the peaks of this sample (see Figure 2.2). The obtained correlations for SDZ, 4-(2-iminopyrimidin-1(2H)-yl)aniline and 4-hydroxy-SDZ were high ($R^2 > 0.99$) and significant (t-test) with a probability of 99%.

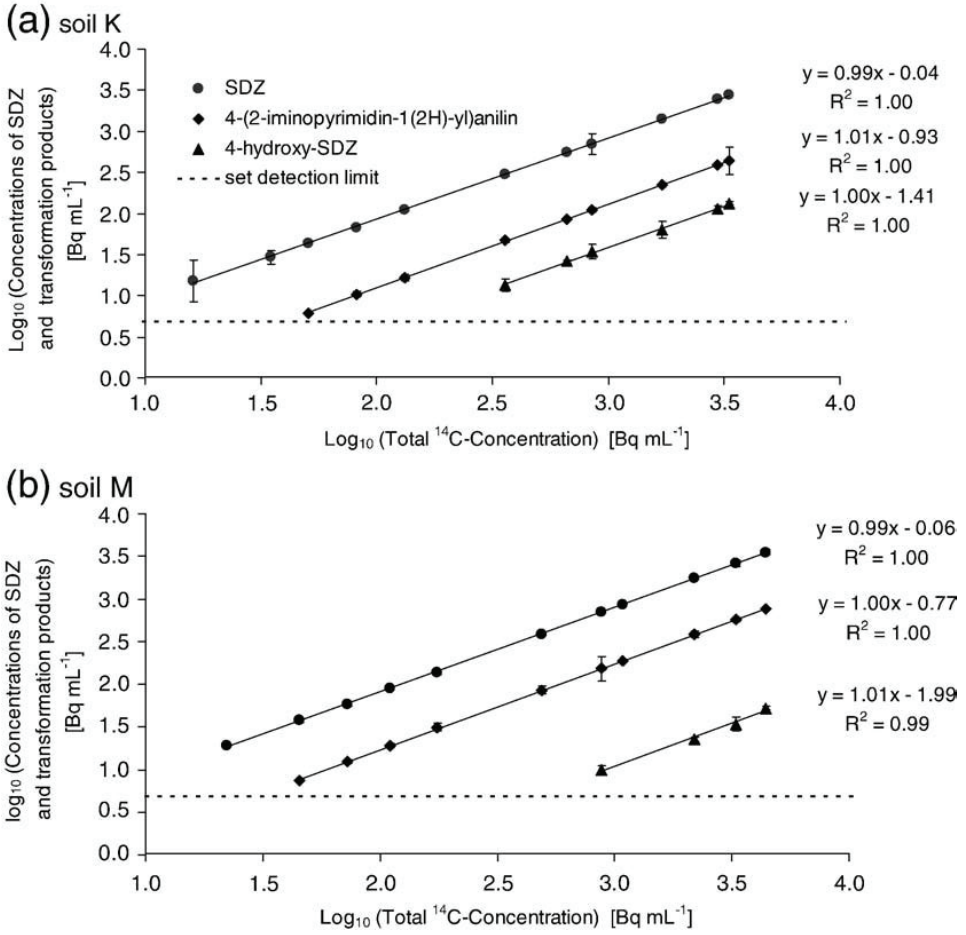

Figure 2.2. Correlation curves for the Liquid Scintillation Counting measurements of SDZ, 4-(2-iminopyrimidin-1(2H)-yl)aniline and 4-hydroxy-SDZ for one outflow sample of (a) the Kaldenkirchen soil (K) and (b) the Merzenhausen soil (M). Bars indicate the root mean square deviation.

In order to quantify the resident concentration profiles of ^{14}C-SDZ in the soil column, the column was cut into slices of 0.5 or 1 cm thickness at the end of the leaching experiments. Only the total amount of radioactivity was measured in the soil since extraction efficiencies are on a relatively low level and vary for fresh (> 70%) and aged (> 45%) SDZ-residues (Förster et al., 2008). For each slice three replicates of 0.5 g oven-dried (105°C), grounded and homogenized soil were combusted in an oxidizer. After combustion, the evolving gas was washed into a scintillation cocktail (Oxysolve) in which the labeled

CO_2 was trapped. This cocktail was measured with LSC. Blanks were run before and after the samples to check for background and cross contamination. The efficiency of the combustion process (>98%) was ascertained by combusting samples spiked with a known amount of the model compound ^{14}C-Anilazine prior and after the samples of the experiment.

2.3.3 Theory of solute transport

Water flow and solute transport in the repacked soil columns were treated as one-dimensional transport problems in the mathematical solutions. The convection–dispersion equation (CDE) is commonly used to describe the transport of solutes. For conservative tracers, like chloride, it can be written for steady state flow conditions as:

$$\frac{\partial C}{\partial t} = -v\frac{\partial C}{\partial z} + D\frac{\partial^2 C}{\partial z^2} \qquad (2.2)$$

where t is time [T], v is pore-water velocity [L T^{-1}], C is solute concentration in the liquid phase [M L^{-3}], D is dispersion coefficient [L^2 T^{-1}] and z is depth [L]. The chloride BTCs were used to estimate the parameters v and D by a non-linear parameter estimation procedure based on the Levenberg-Marquardt algorithm. We used the CXTFIT code (Toride et al., 1999), which analytically solves the CDE for the appropriate boundary conditions, i.e. a flux-type upper boundary condition and a zero gradient at the lower boundary. With the estimated transport parameters and the experimentally determined Darcian flow velocity, q, the volumetric water content, $\theta = q/v$, and the dispersivity, $\lambda = D/v$, were calculated and used to fix the water flow for the transport simulations of the reactive tracer SDZ.

For modeling the transport of SDZ, we used an isotherm-based model concept with two reversible and one irreversible sorption site, like in the work of Wehrhan et al. (2007). For this model concept the transport equation can be written as:

$$\frac{\partial C}{\partial t} + \frac{\rho}{\theta}\frac{\partial S}{\partial t} = -v\frac{\partial C}{\partial z} + D\frac{\partial^2 C}{\partial z^2} - \mu \qquad (2.3)$$

where θ is the water content [$L^3 L^{-3}$], ρ is bulk density [$M L^{-3}$], S is the adsorbed solute concentration [$M M^{-1}$] and μ [$M L^{-3} T^{-1}$] is a term that accounts for degradation, which is used here to mimic irreversible sorption (Baek et al., 2003).

The adsorbed solute concentration, *S,* is defined as the sum of the solute concentration adsorbed at the equilibrium sorption site S_1 and the rate-limited sorption site S_2 [$M M^{-1}$].

$$S = S_1 + S_2 \tag{2.4}$$

S_1 and S_2 are described as:

$$S_1 = fK_f C^m \tag{2.5}$$

$$\frac{\partial S_2}{\partial t} = \alpha_2((1-f)K_f C^m - S_2) \tag{2.6}$$

where K_f [$M^{1-m}_{solute} L^{3m} M^{-1}_{soil}$] is the Freundlich coefficient and m [-] is the Freundlich exponent, f [-] is the fraction of total sorption sites which are in equilibrium with the concentration in the liquid phase and α [T^{-1}] is the sorption rate coefficient. The transport parameters were fitted to the $\log_{10}$-transformed concentration data so that the BTC tailing got an increased weighting. To account for differences in the number of data points and the absolute concentration values, the data of the profiles were weighed with a factor, *w,* according to

$$w = \frac{n_{profile}}{n_{BTC}} \frac{\sum_{i=1}^{n_{BTC}} C_{i,BTC}}{\sum_{i=1}^{n_{profile}} C_{i,profile}} \tag{2.7}$$

where n accounts for the number of data points in the respective BTC and concentration profile and C_i are the measured concentrations at time i for the BTC expressed in mass of SDZ per volume of solution and the measured concentrations at depth i in the soil profile expressed in mass of SDZ per volume of soil.

The results of Wehrhan et al. (2007) showed that both an isotherm-based and an attachment/detachment model with two reversible and one irreversible sorption site were able to describe the measured SDZ-BTCs in soil columns of a silty loam, but not the ^{14}C-distribution in the soil column profiles. In these two models irreversible sorption was treated as a first-order process. In this study we test two additional approaches to account

for irreversible sorption. In a first approach we assume higher-order irreversible sorption according to the orders of chemical reactions and in a second approach we used an exponential model, like it was applied for example in Elovich´s equation (Zeldowitsch, 1934). For model approach 1, the term used to calculate irreversible sorption μ was calculated as

$$\mu = \beta C^k \tag{2.8}$$

where β is the irreversible rate coefficient [$L^{3(k-1)}M^{1-k}T^{-1}$] and k [-] is an exponent. Notice that for k=1, irreversible sorption is described by a first-order process. In the second approach μ is expressed as:

$$\mu = \beta \exp(kC) \ , \tag{2.9}$$

where β is again the irreversible rate coefficient [$M\ L^{-3}\ T^{-1}$]and k [L^3M^{-1}] is now a factor to enlarge the exponent in the exponential function.

We used the finite element code Hydrus6.0 (Šimůnek et al., 1998) to solve the convection-dispersion equation for solute transport and modified it to account for the two irreversible sorption concepts. We coupled Hydrus6.0 with the non-linear parameter estimation code PEST (Doherty, 2002) which estimates the transport parameters using the Gauss-Levenberg-Marquardt algorithm. For the optimal parameter set, the sum of squared deviations between model-generated and experimental observations, expressed by the objective function Φ, is reduced to a minimum:

$$\Phi = \sum_{i=1}^{m} (w_i r_i)^2, \tag{2.10}$$

where m is the total number of the observed data points and model outcomes, w_i is a weighting factor for the i´th observation and r_i is the difference between the i´th modeloutcome and the corresponding observed value (Doherty, 2002).

2.4 Results & Discussion

The measured BTCs and the model fits with the CDE are shown in Figure 2.3.

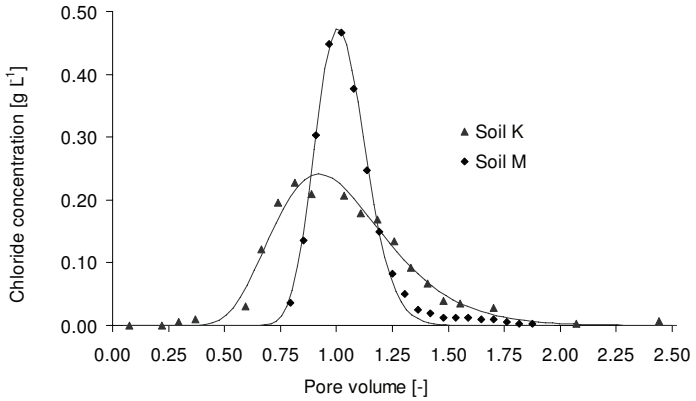

Figure 2.3. Chloride breakthrough curves for the Kaldenkirchen soil (K) and the Merzenhausen soil (M). Symbols represent measurements and lines model predictions using the convection–dispersion equation.

The higher spreading in soil K, expressed by a larger dispersivity, causes a lower peak concentration for chloride than in soil M. The estimated transport parameters are listed in Table 2.3. In both soils the physical equilibrium CDE was able to describe the chloride BTCs and therefore, we assumed that chloride transport was not affected by non-equilibrium water flow processes.

Table 2.3: Transport parameters for the conservative tracer chloride.

	v [cm h^{-1}]	D [cm^2 h^{-1}]	R^2	q [cm h^{-1}]	θ [cm^3 cm^{-3}]	λ [cm]	ρ [g cm^{-3}]
K	0.64 (± 0.02)[a]	0.24 (± 0.04)	0.97	0.26	0.41	0.38	1.31
M	0.49 (± 0.00)	0.030 (± 0.00)	0.99	0.24	0.49	0.063	1.34

v is pore-water velocity, D is dispersion coefficient, the R^2-value is a measure of the relative magnitude of the total sum of squares associated with the fitted equation, q is the experimentally determined Darcian flux density, θ is water content, λ is dispersivity and ρ is the bulk density.
[a] values between brackets indicate 95% confidence interval.

Figure 2.4 shows the BTCs for ^{14}C, SDZ, 4-(2-iminopyrimidin-1(2H)-yl)aniline and 4-hydroxy-SDZ in both soils and additionally for an unknown product which was not identified in soil M. 4-(2-iminopyrimidin-1(2H)-yl)aniline was found as a photo-degradation product of SDZ by Boreen et al. (2005).

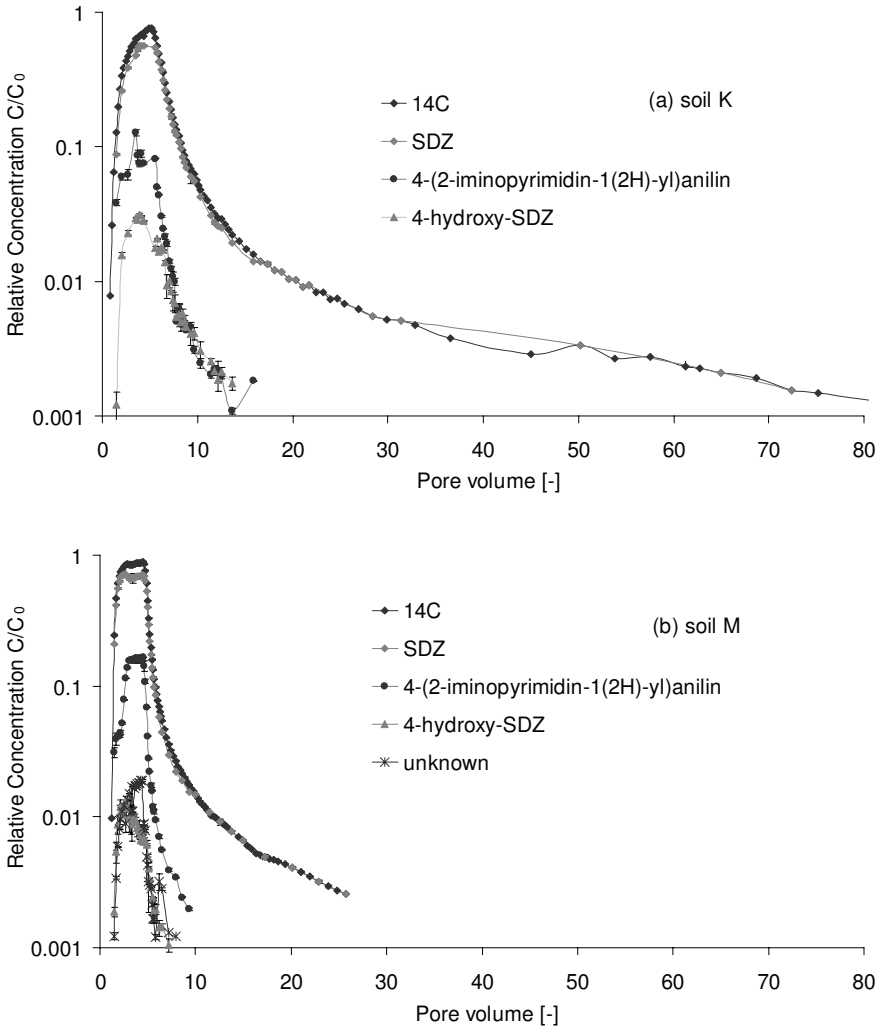

Figure 2.4. Semi-log plots of the measured BTCs of SDZ and its transformation products in (a) the Kaldenkirchen soil (K) and (b) the Merzenhausen soil (M). Time is expressed as pore volume. Bars indicate the root mean square deviation.

In additional experiments we observed an increase of this product after exposure of SDZ-solutions to light (data not shown). The outflow samples were exposed to light in the fraction collector (normal light conditions in the laboratory) and we assume that the transformation had occurred at least partly in the tubes and not in the soils. Therefore this product was added to SDZ for the modeling process. The highest ^{14}C-concentrations in the BTCs amounted to 76% of the applied ^{14}C-concentration for soil K and 88% for soil M. The contribution of transformation products to the total concentration was low for both soils, with on average 4.8% in soil K and 2.9% in soil M, after adding 4-(2-iminopyrimidin-1(2H)-yl) to SDZ (Table 2.4).

Table 2.4: Mass recoveries and the mean distribution of SDZ and the transformation products in the outflow samples of the two soils

	^{14}C eluted [%]	^{14}C in profile [%]	^{14}C total [%]	SDZ [%]	4-(2-iminopyrimidin-1(2H)-yl)aniline [%]	4-hydroxy-SDZ [%]	Unknown [%]
K	84.9	11.6	96.5	86.2	9.0	4.8	-
M	91.4	7.8	99.2	84.1	13.0	1.2	1.7

^{14}C-totals are the mass balances for the two experiments. The percentages for sulfadiazine and the transformation products represent the average parts in the outflow samples. If measured value below the set detection limit of 1.2 Bq they were set to zero.

With this we found a remarkable lower part of transformation products as Wehrhan et al. (2006) who detected 43% of the total radioactivity in the transformation products in a soil column study with a corresponding experimental setup but with a different soil type.
The ^{14}C-peak is pointed in soil K, whereas it reached a semi-plateau after a strong increase of concentration in soil M. This might point at different sorption kinetics. After the peak maxima the decrease of concentration is faster in soil M. Nevertheless, the ^{14}C-BTCs in both soils are characterized by an extended tailing. The BTCs of our study have similar shapes as the corresponding curve (column B) of Wehrhan et al. (2007), which was run under the same boundary conditions but with a different soil type. With total mass balances of almost 100%, the eluted amount of ^{14}C is lower in soil K (85%) than in soil M (91%). Speciation could be a possible reason for this. The distribution of species in the two soils was calculated according to Schwarzenbach et al. (2003). For soil K, 80.3% consisted of the neutral species and 19.2% of the anionic species. For soil M the amount of the less sorbing anionic species was higher with 35.5%. Although the difference between the measured pH-values in the soils after the experiments was not high (Table 2.1), the

distribution of species is different since both pH-values are close to pK_{a2} where small changes in the pH-value lead to high changes in the distribution of the species. For other sulfonamides, Kurwadkar et al. (2007) observed a decreased sorption capacity with increasing pH due to the repulsive forces with the predominantly negatively charged soil particles. The percentage of organic carbon which has also a great influence on the sorption behavior of sulfonamides (Thiele-Bruhn et al., 2004) is higher in soil M. Also the CEC is higher in soil M but due to the high pH-values the part of the cationic species is negligible.

The shape of the measured concentration profiles looked different (Figure 2.5). Although most of the ^{14}C mass was found in the uppermost layers of both soils, the ^{14}C-profile was more curved in soil M, with higher concentrations in the surface layer and

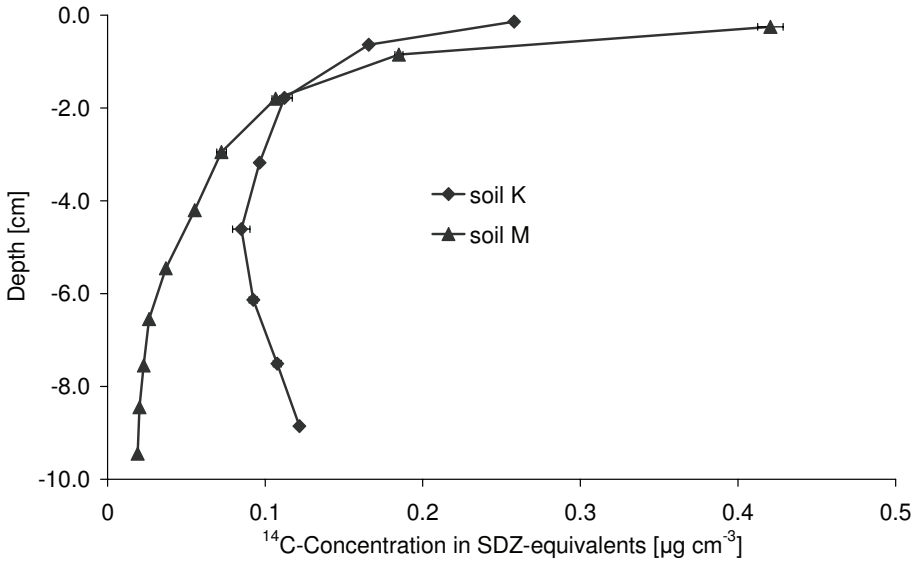

Figure 2.5. ^{14}C distributions in the soil column profiles of the Kaldenkirchen soil (K) and the Merzenhausen soil (M). Bars indicate the root mean square deviation.

lower concentrations in the bottom layer. The profile of soil K was additionally characterized by an increased ^{14}C-concentration below a depth of 6 cm. This increase may result from an accidental compression of the soil during the cutting procedure when the soil was too wet. Various authors have observed incomplete breakthrough of sulfonamides (Boxall et al., 2002; Drillia et al., 2005; Kay et al., 2004; Kay et al., 2005a). Kreuzig & Höltge (2005) detected 64% of the applied amount of ^{14}C-SDZ in the first 5 cm of a

lysimeter, with decreasing amounts down to greater depths. Similar ^{14}C-SDZ distributions in soil columns were reported by Wehrhan et al. (2007), who found most of the applied ^{14}C-SDZ in the first three centimeters of soil columns, except for a short application duration with a high input concentration. Similar patterns of concentration profiles were for example found and successfully modeled for the transport of colloids (Bradford et al., 2002) or the endocrine disruptor testosterone (Fan et al., 2007). According to these studies such concentration profiles can be explained by depth-dependent processes like blocking, filtration or straining or a high transformation into a daughter product with different sorption properties as the parent compound. For a solute like SDZ we do not have any indication for depth-dependent filtration processes and a fast transformation into a daughter product seemed also not likely, since the detected transformation products in the outflow of the soil columns show a high mobility in soil columns (unpublished data) and in literature we found no evidence of a strong sorbing transformation product which is immediately developed after contact to soil.

Figures 2.6 und 2.7 show the modeling results for ^{14}C-BTCs and -distributions for both modeling approaches of irreversible sorption. The fitted parameters of the various models are listed in Table 2.5. First, we fitted the model on the BTC data only, describing irreversible sorption with a first order process. These models (K/M 1- 1st order only BTC) described the ^{14}C-BTCs quite well in both soils, although we observed a systematical underestimation of the measured concentrations at the beginning of the descending branch of the BTC and at longer times in the tailing, and an overestimation in between. For soil K, the leached concentrations were notably underestimated after 600 h, which corresponds to about 50 pore volumes. Notice that the duration of the leaching experiment was 1200 hours for soil K compared to 500 hours for soil M. One reason for this notable underestimation may be that we measured fewer samples at the end of the leaching experiment and so the weighting of this part was lower. The kinetic sorption rate coefficient, α, was three times higher in soil M, which means that sorption approaches equilibrium faster in soil M than in soil K. The Freundlich coefficient, K_f, was lower in soil M, which indicates a lower sorption potential. Due to the larger clay content in soil M we expected a larger specific surface area of the mineral constituents in this soil together with a higher sorption. Also the CEC and the concentration of total organic matter are higher in soil M. One explanation for the lower observed sorption may be again the higher amount of the less sorbing anionic SDZ-species in soil M caused by the higher pH in this soil. The irreversible rate coefficient

,β, was larger for soil K than for soil M, which was also reflected in the lower mass of ^{14}C, detected in the leachate for soil K. For parameter *f* we obtained a value very close to zero in previous model steps which indicated that equilibrium sorption was negligible. Therefore this parameter was fixed to zero for all model scenarios which means that our model concept was reduced to a two-site model with one reversible (kinetic) and one irreversible site. Also the parameter *k* was fixed for all models, since the irreversible rate coefficient, β, and *k* appeared to be highly correlated.

In a second step we fitted the models simultaneously on the ^{14}C-BTCs and ^{14}C-concentration profiles, still calculating irreversible sorption with a first order process. Figure 2.7 illustrates that the shape of the measured concentration profiles cannot be described with this model concept since it is not flexible enough to describe the concentration profiles properly. Constraining the parameters on both the BTCs and the concentration profile causes a shift in the predicted concentration profiles, but without affecting their shape and the shape of the BTC. The value for Φ is minimized by changing the rate coefficient for irreversible sorption, which results in slightly different eluted amounts of SDZ from the soil column.

In a third step we fitted the models on the ^{14}C-BTCs and ^{14}C-concentration profiles assuming higher order sorption processes and exponential relations for irreversible sorption. For model approach 1, we increased the order of sorption from 1 to 5. For soil K the lowest value for the objective function Φ was obtained for 2nd order irreversible sorption, therefore only this curve is shown. Figure 2.6 illustrates that the increase of the order had no major effect on the prediction of the ^{14}C-BTCs, whereas the curvature of the concentration profiles increased with increasing order (Figure 2.7). The same effect can be observed if factor *k* is increased in the exponential model approach 2. For soil K the lowest value of Φ_{total} was observed with model approach 2 and a factor of 9, indicating that this model fits the data best. But this model was still not able to reproduce the measured shape correctly. With higher factors the goodness of fit could not be improved. In general changes in the objective function Φ of the different models were mainly governed by changes in $\Phi_{profile}$. The eluted amounts of ^{14}C for soil K (between 81 and 88%) are predicted well compared to the measured 85%.

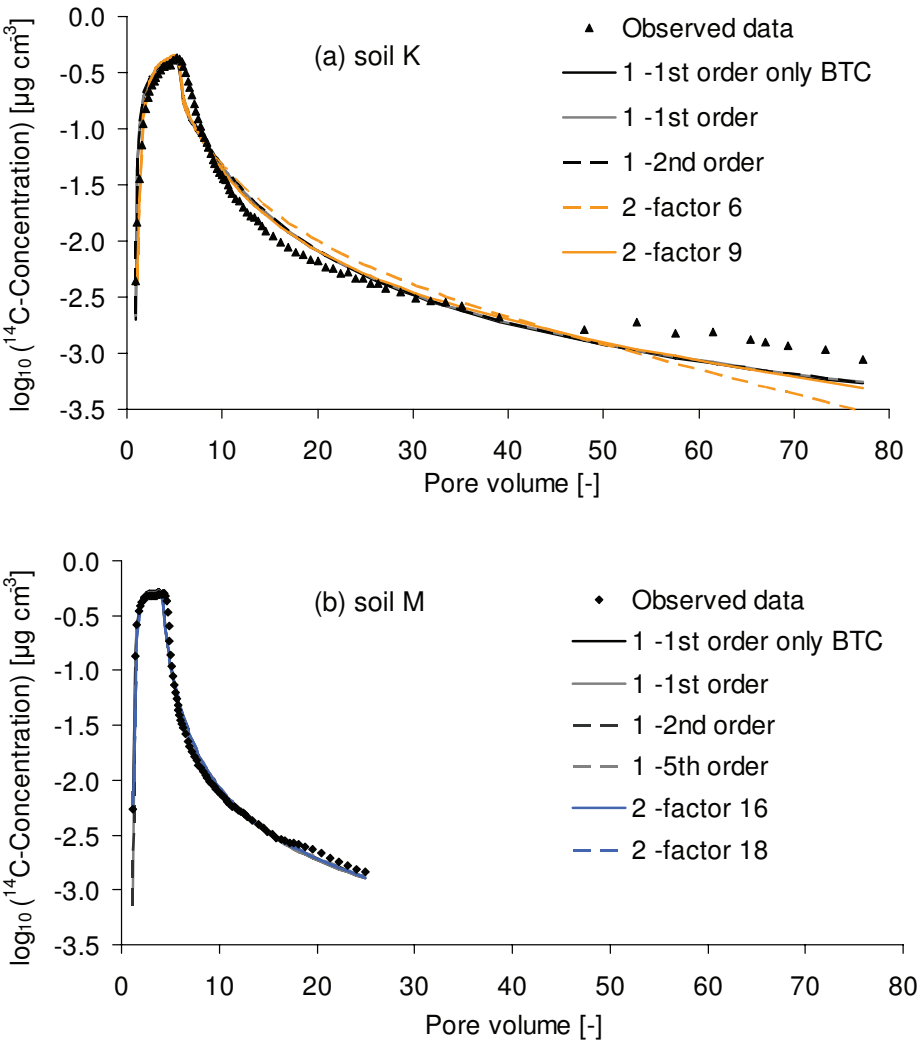

Figure 2.6. ^{14}C-breakthrough curves of (a) the Kaldenkirchen soil (K) and (b) the Merzenhausen soil (M) with the fitted two-site two rates (2S2R) Freundlich models.

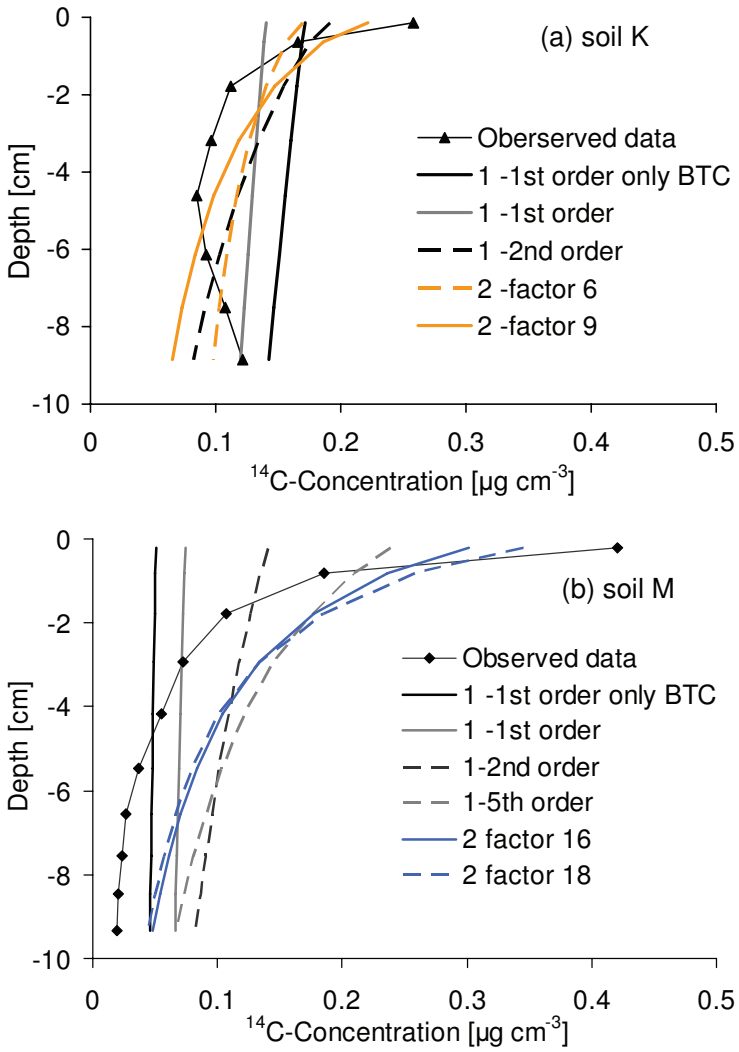

Figure 2.7. ^{14}C-concentration profile in the soil columns of (a) the Kaldenkirchen soil (K) and (b) the Merzenhausen soil (M) with the fitted two-site two rates (2S2R) Freundlich models.

Table 2.5: Fitting parameters for the Freundlich sorption models for ^{14}C-BTCs

	α [h^{-1}]	K_f [$\mu g^{1-m} cm^{3m} kg^{-1}$]	m	β [$cm^{3(k-1)} mg^{1-k} h^{-1}$][a] /[$\mu g\ cm^{-3}\ h^{-1}$][b]	k [-][a]/ [$cm^3 \mu g^{-1}$][b]	Φ_{total}	Φ_{BTC}	$\Phi_{profile}$	R^2	Eluted [%]
K - 1 –1st order only BTC	4.40 x 10^{-2} (±4.98 x 10^{-3})[d]	3.20 x 10^{-1} (±3.62 x 10^{-2})	3.08 x 10^{-1} (±4.44 x 10^{-2})	1.09 x 10^{-2} (±7.07 x 10^{-3})	1[c]	2.29	2.29	-	0.98	81.4
K ^{14}C- 1 –1st order	4.42 x 10^{-2} (±7.21 x 10^{-3})	3.19 x 10^{-1} (±4.54 x 10^{-2})	3.06 x 10^{-1} (±6.63 x 10^{-2})	8.93 x 10^{-3} (±9.96 x 10^{-4})	1[c]	5.15	2.31	2.84	0.98	83.9
K ^{14}C- 1 –2nd order	4.73 x 10^{-2} (±6.42 x 10^{-3})	3.04 x 10^{-1} (±3.60 x 10^{-2})	3.08 x 10^{-1} (±5.24 x 10^{-2})	2.27 x 10^{-2} (±2.29 x 10^{-3})	2[c]	3.83	2.29	1.54	0.99	84.7
K ^{14}C- 2 – factor 6	4.23 x 10^{-2} (±7.25 x 10^{-3})	3.88 x 10^{-1} (±2.85 x 10^{-2})	2.01 x 10^{-1} (±2.25 x 10^{-2})	1.41 x 10^{-4} (±1.49 x 10^{-5})	6[c]	4.80	3.15	1.65	0.98	87.6
K ^{14}C- 2 – factor 9	5.57 x 10^{-2} (±5.81 x 10^{-3})	3.21 x 10^{-1} (±2.42 x 10^{-2})	2.11 x 10^{-1} (±1.04 x 10^{-2})	5.05 x 10^{-5} (±4.52 x 10^{-6})	9[c]	2.89	1.73	1.15	0.99	82.0
M ^{14}C- 1 –1st order BTC only	1.48 x 10^{-1} (±3.31 x 10^{-2})	1.69 x 10^{-1} (±1.09 x 10^{-2})	2.22 x 10^{-1} (±4.00 x 10^{-2})	2.09 x 10^{-3} (±3.53 x 10^{-4})	1[c]	1.29	1.29	-	0.99	91.9
M ^{14}C- 1 –1st order	1.48 x 10^{-1} [c]	1.69 x 10^{-1} [c]	2.22 x 10^{-1} [c]	3.91 x 10^{-3} (±2.23 x 10^{-5})	1[c]	41.94	1.23	40.72	0.89	88.3
M ^{14}C- 1 –2nd order	1.48 x 10^{-1} [c]	1.69 x 10^{-1} [c]	2.22 x 10^{-1} [c]	1.34 x 10^{-2} (±6.18 x 10^{-4})	2[c]	32.29	1.49	30.80	0.91	84.6
M ^{14}C- 1 –5th order	1.48 x 10^{-1} [c]	1.69 x 10^{-1} [c]	2.22 x 10^{-1} [c]	1.29 x 10^{-1} (±1.80 x 10^{-2})	5[c]	19.70	1.21	18.49	0.95	82.8
M ^{14}C- 2 – factor 14				1.11 x 10^{-6} (±8.28 x 10^{-8})	16[c]	11.11	1.05	10.1	0.97	81.8
M ^{14}C- 2 – factor 18				4.35 x 10^{-7} (±2.11 x 10^{-8})	18[c]	9.45	1.22	8.24	0.98	81.0
Parameters of Wehrhan et al. 2007	2.76 x 10^{-2} [c]	6.08 x 10^{-1} [c]	4.54 x 10^{-1} [c]	2.53 x 10^{-2} [c]	1[c]					59.0

[a] unit for model approach one; [b] unit for model approach two; [c] value was fixed, [d] value between brackets indicate 95% confidence interval.

For soil M Φ_{total} decreased with increasing order of the irreversible sorption rate in approach 1 and with increasing factor in approach 2. These changes were also mainly governed by changes in $\Phi_{profile}$. Model approach 2 with a factor of 18 described the ^{14}C-profile best. In soil M the eluted amounts of ^{14}C are predicted well with the first-order rate models, whereas they are underestimated with all the other models. These differences in eluted masses are visible in the peak concentrations in non-logarithmic plots (not shown). Irrespective of the model concept used to calculate irreversible sorption, for soil K the optimized values for the parameters α, K_f and m are in the same range as for the model which was fitted to ^{14}C-BTC data only. In previous model steps we observed the same for soil M, but the confidence intervals for all fitted parameters were large, due to the great contribution of the concentration profile to the objective function, i.e. a poor fit. Therefore we used the optimized parameters α, K_f and m from the model which was fit to the ^{14}C-BTC data only and fixed them in all further simulations for soil M which included measurements of the ^{14}C-concentration profile in the objective function. The models which were fit to the ^{14}C-BTCs only are supposed to obtain the best fits for the ^{14}C-BTCs for both soils since the profile is not considered in the objective function. Nevertheless we obtained lower values for the objective function of the BTC (Φ_{BTC}) with some models which include the measurements of the ^{14}C-concentration profiles (K ^{14}C 2 -factor 9; M ^{14}C 1 -1st order, M ^{14}C 1 -5th order, M ^{14}C 2 -factor 14 and 18). The reason for this is that the model output contained infinite values after $\log_{10}$-transformation for some data points and these data points were excluded from the calculation of the objective function Φ.

Figure 2.8 shows model predictions for the ^{14}C-BTC of soil K using the fitted parameters of soil M (M 1- 1st order only BTC) and soil column B of Wehrhan et al. (2007), who obtained higher values for K_f and m (Table 2.5). Although the transport parameters of the three soils were quite different, the rise of the BTC was predicted quite well, irrespective of the differences in parameter values that describe the sorption capacity, i.e. the Freundlich sorption isotherm. Peak arrival times seem to be more affected by sorption kinetics than sorption capacity. The irreversible rate coefficient determines the amount of mass that can be transported through the column in a certain time, with lower amounts of leached mass for the higher rate coefficients. The peak maximum is largely affected by the reversible sorption rate coefficient, α, with the larger value for the higher peak value.

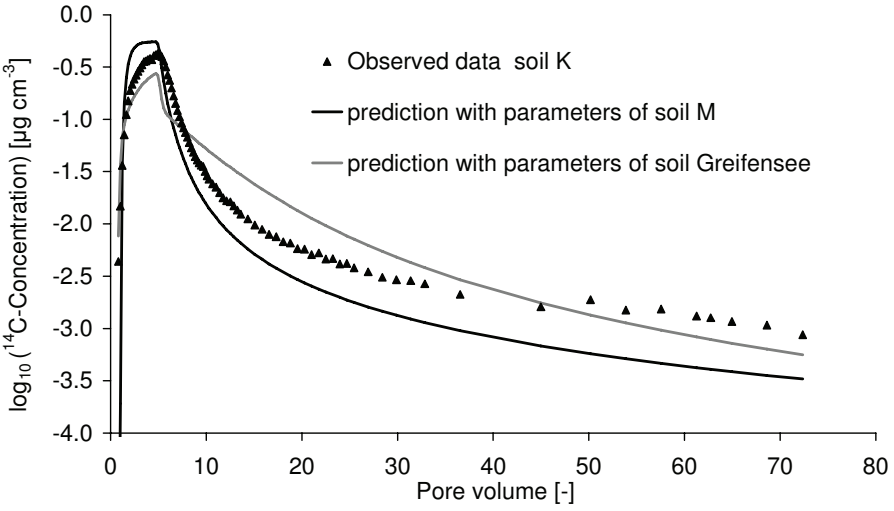

Figure 2.8. Measured ^{14}C-breakthrough curve of the Kaldenkirchen soil (K) and model predictions with fitted parameter sets of the Merzenhausen soil (M) and the Greifensee soil used by Wehrhan et al. (2007).

Up to now we used the ^{14}C data to determine the transport parameters. Since we measured the SDZ-BTCs explicitly, we followed an approach to fit the transport parameters to the measured SDZ-BTCs, by interpreting the effective first-order rate coefficient as being comprised of irreversible sorption and transformation. However, since only 4.8% (soil K) and 2.9% (soil M) of the applied SDZ was found as 4-hydroxy-SDZ in soil K and as 4-hydroxy-SDZ and an unknown transformation product in soil M, simulations concerning the estimation of transport parameters for SDZ itself proved to be not meaningful. The model concepts seem not sensitive enough to deal with such minor concentration changes in the BTCs of ^{14}C and sulfadiazine.

2.5 Conclusions

The transport and transformation of SDZ were studied in laboratory soil column experiments. An analytical method for the detection of SDZ and its transformation products 4-hydroxy-SDZ and 4-(2-iminopyrimidin-1(2H)-yl)aniline was developed with a detection limit of 0.5 µg L−1.

With this the experiments revealed first insights in the transformation of SDZ during the transport in soil columns. Aside from a low amount of 4-hydroxy-SDZ, 4-(2-iminopyrimidin-1(2H)-yl)aniline, known as a photo-degradation product of SDZ, was

detected in the outflow of the soil columns. Future experiments are necessary to asses whether this transformation is a possible degradation process which reduces the persistence of SDZ in soils. Under the given experimental conditions SDZ showed a high leaching potential but also a tendency to accumulate in the uppermost layers of the soil columns, probably due to the formation of irreversibly bound residues. A comparison of the model parameters confirmed a higher leaching potential for the silty loam than for the loamy sand and showed that the description of the concentration profiles in the soil columns is mainly governed by the rate coefficient for irreversible sorption. The estimation of the ^{14}C-concentration profiles in the soil columns could be improved using two empirical approaches to account for irreversible sorption, but the concentration profiles can still not be predicted correctly. The sorption process which leads to irreversible sorption of SDZ is still not well understood and requires further investigations.

3 Transport of sulfadiazine in undisturbed soil columns: the effect of flow rate and applied mass[2]

3.1 Objectives

The objective of chapter 3 was to investigate SDZ transport in dependence of flow rate and applied input concentration/mass using five undisturbed soil columns of the loamy sand. Measured BTCs and concentration profiles of different experiments were modeled with common parameter sets using an attachment/detachment based model approach.

3.2 Introduction

Introduction of antibiotic substances in the environment has become a serious concern in the last decade. Through application of manure or sewage sludge on agricultural fields these antibiotics are introduced in soils (Jørgensen and Halling-Sørensen, 2000) where they may affect microbial processes and community structures (Hammesfahr et al., 2008, Kotzerke et al., 2008) or may be leached to the groundwater (Sacher et al., 2001; Hamscher et al., 2005; Focazio et al., 2008).

Our target substance SDZ belongs to the chemical class of sulfonamides which was frequently detected throughout various environmental compartments and recently classified as relevant to the environment in Germany (Bergmann et al., 2008). The understanding of sorption and transport mechanisms is important to assess the spreading of SDZ in the environment, especially its leaching potential from soils into groundwater. Compared to antibiotics from other chemical classes, SDZ has a lower sorption coefficient, indicating good water solubility and a higher mobility (Thiele-Bruhn et al., 2004). Experimental SDZ sorption data could be best described as a nonlinear (Thiele-Bruhn et al., 2004) non-equilibrium process with sorption coefficients increasing with time (Förster et al., 2009, Wehrhan et al., 2009). This non-equilibrium or kinetic process may be explained by diffusion processes into the intra-particle pore systems or organic matter and was also

[2]adapted from: Unold, M., R. Kasteel, J. Groeneweg and H. Vereecken (2009). Transport of sulfadiazine in undisturbed soil columns: the effect of flow rate and applied mass. Submitted to Journal of Environmental quality.

found for pesticides like atrazine (Park et al., 2004). Sorption hysteresis was also reported (Sukul et al., 2008a, Wehrhan et al., 2009). While this could be partly explained with a kinetic process having slow desorption, also irreversible sorption of SDZ via covalent bonding to organic substances was found (Bialk et al., 2008). In transport experiments, sorption hysteresis became visible in incomplete breakthroughs where parts of the substance were retained in the uppermost soil layers (Kreuzig et al., 2005; Unold et al., 2009a,b; Wehrhan et al., 2007). Measured breakthrough curves (BTCs) showed extended tailings which can be explained by slow kinetic processes or non-linear sorption behavior. Furthermore, the pH value (Kahle and Stamm, 2007a; Kurwadkar et al., 2007) as well as the amount and composition of organic material (Kahle and Stamm, 2007b; Thiele-Bruhn et al., 2004) affected sorption of SDZ.

Several studies indicated that transformation of sulfonamides in soils occurs. This was shown for acetylation (Burkhardt & Stamm 2007; Wehrhan, 2006) or hydroxylation processes (Unold et al., 2009a,b; Wehrhan 2006). The hydroxylated form of SDZ, 4-OH-SDZ (N^1-2-(4-hydroxypyrimidinyl)benzenesulfanilamide), was also determined as one of the main metabolites of SDZ in pig manure (Lamshöft et al., 2007). 4-OH-SDZ was found to be still microbial active (Nouws 1989) which means that its fate has to be considered, too. An-SDZ (4-[2-iminopyrimidine-1(2H)-yl]-aniline) was identified as a photo degradation product of SDZ (Sukul et al., 2008b), but it was also detected in transport experiments with soil performed in the dark (Unold et al., 2009b). To our knowledge, potential adverse effects of the An-SDZ are unknown.

SDZ concentrations in manure and the amounts of manure applied to fields vary which results in different masses of SDZ reaching the field. Also the flow rate in the field is not constant due to rainfall events and evaporation which results in different pore-water velocities. Effects of concentration and total applied mass on SDZ transport were revealed in transport experiments in a silty loam conducted by Wehrhan et al. (2007). They found that when the same mass of SDZ was applied by varying input concentration and pulse duration, remarkably more mass was eluted in the experiment with the lower input concentration. But when SDZ solutions with different concentrations were applied for the same time, more mass eluted in the experiment with the higher input concentration. In general, less retardation can be expected in higher concentration ranges for non-linear sorbing solutes with adsorption isotherms that exhibit a convex shape with respect to the solute concentration, like SDZ. The concentration of non-linear sorbing substances

determines also the time which is needed to reach equilibrium. Braida et al. (2001) showed that for PAHs sorption equilibrium was reached faster at higher concentrations.

Discussions in the literature on the effect of flow rate on sorption are ambiguous. While some researchers observed changes in reaction rates with pore water velocity (Brusseau, 1992; Kim et al., 2006) others did not (Deng et al., 2008). Due to the pronounced differences in experimental results the hypothesis was developed that the relationship between adsorption rate and pore water velocity is not simply determined by the contact time between the solute and the soil surface (Zhang and Lv, 2009). Based on pore scale simulations, Zhang and Lv (2009) and Zhang et al. (2008) proposed that different reaction rates with pore water velocity are caused by heterogeneous sorption on the microscopic scale.

Numerical analysis of experimental data allows the quantification and partly the identification of governing transport processes. Parameter estimates obtained from a fit to data can be used for the prediction of substance behavior. So far, attempts to mathematically describe SDZ transport in soil columns have been very difficult due to the complexity of the sorption processes. Besides irreversible sorption, reversible kinetic sorption has to be considered. Wehrhan et al. (2007) could describe BTCs of SDZ best with an attachment/detachment model which included two reversible kinetic sorption sites and one kinetic irreversible sorption site. Unold et al. (2009a,b) used a fully kinetic model with one reversible kinetic sorption site and one irreversible sorption site. Sorption on the reversible sites was described by the Freundlich sorption isotherm. The study of Wehrhan et al. (2007) revealed that, although one model concept was able to fit all BTCs, the estimated parameters differed for BTCs made with different boundary conditions i.e., input concentration and pulse duration.

The aims of the study were i) to investigate the effect of different input concentrations and flow velocities on SDZ transport and ii) to investigate differences and similarities in fitted parameter sets by simultaneously fitting BTCs obtained under different experimental conditions. Measured ^{14}C-breakthrough curves and concentration profiles were modeled using two model concepts based on the convective-dispersive transport model. The first model described the sorption process with a two-site model with one reversible kinetic (described by Freundlich sorption) and one irreversible kinetic sorption site. This model was also used for describing the transformation of SDZ into 4-OH-SDZ and An-SDZ. The second model was based on the attachment/detachment approach using

two reversible kinetic and one irreversible sorption site. Using this approach, model parameters were fitted simultaneously to selected experiments in order to test if a common set of parameters can be found.

3.3 Material & Methods

3.3.1 Soil

Transport experiments on undisturbed soil columns were performed in order to study the effect of concentration and flow rate on the transport of SDZ. The soil, taken from the plow layer of an agricultural field near Kaldenkirchen (Germany), was classified as loamy sand (FAO) with mass fractions of 4.9% clay, 26.7% silt and 68.5% sand, a pH value of 6 (0.01 M $CaCl_2$), a mass fraction of organic carbon of 1.07% and a cationic exchange capacity of 7.8 $cmol_c kg^{-1}$ (Förster et al., 2008, Unold et al., 2009b).

Transport experiments were carried out on five PVC columns containing undisturbed soil material. The experimental conditions are presented in Table 3.1. In the subsequent, we will refer to the experiments and soil columns by using its respective capital letter. The soil columns had an inner diameter of 8.5 cm and a height of 10 cm and were taken from the upper 30 cm of the field according to Unold et al. (2009b). To facilitate undisturbed sampling, a metal adapter was mounted at the front end of the column. The undisturbed soil columns were fixed on a porous glass plate, having a high conductivity and an air-entry value higher than 100 mbar.

Table 3.1: Experimental conditions for the different soil column experiments

Exp.	Flow rate [cm h^{-1}]	C_{input} SDZ [mg L^{-1}]	SDZ-Pulse duration [h]	Irrigation	ρ[a] [g cm^{-3}]	Applied suction [mbar]	M_0[b] [µg cm^{-2}]
A	0.220	0.57	68	Constant	1.58	-4.1	8.38
B	0.197	0.57	68	Constant	1.39	-10.3	8.13
C	0.210	5.7	6.8	Constant	1.36	-9.2	8.52
D	0.051	0.57	68	Constant	1.42	-17.7	1.81
E	0.047	0.57	306	Intermittent	1.39	-23.2	8.15

[a] ρ = bulk density.
[b] M_0 = Total mass of SDZ applied to 1cm² of the soil column.

3.3 Materials & Methods

Prior to the leaching experiments, the soil columns were slowly saturated from the bottom with a 0.01 M $CaCl_2$ solution for approximately 2 days. To avoid splashing of the soil material during the irrigation process, a thin layer of coarse quartz sand was placed on the top of the columns. Soil columns A, B and C were irrigated with a constant flow rate of approximately 0.2 cm h^{-1}; soil columns D and E with a lower flow rate of approximately 0.049 cm h^{-1}. For soil column E the amount of irrigated water per hour was applied at a higher flow rate during 5 minutes, followed by 55 minutes without irrigation.

All soil column experiments were run with a software-controlled experimental setup that was described in more detail by Unold et al. (2009b). Irrigation with the 0.01 M $CaCl_2$ background solution started a few days prior to the leaching experiments in order to establish steady-state water flow conditions in the soil columns. Applied suctions were in a range from -4.1 to -23.2 mbar. They were chosen separately for each soil column to establish a constant pressure head in the soil columns for the given flow rates. This meant that water was only driven by gravity. An electrical conductivity sensor integrated in the experimental setup allowed the on-line measurement of BTCs with the conservative salt tracer $CaCl_2$. These BTCs were used to characterize physical transport mechanisms in the soil columns. Electrical conductivity was related to chloride concentrations by determining a calibration curve with samples of known chloride concentrations. Chloride was applied as a 0.05 M $CaCl_2$-solution in a pulse with one hour duration.

For measuring the BTCs of SDZ the background solution was replaced with the respective SDZ-application solution for the time of the pulse duration (Table 2.1). The outflow of the soil columns was collected in test tubes of a fraction collector. Measured concentrations in the outflow samples were corrected for evaporation losses, which were approximately 2.19 x 10^{-6} L h^{-1}. The transport experiments were performed in the dark in order to prevent photo-degradation. Only during sample collection and preparation, a short exposure of the effluent samples to artificial light occurred. The samples were then stored in the fridge at 5°C until measurements were conducted. After the leaching experiments, the soil columns were cut into slices of 0.5 or 1 cm thickness, in order to detect the ^{14}C-concentrations in the soil column profile.

3.3.2 Analytics of sulfadiazine and transformation products

The application solutions for the different experiments were prepared by adding the adequate amounts of ^{14}C-SDZ (solved in a 0.01 M $CaCl_2$ stock solution) to a 0.01 M $CaCl_2$ solution. ^{14}C-SDZ (IUPAC: 4-amino-N-pyrimidin-2-yl-benzenesulfonamide) was provided by Bayer HealthCare AG (Wuppertal, Germany) as a powder with a purity of 99% and a specific radioactivity of 8.88 MBq mg^{-1}. The pH value of the application solutions was buffered to the pH value of the $CaCl_2$ background solution (pH~5.6) in order to avoid a change of the SDZ-speciation at the beginning and end of the application time.

The total amount of radioactivity in the outflow samples was measured in triplicates with liquid scintillation counting (LSC) for a counting time of 15 minutes. Therefore aliquots of 0.5 mL of each liquid sample were mixed with 10 mL scintillation cocktail (Insta-Gel Plus, Canberra Packard GmbH, Dreieich, Germany). The detection limit of the LSC measurements was 0.4 Bq corresponding to 0.045 ng mass equivalents of SDZ. Samples were corrected for background radiation by an additional measurement of a blank.

For experiment C the concentrations of SDZ and its transformation products in the outflow samples were determined using Radio-HPLC separation. The HPLC-system contained a reversed-phase column (Phenomenex Synergi Fusion RP 80, 250 mm x 4.6 mm) which was eluted with a mixture of water (490 mL) and methanol (10 mL), buffered with 0.5 mL of a 25% phosphoric acid solution. The injection volume was 0.25 mL for each sample. A gradient with an increased amount of methanol was used for peak separation, starting with 100% water for 6 minutes. The methanol fraction increased linearly to 27% till minute 23, then to 37% in the next three minutes and to 47% in the following two minutes. The methanol part reached its maximum with 57% after 30 minutes (Unold et al. 2009b).

Three peaks were distinguished in the drainage water of experiment C. According to their known retention times from standards and previous studies, we identified them as SDZ, 4-OH-SDZ and An-SDZ. Using the HPLC-detector (LB 509 detector, Berthold Technologies, Bad Wildbad, Germany) the detection limit for SDZ and its transformation products was about 3 µg L^{-1} mass equivalents of SDZ. We applied the same measurement technique as in previous studies (Unold et al., 2009a,b) in order to detect SDZ and the transformation products also in samples at lower concentrations. There, the outflow of the HPLC-column was collected according to the retention times of SDZ and the transformation products, and also in-between these time frames for determining background

signals. Subsequently, the radioactivity in the collected samples was measured with LSC as described above. A correction was performed to calculate concentration C_i of compound *i* according to the total measured ^{14}C-concentration ($^{14}C_{total}$) in an aliquot of the respective sample:

$$C_i = \frac{(RA_{i\,uncorrected} - RA_{background})}{\Sigma RA_{j\,corrected}} \; {}^{14}C_{total} \tag{3.1}$$

where $RA_{i,uncorrected}$ is the radioactivity in the respective peak before subtracting the background radioactivity $RA_{background}$ and $RA_{jcorrected}$ is the background corrected radioactivity of compound j in the respective sample. SDZ and its transformation products were quantified, when the measured radioactivity was higher than 1.2 Bq, which was three times the detection limit of the LSC. Otherwise the contribution was set to zero. With this method, the transformation products could be quantified with the help of the specific radioactivity of ^{14}C down to a concentration of 0.5 µg L^{-1} mass equivalents of SDZ. ^{14}C-concentrations in the soil slices of 0.5 or 1 cm thickness were quantified via combustion of the soil in an oxidizer (Robox 192, Zinsser Analytik GmbH, Frankfurt, Germany) and subsequent measurements with LSC. For each slice three replicates of 0.5 g oven-dried (105°C), grounded and homogenized soil were combusted. With the help of blanks before and after the samples, cross contamination was avoided. The efficiency of the combustion process (> 95%) was controlled by combusting samples spiked with a known amount of ^{14}C-Anilazine prior and after the samples of the different experiments. With the presented method ^{14}C concentrations could be measured without applying extraction methods.

3.3.3 Theory of solute transport

The transport experiments with the unsaturated and undisturbed soil columns were analyzed as one-dimensional transport problems for which uniform and constant water contents and fluxes were assumed in time and space. Solute transport is commonly described using the convection–dispersion equation (CDE). For conservative tracers, such as chloride, and for steady state flow conditions it can be written as:

$$\frac{\partial C}{\partial t} = -v\frac{\partial C}{\partial z} + D\frac{\partial^2 C}{\partial z^2} \tag{3.2}$$

where t is time [T], v is the average pore-water velocity [L T^{-1}], C is the solute concentration in the liquid phase [M L^{-3}], D is the dispersion coefficient [L^2 T^{-1}], and z is depth [L]. Using the chloride BTC, the parameters v and D were estimated with a non-linear parameter estimation procedure based on the Levenberg-Marquardt algorithm. Therefore we used the CXTFIT code (Toride et al., 1999), which analytically solves the CDE for the appropriate boundary conditions, i.e., a flux-type upper boundary condition and a zero concentration gradient at the lower boundary. The estimated transport parameters (i.e., v and D) and the experimentally determined Darcian flux density, q, were used to evaluate the volumetric water content, $\theta=q/v$, and the dispersivity, $\lambda=D/v$. With the help of these parameters the water flow in the soil columns was characterized. They were fixed for the subsequent transport simulations of SDZ and its transformation products.

SDZ transport was described using two model concepts previously applied to describe SDZ transport and implemented in Hydrus-1D version 4.03 (Šimůnek et al., 2008). The first one was an isotherm-based model with one reversible kinetic sorption site described by Freundlich sorption and one irreversible sorption site (Unold et al., 2009a). Note that instantaneous sorption was omitted from the model. For this model concept the transport equation can be written as:

$$\frac{\partial C_k}{\partial t}+\frac{\rho}{\theta}\frac{\partial S_k}{\partial t}=-v\frac{\partial C_k}{\partial z}+D\frac{\partial^2 C_k}{\partial z^2}-\mu_k C_k-\mu_k` C_k+\mu_{k-1}` C_{k-1} \quad \text{k=1,2} \tag{3.3}$$

where θ is the water content [L^3 L^{-3}], ρ is bulk density [M L^{-3}], S is the adsorbed solute concentration at the reversible kinetic sorption site [M M^{-1}] and μ [T^{-1}] is a first-order rate coefficient which is used here to mimic irreversible sorption (Baek et al., 2003). For fitting the BTCs of the two SDZ transformation products, the first-order transformation rate $\mu_k`$ [T^{-1}] which accounts for the transformation of SDZ (k=1) into 4-OH-SDZ or An-SDZ (k=2) was included in the equation. Transformation of SDZ was assumed to occur in the liquid phase only, since fixation processes on soil surfaces and within pores may protect the SDZ molecules from degradation processes (Thiele-Bruhn 2003). For fitting the ^{14}C-BTCs the terms describing transformation and formation were omitted. For the isotherm-based approach, S_k is described as:

$$\frac{\partial S_k}{\partial t}=\alpha_k(K_{f,k}\,C_k^{\,m_k}-S_k), \tag{3.4}$$

where $K_{,f,k}$ [$M_{solute}^{1-m}\ L^{3m}\ M_{soil}^{-1}$] is the Freundlich coefficient, m_k [-] is the Freundlich exponent and α_k [T^{-1}] is the sorption rate coefficient (van Genuchten and Wagenet, 1989).
Wehrhan et al. (2007) used an attachment/detachment concept, with two reversible kinetic sorption sites and one irreversible sorption site in which all processes were first-order and rate-limited. Reversible attachment/detachment processes are given by:

$$\frac{\partial S_i}{\partial t} = \frac{\theta}{\rho}\beta_i C - \gamma_i S_i \qquad i = 1,2,3 \tag{3.5}$$

where i represents the i^{th} sorption site and β_i [T^{-1}] and γ_i [T^{-1}] are the attachment and detachment rate coefficients for the corresponding sorption sites S_i. The irreversible sorbed mass (S_3) was calculated according to equation 3.5 with γ_3 fixed to zero. The sum of reversible and irreversible sorption sites represents the total amount of sorbed solute per dry mass of soil:

$$S = S_1 + S_2 + S_3 \tag{3.6}$$

To account for differences in the number of data points and in absolute values, the data of the concentration profiles were weighed with a factor, *w,* according to

$$w = \frac{n_{profile}}{n_{BTC}} \frac{\sum_{j=1}^{n_{BTC}} C_{j,BTC}}{\sum_{l=1}^{n_{profile}} C_{l,profile}} \tag{3.7}$$

where *n* is the number of data points in the respective BTCs and soil profiles, $C_{j,BTC}$ are the measured concentrations at time j for the BTC expressed in mass of SDZ per volume of solution and $C_{l,profile}$ are the measured concentrations at depth *l* in the soil profile expressed in mass of SDZ per volume of soil. The data of the BTCs had unit weight.
Simultaneous parameter estimation was performed by coupling Hydrus1D (version 4.03) with PEST (Doherty, 2002) which estimates the transport parameters using a Gauss-Levenberg-Marquardt algorithm. The optimal parameter set was obtained by minimizing the least squares objective function Φ:

$$\Phi = \sum_{i=1}^{n} (w_i r_i)^2, \qquad (3.8)$$

where n is the total number of the observed data points and model outcomes, w_i is a weighting factor for the i´th observation and r_i is the difference between the i´th model outcome and the corresponding observed value (Doherty, 2002).

Both the ^{14}C-BTCs and concentration profiles were included in the objective function. The data points of the soil column profiles were weighed according to Equation 3.7. ^{14}C-measurements in the drainage water were log-transformed since otherwise it was not possible to capture the tailings of the BTCs adequately. Consequently, we obtained less good agreement for the peak concentrations.

The development of transformation products and their transport could only be investigated in soil column C. For soil columns A and B, we observed a white clouding in the samples, possibly caused by a precipitation reaction, which made the HPLC-measurement impossible; for soil columns D and E the concentrations of SDZ and the transformation products in the outflow samples were below the detection limit. We used the isotherm-based approach to describe the transformation process of SDZ since this approach described the data of experiment C better. The model parameters were fitted to the $\log_{10}$-transformed concentrations in the drainage water. BTCs of the transformation products were modeled by fitting the transformation of SDZ into each of the products separately in two separate model runs using the procedure proposed by Unold et al. (2009b). First, the reversible sorption parameters (K_f, m, α) of SDZ were fitted where transformation into both transformation products was described by one effective transformation rate. In the next steps, these reversible sorption parameters of SDZ were fixed to the parameters fitted for the SDZ BTC, while the parameters for irreversible sorption and transformation of SDZ were fitted together with the transport parameters of the respective transformation product. Irreversible sorption of the transformation products was neglected in order to avoid parameter interactions with the transformation rate. The profile data were included in the objective function to fit the ^{14}C- and SDZ BTCs according to equation 3.7, but not in the fits for the transformation products since the amount of SDZ which degraded into the other transformation product was added to irreversible sorption of SDZ. This resulted in higher irreversible sorption rates for SDZ (Table 3.5) which would lead to an overestimation of the irreversibly sorbed amount.

3.3 Materials & Methods

After modeling the single experiments, several parameter combinations were simultaneously fitted to three or four experiments performed at a constant flow rate using the attachment/detachment approach. In a first run, all five parameters (β_1, β_2, β_3, γ_1, γ_2) were fitted concurrently to the experiments conducted with the low concentration (A, B & D). The profile data were included in the fit with the same weight as calculated for the single BTCs. Since experiments A and B were replicates, both the weights for the BTC and concentration profile data of experiment D were multiplied with a factor of two. In the second run, the same procedure was followed for the experiments performed at the higher flow rate (A, B & C). Finally, the five parameters were simultaneously fitted to all four experiments (A, B, C &D). To investigate the influence of the attachment (β_1) and detachment rate (γ_1) of one reversible sorption site on the goodness of fit, one additional model run was performed. For this purpose the attachments rates β_2 and β_3 as well as the detachment rate γ_2 were fitted to all four experiments simultaneously while β_1 was fitted separately to the four single experiments, together with one value "ratio", defined as β_1/γ_1. Using this ratio, γ_1 could be calculated for each BTC separately.

3.4 Results & Discussion

3.4.1 Chloride Breakthrough Curves

The BTCs of chloride are shown in Figure 3.1, where concentrations are transformed by dividing the measured concentrations with the applied mass of chloride per cm², M_0, to compare the BTCs of the experiments with different masses.

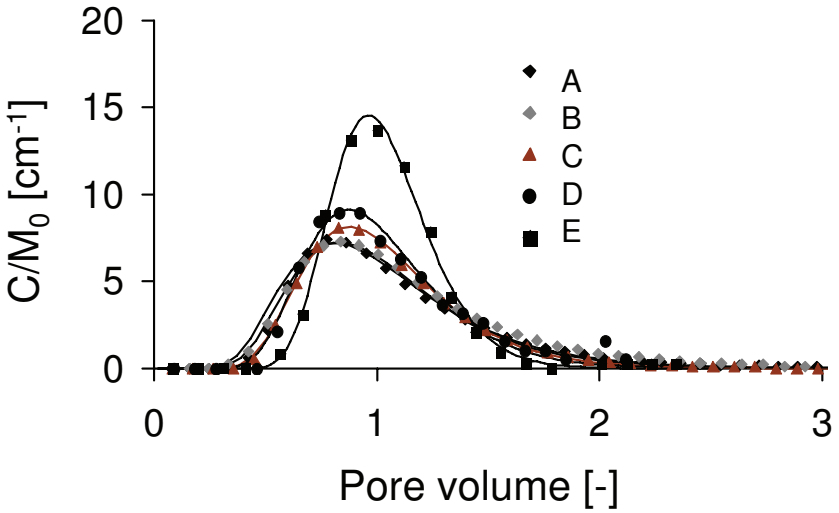

Figure 3.1. The measured breakthrough curves of chloride (symbols) fitted with the convection-dispersion equation (solid lines) for the five experiments. Time is expressed as dimensionless pore volumes, i.e., the time needed to replace all water in the soil column. Concentrations were transformed by dividing through the applied mass of chloride per m², M_0.

The parameters of the CDE fit are listed in Table 3.2. Chloride breakthrough curves were described well for all five experiments using the convection-dispersion equation. We therefore concluded that no physical non-equilibrium processes affected solute transport in the columns. Soil column E with the lowest dispersivity had the highest peak concentration which hints at a more homogeneous pore structure, followed by soil columns D and C. Note that the chloride BTC for experiment E was conducted at a constant flow rate, due to a failure in the experiment conducted with the intermittent flow rate. However, a chloride BTC, measured under transient flow conditions in the same column (data not shown) with a slightly higher flow rate did not indicate towards the presence on physical non-equilibrium-

processes and it showed also a pronounced peak. Therefore, it can be stated that the low dispersivity was not an effect of the transient flow regime. Also a previous study (Unold et al., 2009b) showed that it was not possible to generate macropore flow conditions using higher flow rates in undisturbed soil columns of the same soil.

Table 3.2: Transport parameters for the conservative tracer chloride. V is pore-water velocity, D is dispersion coefficient, R^2 is coefficient of determination, ρ is bulk density, q is flux density, λ is dispersivity, and θ is water content.

soil column	*v* [cm h^{-1}]	D [cm^2 h^{-1}]	R^2	ρ [g cm^{-3}]	q [cm h^{-1}]	λ [cm]	θ [cm^3 cm^{-3}]
A	0.65 (± 0.01)[a]	0.48 (± 0.03)	0.99	1.58	0.220	0.74	0.34
B	0.62 (± 0.005)	0.53 (± 0.02)	1.0	1.39	0.197	0.85	0.32
C	0.63 (± 0.004)	0.36 (± 0.01)	1.0	1.36	0.210	0.57	0.33
D	0.16 (± 0.01)	0.076 (± 0.01)	0.97	1.42	0.051	0.48	0.32
E	0.18 (± 0.002)	0.042 (± 0.003)	0.99	1.49	0.047	0.24	0.26

[a] values between brackets indicate 95% confidence interval.

Calculated water contents were fairly constant for the constant irrigation experiments except for experiment E where the water content was lower. This is in agreement with the lower suction applied to the bottom of the soil column compared to the other experiments. In case of experiment D the lower flow rate seemed to have a minor effect on the water content.

3.4.2 ^{14}C Breakthrough Curves

The measured BTCs and concentration profiles for ^{14}C-SDZ in the various experiments are presented in Figure 3.2. The peak concentrations in the experiments with the short SDZ pulses (C and D) were reached earlier (time expressed in pore volumes (PV)) than the peak concentrations in the experiments with the longer pulses. Even though the characterization of the physical transport was slightly different, the similarity between replicate experiments A and B showed that the BTC experiments were repeatable. Total mass recoveries (Table 3.3) were generally greater than 95% except for experiment E. The missing mass can be attributed to the experimental errors introduced by the slicing procedure of the soil material in the column. There, small variations in the thickness of the

slices can lead to errors in the mass balance. These errors are expected to be larger than errors in the measurements of liquid concentrations. Experiments with the higher and lower flow rates could be distinguished by means of their eluted mass (Table 3.3). Distinct higher eluted amounts of mass were found in the experiments with the higher flow rate, probably due to less contact time.

Table 3.3: Mass recovery of ^{14}C in the breakthrough curves and the concentration profiles, as well as transformation products in the drainage water of experiment C.

	^{14}C in breakthrough curves [%]	^{14}C in the soil Profile [%]	SDZ [%]	OH-SDZ [%]	An-SDZ [%]
A	57.4	37.6	n.d[a]	n.d	n.d
B	59.5	39.3	n.d	n.d	n.d
C	71.4	30.5	61.7	16.9	21.4
D	10.8	86.0	n.d	n.d	n.d
E	19.1	72.9	n.d	n.d	n.d

n.d[a] concentration was not determined

Also the experiments with the high and low input concentrations differed. The eluted amount was highest for experiment C (71%) which was performed at the high flow rate and with the high input concentration. For experiments A and B which were conducted at the same flow rate but with the low input concentration the eluted mass was lower (57-60%). Only 19% (D) and 11% (E) of the applied mass were eluted in the experiments with the lower flow rates. This trend of higher eluted masses with higher flow rates was supported by the results of a previous experiment made with a soil column repacked with the same soil near saturation (Unold et al., 2009a). This experiment was conducted at a slighted higher flow rate (0.25 cm h^{-1}),which resulted in a higher eluted mass (85%). Srivastava et al. (2009) conducted transport experiments with the sulfonamide sulfadimethoxine in two soils and a sand in repacked soil columns with a remarkably higher flow rate (~9.2 cm h^{-1}) than in our study and found mass recoveries in the effluent > 90%.

Except for experiment E, the BTCs were characterized by a steep increase of concentrations in the drainage water. This difference in the rise of the BTC may be attributed to the different flow regimes for SDZ (intermittent vs. constant irrigation). After the peak maxima were reached, concentrations decreased initially fast and then slower in all

experiments, ending in an extended tailing. This tailing, which was also observed in previous experiments, proved to be typical for sulfadiazine transport.

The differences in eluted amounts of mass were also reflected in the ^{14}C-concentration profiles, with the higher mass recoveries in the experiments with the lower flow rate. Experiments conducted at the lower flow rate showed a trend of continuously decreasing concentrations with depth, whereas the concentration profiles conducted at the higher flow rate were quite curved. Compared to previous experiments (Unold et al., 2009a, Wehrhan et al., 2007), the concentration profiles were more irregular which may be attributed to the usage of undisturbed soil columns.

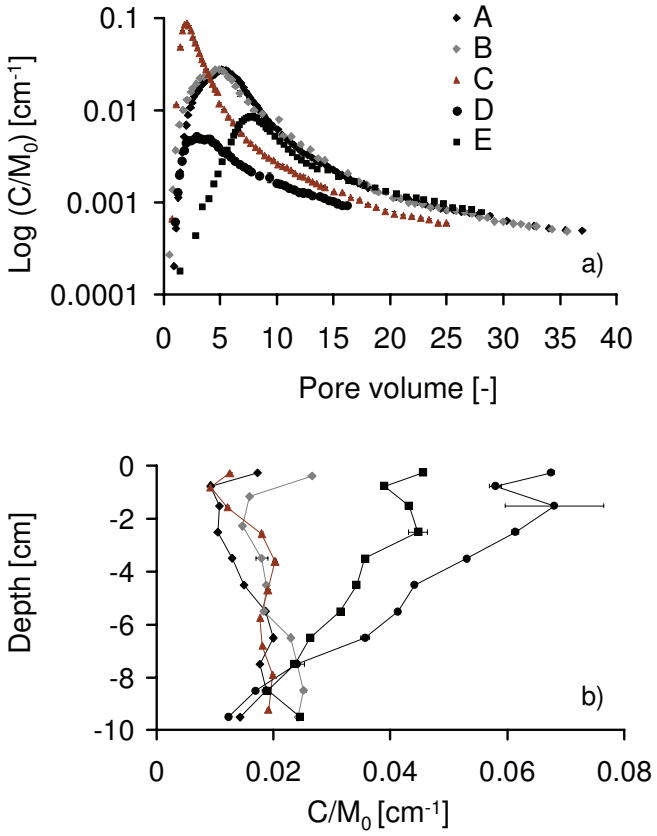

Figure 3.2. (a) ^{14}C breakthrough curves and (b) concentration profiles of ^{14}C in the soil column for the five experiments. Time is expressed as pore volume, bars indicate standard error. Concentrations were transformed by dividing through the applied mass of SDZ per cm^2, M_0.

3.4.3 Transformation of Sulfadiazine

Figure 3.3 presents the BTCs of ^{14}C, SDZ, 4-OH-SDZ and An-SDZ for experiment C. The peak maxima of the breakthrough curves of SDZ and its transformation products did not appear at the same time (expressed as pore volume) in the drainage water as they did in previous studies with the same soil (Unold et al., 2009a,b). Whereas the concentration peaks of SDZ and ^{14}C coincided, the An-SDZ peak appeared shortly before and the 4-OH-SDZ peak appeared shortly after the ^{14}C peak. From experiments with manure (Unold et al., 2009b), in which 4-OH-SDZ was initially present, we know that this transformation product was more mobile than SDZ. The fast appearance of An-SDZ on the other hand hinted at an even faster transport. To our knowledge no quantitative information on sorption and transformation behavior of SDZ-transformation products in soil exists.

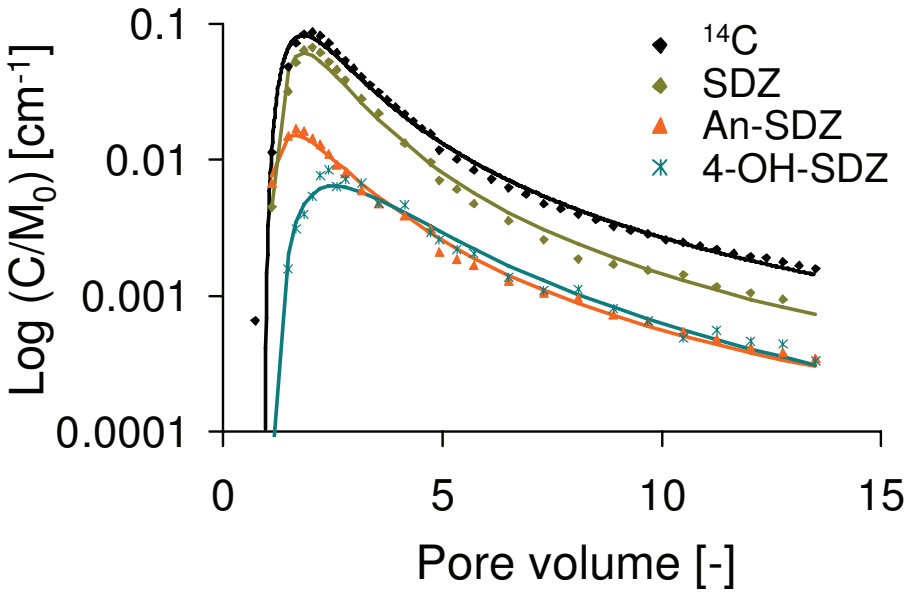

Figure 3.3. Breakthrough curves of ^{14}C, SDZ, 4-OH-SDZ and An-SDZ of experiment C. Symbols represent measurements and solid lines model predictions using the isotherm-based concept of the convection-dispersion equation with transformation. Concentrations were transformed by dividing through the applied mass of SDZ per cm^2, M_0.

3.4.4 Modeling Results

3.4.4.1 ^{14}C-BTCs: single fits

Each experiment was fitted with the isotherm-based and the attachment/detachment approach. We did not include ^{14}C-concentrations in the drainage water below 0.006 µg mL^{-1} in the objective function for experiment A (3 data points) and experiment C (1 data point). This is justified by the severe impact of concentrations equaling zero on the objective function when using log-transformed values. Figure 3.4 shows the results and the respective parameter estimates are listed in Table 3.4. Compared to a previous study (Unold et al., 2009a), K_f and *m* were not highly correlated, so both parameters were fitted.

Except for experiment C, the attachment/detachment model described all experiments better than the isotherm-based model in terms of the sum of squared weighed residuals (Table 3.4). While the difference in model performance was quite small for experiment C, distinct differences in the prediction of the BTCs were found between both model approaches for the other experiments, where the isotherm-based model was not able to correctly capture the tailings (Figure 3.4). Both model approaches failed to describe the rise of the peak of experiment E but the tailing was well captured with the attachment/detachment approach. The sorbed mass was predicted well on average for experiments A, B, and C for both model approaches. However, the fairly curved measured concentration distribution with depth could not be captured by the models. For experiment D and E, the concentration profile data could be described quite well below -2 cm. One kinetic sorption site in the attachment/detachment approach showed considerably faster ad- and desorption rates for all experiments, hinting on the fact that sorption of SDZ was characterized by a fast and a slow reversible process in addition to irreversible sorption.

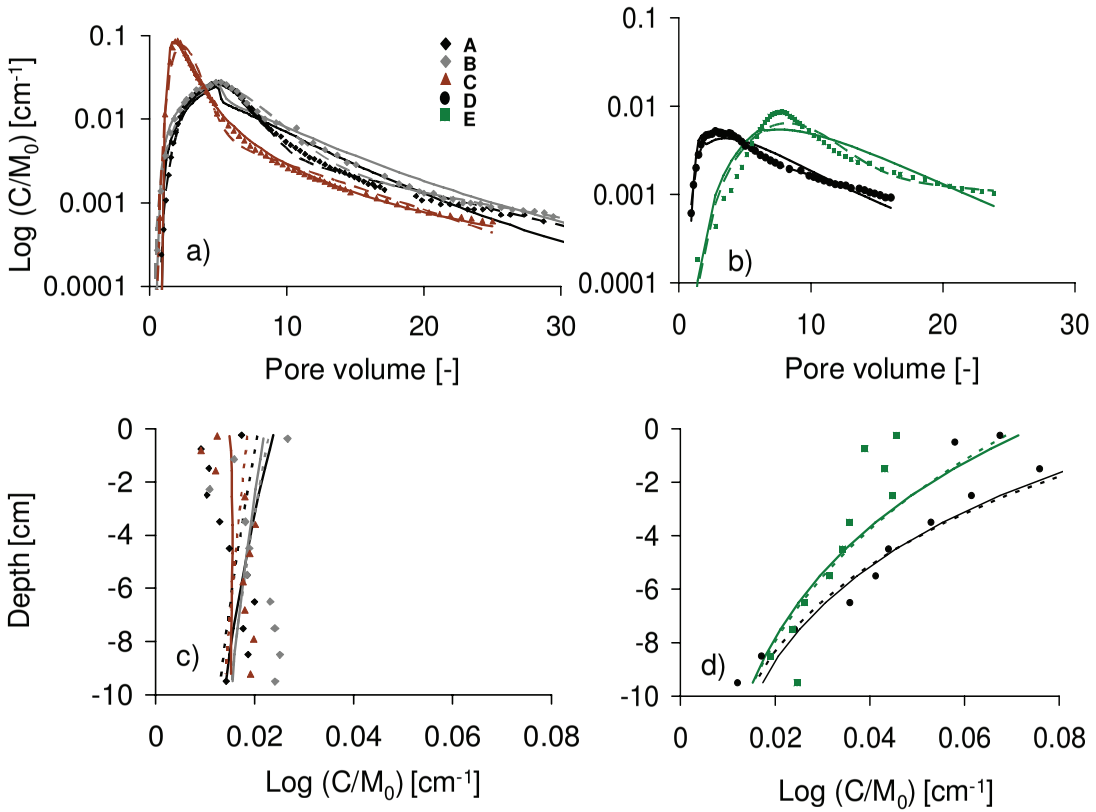

Figure 3.4. ^{14}C breakthrough curves for (a) the high flow rate and (b) the low flow rate; ^{14}C concentration profiles for (c) the high flow rate and (d) the low flow rate. Symbols represent measurements, solid lines are model predictions for the isotherm-based approach and dashed lines are model predictions for the attachment/detachment approach. Concentrations were transformed by dividing through the applied mass of SDZ per cm^2, M_0.

Table 3.4: Fitted parameters for the log-normalized ^{14}C-BTCs and concentration profiles for all experiments using attachment/ detachment and isotherm-based models. Presented are the irreversible sorption rate coefficients (μ, β_3) for SDZ, attachment- (β_1, β_2) and detachment rates (γ_1,γ_2) for the kinetic reversible sorption as well as the Freundlich parameters (K_f, and *m*) and the kinetic rate coeffient (α).

	β_3 [h^{-1}]	β_2 [h^{-1}]	γ_2 [h^{-1}]	β_1 [h^{-1}]	γ_1 [h^{-1}]	R^2 [b]	Φ_{BTC} [c]	$\Phi_{profile}$ [c]	Eluted [%]
A	0.033 (± 0.002)[a]	0.025 (± 0.002)	0.0067 (± 0.0005)	0.33 (± 0.02)	0.14 (± 0.01)	0.99	0.28	0.015	59.7
B	0.030 (± 0.005)	0.019 (± 0.003)	0.0052 (± 0.001)	0.26 (± 0.04)	0.090 (± 0.02)	0.99	0.29	0.007	61.7
C	0.022 (± 0.004)	0.020 (± 0.002)	0.0094 (± 0.001)	1.35 (± 0.1)	0.82 (± 0.1)	0.99	0.32 [d]	0.017	70.0
D	0.036 (± 0.0005)	0.022 (± 0.001)	0.0031 (± 0.0003)	0.12 (± 0.006)	0.045 (± 0.005)	0.99	0.025	0.001	10.6
E	0.025(± 0.02)	0.017 (± 0.02)	0.00083 (± 0.002)	0.18 (± 0.02)	0.035 (± 0.007)	0.96	0.69	0.020	17.1
	μ [h^{-1}]	**K_f [$\mu g^{1-m} cm^{3m} g^{-1}$]**	**m [-]**	**α [h^{-1}]**		**R^2**	**Φ_{BTC}**	**$\Phi_{profile}$**	**Eluted [%]**
A	0.039 (± 0.005)	0.57 (± 0.06)	0.61 (± 0.04)	0.032 (± 0.003)		0.94	2.36	0.005	54.9
B	0.029 (± 0.005)	0.58 (± 0.06)	0.58 (± 0.04)	0.030 (± 0.003)		0.98	0.66	0.001	62.3
C	0.016 (±0.005)	0.44 (±0.02)	0.36 (±0.01)	0.39 (±0.07)		1.0	0.10	0.010	71.5
D	0.036 (± 0.001)	0.34 (± 0.07)	0.56 (± 0.06)	0.015 (± 0.001)		0.96	0.25	0.001	10.9
E	0.032 (± 0.002)	0.83 (± 0.07)	0.75 (± 0.001)	0.011 (± 0.001)		1.0	1.15	0.023	17.1

[a]Values in parenthesis represent 95% confidence limits.
[b] R^2 = coefficient of determination.
[c] Φ = Sum of squared weighed residuals.
[d] Φ_{BTC} was calculated without considering the first 3 data points in order to make it comparable with Φ_{BTC} for the isotherm based approach.

The experiment with the high input concentration (C) showed distinct differences compared to the other experiments. In the attachment/detachment approach pronounced higher attachment/detachment rates for the faster reversible kinetic sorption sites were observed compared to the other experiments, meaning that sorption can be approximated by an instantaneous process. This was confirmed with the isotherm-based model concept, where the kinetic sorption rate, α, was almost one order of magnitude higher than for the other experiments. In the case of instantaneous sorption both model approaches are equivalent. This is supported by the similar values obtained for the kinetic sorption rate, α, in the equilibrium approach and for the ratio of the detachment and attachment rate (γ_2/β_2) for the slower sorption site in the attachment/detachment approach. Although the other fitted parameters (β_2, β_3, γ_3, K_f, m, μ) in the two models differed between the five experiments, the absolute differences among them were generally small. The experiments with the lower flow rate D and E had slower ad- and desorption rates at the fast sorption site than the experiments with the higher flow rate.

The ratio between the attachment and detachment rates (β_i/γ_i) represents the sorption affinity to the respective sorption site (Wehrhan et al., 2007). Calculated sorption affinities were higher for the slower reversible sorption site than for the faster reversible sorption site in all experiments. For the experiments with the lower flow rate (D & E) sorption affinities at the slower reversible sorption site were on average more than two (D) or seven (E) times higher than for the experiments conducted at a higher flow rate. This resulted in higher reversibly sorbed parts of the total applied mass in experiments D (6.2%) and E (18.8%) at the end of the leaching experiments, accompanied by a lower eluted amount of ^{14}C. Since the attachment rate for the slower reversible sorption process was quite similar for all experiments, its sorption affinity was mainly determined by the value of the detachment rate. As is visible from the higher eluted amounts in experiment C, both reversible sorption sites had lower sorption affinities compared to the other experiments.

The rate for irreversible sorption was in the same range for both model approaches, had the same order of magnitude as the attachment rate for the slower reversible sorption site and was inversely related to the amount of eluted mass for experiments A, B, C and D. This trend was not confirmed by experiment E which had a relatively low irreversible sorption rate, but also a low amount of eluted mass. Overall the large difference in sorbed amounts between experiments with the higher and lower flow rates was most probably caused by the differences in contact time. The characteristic time scale of the experiments

($1/\gamma_3$) was on average one and a half day. Thus due to the longer residence time in the soil column, much more ^{14}C could adsorb in the experiments with the lower flow rate.

The attachment/detachment concept, commonly used to predict particle transport, had the disadvantage that it did not consider concentration-dependent processes which were reported for SDZ sorption (Thiele-Bruhn et al., 2004). Also the presented data and modeling results in this study showed that SDZ transport was highly dependent on concentration. In previous studies (Unold et al., 2009a,b) where higher outflow concentrations were observed, the 2-site kinetic model was able to describe the BTCs quite well. This supports the results of Braida et al. (2001), who found that sorption equilibrium for non-linear sorbing substances was reached faster at higher concentrations. However, the flexibility of the 3-site attachment/detachment model was needed to describe the BTCs of the experiments with the low input concentration which corresponds to the finding of Wehrhan et al. (2007).

Compared to the results of Wehrhan et al. (2007), we observed an opposite trend. When the same mass of SDZ was applied during a short and a long pulse, more mass was eluted in the experiment with the high concentration in our study. The higher eluted mass for the experiment with the high concentration in our study may be explained by a lower sorption capacity of the loamy sand compared to the silty loam of Wehrhan et al. (2007) which had higher contents of clay and organic material. Since the pH values of both soils were almost equal, pH dependent sorption behavior of SDZ should not have caused the difference. This highlights the importance of soil properties like clay content and organic matter content as important factors in explaining differences in SDZ transport.

The fitted parameters for experiments A and B using the isotherm-based approach can be compared to one experiment of Unold et al. (2009a), where SDZ was applied using the same input concentration for the same pulse duration to a repacked soil column of the same soil, but at a slightly higher flow rate. In our study, higher Freundlich coefficients and exponents were found as well as a higher rate coefficient for irreversible sorption which explained the lower eluted mass. Equilibrium was reached slightly faster in the previous study.

3.4.5 Fitting the BTCs of SDZ and its transformation products for experiment C

The transport of SDZ and its transformation products was only investigated for soil column C for which these data were available. The results are presented in Table 3.5 and Figure 3.3. In the fit to the SDZ BTC without considering the transformation products, the transformation rate accounted for the degraded amount of SDZ into both daughter products.

Table 3.5: Fitted parameters for the breakthrough curves of ^{14}C, SDZ and the transformation products 4-OH-SDZ and An-SDZ of experiment C, including the degradation rates from SDZ into the respective transformation products, the irreversible sorption rate coefficient (μ) for SDZ and the fitted Freundlich parameters (K_f, and *m*) as well as the kinetic rate coefficient (α) for SDZ or the transformation products.

	$\mu`_{SDZ}$ [h^{-1}]	μ_{SDZ} [h^{-1}]	K_f [μg^{1-m} cm^{3m} g^{-1}]	*m* [-]	α [h^{-1}]	R^2 [b]	Φ_{BTC} [c]
^{14}C[d]	n.d.	0.020 (±0.002)	0.43 (±0.008)	0.40 (±0.02)	0.37 (±0.03)	1.0	0.07
SDZ	0.021 (±0.01) [a]	0.024 (±0.01)	0.39 (±0.02)	0.46 (±0.04)	0.51 (±0.08)	0.99	0.10
4-OH-SDZ	0.0093 (±0.001)	0.035 (±0.01)	0.19 (±0.03)	0.50 (±0.05)	0.20 (±0.02)	0.99	0.10
An-SDZ	0.014 (±0.001)	0.029 (±0.007)	0.077 (±0.01)	0.30 (±0.07)	0.12 (±0.02)	0.99	0.05

[a] effective transformation rate from SDZ into both, 4-OH-SDZ and An-SDZ
[b] R^2 = correlation coefficient
[c] Φ = Sum of squared weighed residuals
[d] data points in the tailing are only included where measurements of SDZ were available to make Φ comparable.

The applied model adequately described the BTCs of the transformation products. According to the fitted Freundlich parameters, the sorption capacity of the three solutes decreased in the order SDZ > 4-OH-SDZ > An-SDZ. This finding was consistent with a previous study (Unold et al., 2009b), where the transport behavior of these transformation products, formed in experiments with SDZ-solution, was described with the same model for the same soil. There the sorption capacity for both transformation products was lower than in our study whereas the sorption capacity for SDZ was higher. The differences for the transformation products may be partly attributed to high parameter uncertainties in the previous paper as well as to different application conditions. Sorption of the transformation products was non-linear, like for SDZ. According to the higher parts of An-SDZ in the outflow samples, the transformation rate from SDZ into An-SDZ was higher than for SDZ

into 4-OH-SDZ. Contrary to An-SDZ, the peak arrival time of 4-OH-SDZ could not be correlated to the sorption capacity, since the peak of 4-OH-SDZ appeared shortly after the peaks of SDZ and ^{14}C for which the sorption capacities were higher.

An apparent DT_{50} value for the dissipation of SDZ from the liquid phase by irreversible sorption and transformation was calculated as 0.64 d. This value is lower, but in the same order of magnitude than the DT_{50} value of 3 days determined for SDZ dissipation in a silty clay loam soil by Kreuzig et al. (2005) and the DT_{50} value of 3.5 days for the sulfonamide sulfochloropyridazin in a sandy loam with manure application (Blackwell et al., 2007). Förster et al. (2009) found a higher DT_{50} value (19 d) for SDZ with manure application ($CaCl_2$-fraction) in the same sandy soil as was used in this study.

Figure 3.3 shows that the shapes of the ^{14}C and SDZ BTCs were quite similar. When the isotherm-based model was fitted to both of them the estimated parameters values were not the same, but differences were small. Therefore, the transport of SDZ can be reasonably well described by fitting the ^{14}C data in this case.

3.4.6 Simultaneous fitting of the steady-state flow experiments

Apart from the physical characterization of the water flow, one set of transport parameters should be able to describe the measured BTCs for all experimental conditions, in case the model reflected all relevant processes. However, as Table 3.5 shows, the estimated parameter sets differed among the various experiments. With the help of the simultaneous modeling of three or four experiments, we tested if a common set of parameters existed which was able to describe all experiments. We used the attachment/detachment model for the simultaneous fitting, since it better described the measured BTCs for most experimental conditions. Experiment E was not included, since either the transient (intermittent) flow regime or the soil itself clearly affected the transport of the reactive tracer SDZ.

Figure 3.5 shows that the general shapes of all BTCs conducted under steady-state flow conditions could be described quite well for the various simultaneous parameter fits. Peak arrival times were predicted correctly, although the common sets of parameters were not able to compensate the different eluted masses observed in the single experiments which led to over- and underestimations of the peak heights. Also the slopes of the tailings were

not adequately captured. As could be expected, the sum of squared weighed residuals (ϕ) was higher for the simultaneously fitted models than for those fitted to the individual BTCs.

In the model run in which all five parameters were fitted to the experiments with the lower concentration (A, B, D) the description of experiments A and B was better than for the model that was fitted to the experiments conducted at the high flow rate (A, B, C). This was probably caused by the more pronounced difference in absolute parameter values of experiment C compared to the other experiments, especially for the parameter values describing the faster reversible sorption process (β_1, γ_1). The influence of these two parameters on the modeling results was further investigated by fitting the attachment rate β_1 individually to each BTC, together with an additional ratio of β_1/γ_1 instead of γ_1. As became visible in the sum of squared weighed residuals, the performance of this model run led to the best descriptions of the single BTCs using simultaneously fitted parameters, especially for experiments A and B for which the parameters for the single BTCs lay in most cases between the estimated values for experiments C and D. For experiments C and D ϕ was in same range as for the models fitted either to experiments A, B and D or A, B and C.
For the model run in which all parameters were fitted simultaneously to experiments A, B, C and D, ϕ was remarkably higher for all BTCs. This confirmed the hypothesis that the process described by the faster attachment/detachment rates was the main difference between the investigated experiments. A higher flexibility in these rates led to pronounced better descriptions of the single BTCs.

Table 3.6: Simultaneously fitted parameters to ^{14}C-BTC and concentration profile data of the experiments with the low concentration (A, B, D) and the experiments with the high flow rate (A, B, C) using the attachment detachment concept as well as fitted parameters for BTCs of experiments A, B, D & C which were either fitted simultaneously (A, B, C, D) or partly individually for the single experiments (A, B, C, D, β_1 variable, ratio).

	ABD	ABC	ABCD β_1 variable, ratio	ABCD
β_3 [h^{-1}]	0.037 (±0.001)	0.027 (±0.004)	0.036 (±0.001)	0.035 (±0.001)
β_2 [h^{-1}]	0.026 (±0.002)	0.022 (±0.003)	0.026 (±0.002)	0.027 (±0.003)
γ_2 [h^{-1}]	0.0047 (±0.001)	0.0076 (±0.001)	0.0056 (±0.0004)	0.006 (±0.0007)
$\beta_{1,A}$ [h^{-1}]	0.21 (±0.02)	0.68 (±0.07)	0.33b (±0.05)	0.57 (±0.08)
$\gamma_{1,A}$ [h^{-1}]	0.10 (±0.01)	0.38 (±0.05)	0.16 [b]	0.33 (±0.05)
$\beta_{1,B}$ [h^{-1}]	0.21 [d]	0.68 [d]	0.27 (±0.09)	0.57 [d]
$\gamma_{1,B}$ [h^{-1}]	0.10 [d]	0.38 [d]	0.13 [b]	0.33 [d]
$\beta_{1,C}$ [h^{-1}]	-	0.68 [d]	1.09 (±0.1)	0.57 [d]
$\gamma_{1,C}$ [h^{-1}]	-	0.38 [d]	0.53[b]	0.33 [d]
$\beta_{1,D}$ [h^{-1}]	0.21 [d]	-	0.13 (±0.03)	0.57 [d]
$\gamma_{1,D}$ [h^{-1}]	0.10 [d]	-	0.063[b]	0.33 [d]
ratio	-	-	2.05[a] (±0.09)	-
R^2	1.0	0.99	1.0	0.99
$\Phi_{BTC\ A}$	1.43 (0.28) [c]	2.95	0.57	2.18
$\Phi_{Profil\ A}$	0.01 (0.015) [c]	0.0048	0.0046	0.0079
$\Phi_{BTC\ B}$	0.88 (0.29)[c]	1.81	0.66	1.33
$\Phi_{Profil\ B}$	0.0022 (0.007) [c]	0.002	0.002	0.0019
$\Phi_{BTC\ C}$	-	5.91 (0.32) [c]	5.55	10.17
$\Phi_{Profil\ C}$	-	0.059 (0.017) [c]	0.00	0.17
$\Phi_{BTC\ D}$	1.15 (0.025) [c]	-	1.27	4.88
$\Phi_{Profil\ D}$	0 (0.001) [c]	-	0.00	0

[a] ratio = $\beta_i/\gamma_{i,}$ fitted simultaneously to all four BTCs
[b] calculated according to $\gamma_1 = \beta_1$/ratio
[c] sum of squared weighed residue for the model fitted to the single BTC
[d] value is fitted simultaneously for experiments A, B and D, A, B and C or A, B, C and D. Confidence interval is presented in the cell of experiment A.

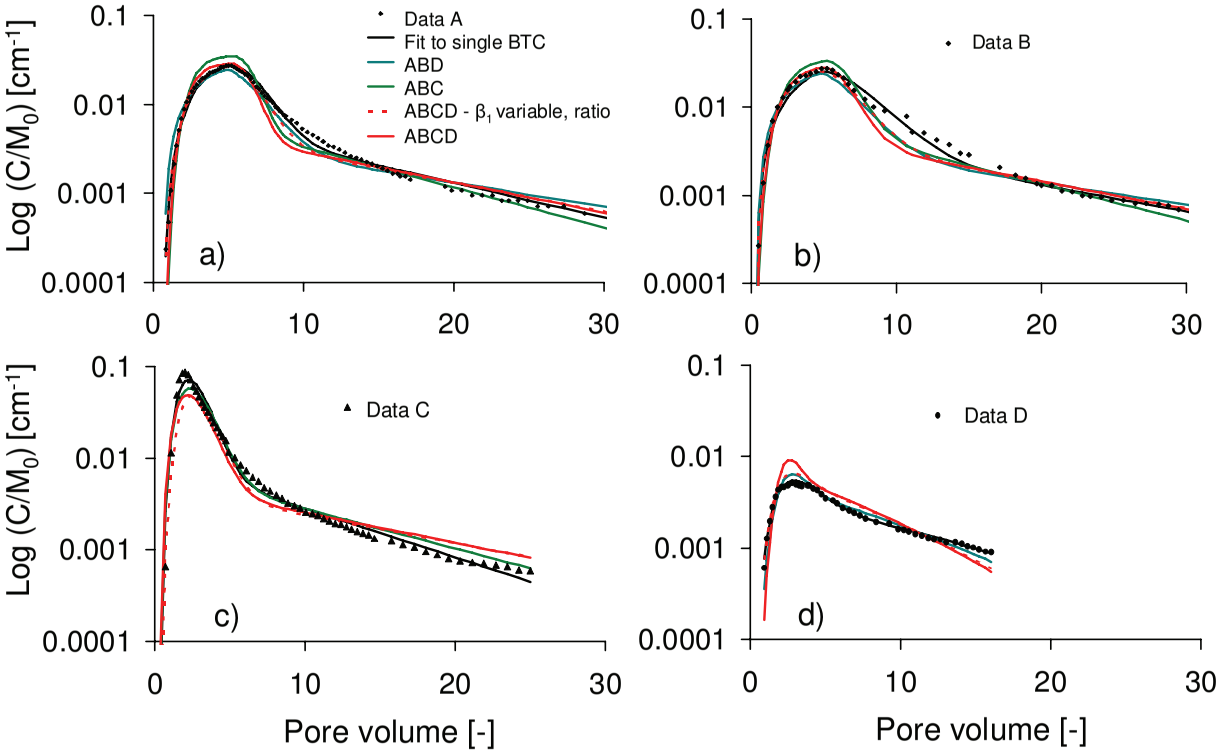

Figure 3.5. Breakthrough curves of experiments A, B, C and D and models fitted to the single BTCs (black lines), simultaneously either to experiments A, B and D (blue lines), A, B and C (green lines), A, B, C and D (red lines) as well as the model for which β_1 was fitted individually to each BTC together with the ratio β_1/γ_1 (dashed red lines). Concentrations were transformed by dividing through the applied mass of SDZ per cm², M_0.

The models in which all parameters were fitted simultaneously (Table 3.6) were used to predict the transport of SDZ in experiment E which was conducted under transient flow conditions. As Figure 3.6 shows, the predictions were quite good, although the rise in concentration was predicted too early and was too steep. The different shape of experiment E in the beginning could possibly be explained by the transient flow regime. Periods without irrigation could have led to longer contact times between SDZ and the soil, which led to higher sorption or different sorption kinetics. Additionally more regions of the soil were reached, due to the higher water content during irrigation with the higher flow rate. In contrast no influence of transient flow conditions on SDZ-transport was found by Unold et al. (2009b) for SDZ application with manure. This may be caused by the influence of manure, as well as a joined effect of the lower flow rate and concentrations in this study.

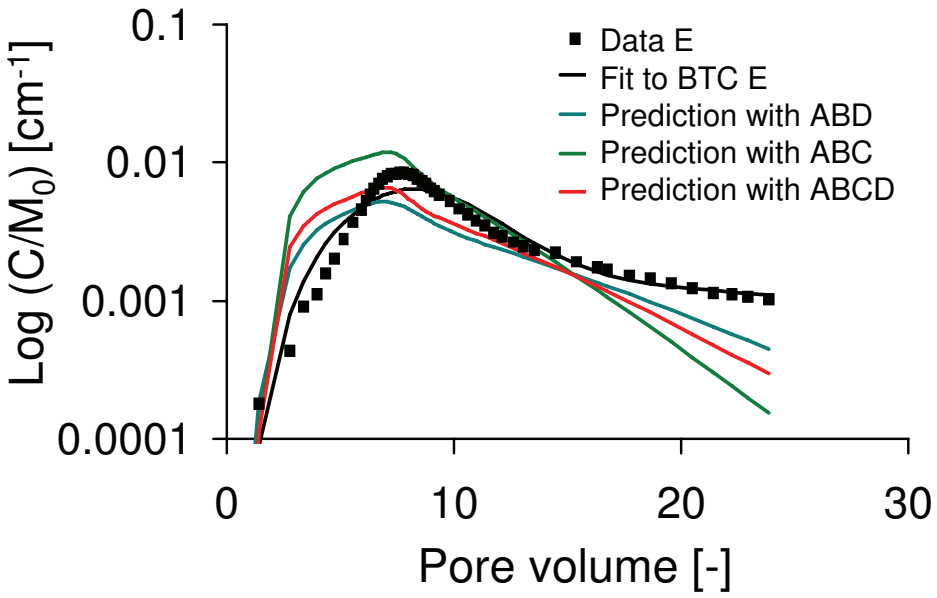

Figure 3.6. Breakthrough curve of experiment E and model predictions using the estimated parameters for the single BTC, the models fitted simultaneously either to experiments A, B and D (blue line), A, B and C (green line) or A, B, C and D (red line). Concentrations were transformed by dividing through the applied mass of SDZ per cm², M_0.

3.5 Conclusions

We conducted transport experiments with SDZ on five undisturbed soil materials using different top boundary conditions and input concentrations. The experiments confirmed that the applied solute mass, i.e. input concentration and pulse duration, and flow rate influenced the transport of sulfadiazine in soil columns. The slower flow rate led to remarkably lower eluted masses of SDZ compared to the experiments with the higher flow rate. Eluted masses were also moderately lower for the experiments with the low input concentration than for the high input concentration. The parameterization of the BTCs of total- ^{14}C proved to be appropriate to predict SDZ transport. While a two-site isotherm-based model approach was able to describe the transport of sulfadiazine applied at the high input concentration, sorption kinetics became more dominant in the lower concentration range and at the slower flow rate, where a three-site attachment/detachment model better fitted the measured BTCs. The description of the concentration profiles with the two model concepts was similar with the two model approaches. The parts of transformation products in the effluent of soil column C were substantial, with 17% for 4-OH-SDZ and 21% for An-SDZ. Modeling revealed a higher mobility for the transformation products than for SDZ, with a higher sorption capacity for 4-OH-SDZ than for An-SDZ. The modeling process using the attachment/detachment concept arranged sorption into a faster and a slower reversible kinetic process, as well as irreversible sorption. We concluded from the simultaneous fits that the overall BTC shapes of experiments conducted under steady state flow conditions can be described quite well with one common parameter set. But it was impossible with the estimated parameters to compensate the differences in observed eluted masses in the experiments, which led to over- and underestimation of peak heights and tailings and were mainly described by the attachment- detachment rate of the faster sorption site. Fitting the faster attachment rate individually together with the ratio of the faster attachment and detachment rate clearly improved the simultaneous fits. Transport behavior of SDZ was different for transient flow conditions, which led to a higher retention especially at the slow reversible sorption site. This shows that the prediction of SDZ leaching in the field, where flow conditions are highly variable, still is a challenge. The results imply that the leaching potential of SDZ remarkably decreases for low input concentrations and under soil moisture conditions where low water flow velocities dominate.

4 Transport of manure-based applied sulfadiazine and its main transformation products in soil columns[3]

4.1 Objectives

In chapter 4 the effect of pig manure on SDZ was investigated by comparing experiments conducted using SDZ containing manure with experiments performed with a SDZ-solution. Also the transport of the main metabolites in pig manure, 4-OH-SDZ and N-AC-SDZ, was investigated. The transport of SDZ and the metabolites was described simultaneously using a model including a degradation chain from N-Ac-SDZ into SDZ and from SDZ into 4-OH-SDZ as well as one reversible kinetic and one irreversible sorption site for SDZ and 4-OH-SDZ. For N-Ac-SDZ no irreversible sorption was included.

4.2 Introduction

In recent years, several studies have shown the widespread occurrence of sulfonamide antibiotics in surface waters (Christian et al., 2003; Managaki et al., 2007), groundwaters (Sacher et al., 2001; Hamscher et al., 2005; Focazio et al., 2008) and soils (Höper et al., 2002; Boxall, 2004; Hamscher et al., 2005). The major risk of introducing these substances into the environment is the development and spreading of resistant pathogens (Kemper, 2008), especially since the probability of these chemicals reaching the food chain via drinking water (Batt et al., 2006; Ye et al., 2007) or the root uptake by plants (Dolliver et al., 2007) is high.

The main difference in how antibiotics and other organic contaminants, such as pesticides, are introduced into the environment is the way of their application. While pesticides are intentionally spread over the field, antibiotics are mostly introduced unintentionally with the application of manure (Jørgensen & Halling-Sørensen, 2000). The application of the sulfonamide antibiotic sulfadiazine (SDZ) with incorporation of manure into the root zone, which is a common practice in Germany, may influence soil structure and other

[3] * adapted from: Unold M., J. Simunek, R. Kasteel, J. Groeneweg and H. Vereecken: Transport of manure-based applied sulfadiazine and its main transformation products in soil columns. Vadose Zone Journal, 8, 677-689

conditions affecting the solute transport in the soil profile. The effects of the manure application on soil aggregation were studied by many, including Wortmann & Shapiro (2008). These researchers found that manure application resulted in the formation of macro-aggregates. They concluded that the risk of surface runoff may be greatest shortly after application because macro-aggregates have had no time to develop.

Suspended colloidal material, as found in manure, can facilitate the transport of pollutants in soils. Molecules of organic substances can sorb to small particles (McGechan & Lewis, 2002) and travel along with them at usually rapid un-retarded velocities. Colloid-facilitated transport has been shown, for example, to accelerate the transport of pesticides, phosphates, and heavy metals (Hesketh et al., 2001; de Jonge et al., 2004; Pang and Šimůnek, 2006). McGechan & Lewis (2002) indicated in their review that macropores are the main pathways for colloidal transport since such larger particles are otherwise effectively retained by physical filtration processes (Jarvis et al., 1999; Kretzschmar, 1994).

Due to speciation, sorption of sulfonamide antibiotics to soils (Kurwadkar et al., 2007) and organic material (Kahle & Stamm, 2007b) is strongly dependent on pH. Due to high amounts of NH_4 present in manure, the soil water pH can increase by 1.5 units after the application of manure (Kay et al., 2005a), which may lead to a significantly lower sorption of SDZ.

Several studies focused on the sorption and transport of antibiotics in the presence of manure (Boxall et al., 2002; Kay et al., 2004; Kay et al., 2005a; Kreuzig & Höltge, 2005; Blackwell et al., 2007; Stoob et al., 2007). Antibiotics of the sulfonamide group seem to have a stronger tendency for leaching and overland flow than other antibiotics, such as tetracyclines and tylosin. Blackwell et al. (2007) and Kay et al. (2005b) demonstrated this tendency for sulfachloropyridazine in field and lysimeter studies. Kay et al. (2005a) found no influence of manure on the transport of the tetracycline antibiotic oxytetracycline. In batch studies, Kreuzig and Höltge (2005) observed a tendency of SDZ to form a non-extractable fraction, which remained in the manure matrix. Additionally, the extractable fraction of SDZ in a soil was much lower when SDZ was applied together with manure. In contrast, Thiele and Aust (2004) and Boxall et al. (2002) found decreased sorption of SDZ and other sulfonamide antibiotics in the presence of manure, probably due to the use of different soils and manures in their experiments.

Kreuzig et al. (2005) and Heise et al. (2006) reported that sulfonamides quickly form non-extractable residues in soils. Bialk and Pedersen (2008) showed that the

sulfonamide antibiotic sulfapyridine can be covalently bound to the model humic substance protocatechuic acid, which is one explanation for the observed irreversible sorption behavior of sulfonamides. While degradation of sulfonamides was often observed (Sukul et al., 2008b; Wang, 2006), their mineralization has been found to be relatively low (Loftin et al., 2008; Schmidt et al., 2008).

Various studies have shown that manure from SDZ administered animals contains the parent compound SDZ as well as several transformation products. Lamshöft et al. (2007) studied excretion patterns from pigs that were administered with ^{14}C-SDZ. They detected about 96% of the applied ^{14}C excreted in manure and identified five transformation products in addition to SDZ. While 4-N-acetyl-SDZ (*N*-Ac-SDZ) and 4-hydroxy-SDZ (4-OH-SDZ) were found in larger concentrations, formyl-SDZ and acetyl-hydroxyl-SDZ were found only in trace amounts.

The occurrence of these transformation products cannot be regarded as the result of a degradation process that makes the parent compound harmless, since it is known, for example, that the metabolite 4-OH-SDZ can still be microbially active (Nouws et al., 1989) and that *N*-Ac-SDZ can retransform into the active parent compound SDZ (Berger et al., 1986). There are indications that transformations not only occur during metabolization in animals, but also in soils (Burkhardt et al., 2005; Wehrhan, 2006; Wehrhan et al., 2007) and aqueous solutions (Sukul et al., 2008b).

Up to now, little has been known about the occurrence and fate of transformation products in the environment. This may be due to the lack of reference substances (Diaz-Cruz & Barcello, 2006). Their relevance in environmental assessments was shown by Hilton & Thomas (2003), who detected relatively high concentrations of the acetyl form of the antibiotic sulfamethoxazole in effluent and surface waters, whereas the concentration of the parent compound was lower than the detection limit.

Various types of models are available to simulate the transport of antibiotics. These models need to consider various physical processes involved in the transport of antibiotics, as well as chemical processes, including kinetic and equilibrium sorption and degradation. The process of degradation is usually simulated in transport models as a first-order process. Examples of model applications that considered first-order degradation are, for example, Casey and Šimůnek (2001) and Schaerlaekens et al. (1999) for the transport of trichloroethylene, Casey et al. (2003, 2004, 2005), Das et al. (2004) and Fan et al. (2007) for the transport of hormones, and Papiernik et al. (2007) for the transport of a herbicide.

Das et al. (2004), for example, used a bicontinuum model with first-order degradation to describe the transport of estradiol and testosterone, as well as their daughter products. Similarly, Casey et al. (2003, 2004, 2005) included first-order degradation to describe the transport of estradiol and testosterone, as well as their daughter products. Similar first-order reaction pathways are also often used to describe the simultaneous transport of N species (Hanson et al., 2006), radionuclides (van Genuchten, 1985) or organic explosives (Šimůnek et al., 2006).

The main objectives of this study were to investigate (i) the effects of pig manure on the fate and transport of SDZ in soil columns and (ii) the transport in soil columns of two SDZ transformation products present in applied manure. To achieve these objectives, solute displacement experiments were performed using both repacked and undisturbed soil columns involving two soils. Pig manure containing ^{14}C-SDZ, ^{14}C-4-OH-SDZ, and ^{14}C-N-Ac-SDZ was incorporated into the top of the soil columns. A ^{14}C-SDZ solution was additionally incorporated into one repacked column of each soil. Breakthrough curves and ^{14}C distributions vs. depth were analyzed using a transport model that considered convective–dispersive transport with one kinetic reversible and one kinetic irreversible sorption site. Transformation and sorption rates for the different solutes were determined using an inverse parameter optimization procedure based on the Levenberg–Marquardt algorithm.

4.3 Materials & Methods

4.3.1 Experimental set-up

To study the effects of manure on the transport of SDZ and its transformation products, we conducted experiments on undisturbed and repacked columns of two soils. Soil samples for both the repacked and undisturbed soil columns were collected from the upper 30 cm of two fields with soil types that are typical for agricultural land use in Northrhine-Westpfalia, Germany. A silt loam soil (an Alfisol or Orthic Luvisol) was collected from a field near Jülich-Merzenhausen (denoted below as Soil M), while a loamy sand soil (an Inceptisol or Gleyic Cambisol) was sampled from a field near Kaldenkirchen (denoted below as Soil K). Selected soil properties are shown in Table 4.1.

Table 4.1: Selected physical and chemical properties of the Kaldenkirchen soil (K) and the Merzenhausen soil (M).

	Unit	Soil K	Soil M
Clay (<0.002 mm)[a]	[% mass]	4.9	15.4
Silt (0.002-0.064 mm) [a]	[% mass]	26.7	78.7
Sand (0.064-2.0 mm) [a]	[% mass]	68.5	5.9
pH (0.01 M $CaCl_2$) [b]		6.8	7.4
C_{org} [a]	[% mass]	1.07	1.24
CEC[c]	[$cmol_c kg^{-1}$]	7.8	11.4

[a] Data were measured at the Institut für Nutzpflanzenwissenschaften und Ressourcenschutz of the University of Bonn.
[b] Average pH values in soil column effluents for soil columns with manure.
[c] Data for CEC were taken from Förster et al. (2009).

For the repacked soil columns, the soils were sieved (2 mm) and air dried. During the packing procedure, layers of about 0.5-cm thickness were added to the columns and compacted by weakly pressing with a pestle. Columns constructed of polyvinyl chloride (PVC) with an inner diameter of 8 cm and heights of 10 cm were used for all experiments. The excellent solute mass recoveries in most experiments suggested that we could neglect SDZ sorption onto the PVC material.

Undisturbed soil columns were collected using PVC columns and a metal adaptor with a sharp front attached at one end to facilitate entry into the soil. No roots were visible in the soil, so only fine roots may have existed in the soil columns. The repacked and undisturbed soil columns were mounted on porous glass plates having a high conductivity and an air-entry value >100 mbar. Overall, seven experiments were performed. The experimental conditions for each setup are shown in Table 4.2.

Table 4.2: Experimental conditions for different soil column experiments.

Soil column[a]	soil	Packing	SDZ Appli-cation	Irrigation	ρ [g cm^{-3}]	q [cm h^{-1}]	Applied suction [mbar]
KrepMAN	K	repacked	manure	constant	1.42	0.18	23
KrepSOL	K	repacked	solution	constant	1.37	0.19	41
KundMAN	K	undisturbed	manure	constant	1.49	0.20	10
KundMAN$_i$	K	undisturbed	manure	intermittent	1.40	0.18	10
MrepMAN	M	repacked	manure	constant	1.34	0.19	30
MrepSOL	M	repacked	solution	constant	1.27	0.19	29
MundMAN	M	undisturbed	manure	constant	1.88	0.19	4

[a]The first letter represents soil type (either K or M), columns were either repacked (rep) or undisturbed (und), and either manure (MAN) or a stock solution (SOL) was incorporated into the column; subscript i denotes intermittent infiltration.

While either manure or the SDZ solution was applied to the repacked soil columns, only manure was incorporated into the undisturbed soil columns. The soil columns were slowly saturated from the bottom with 0.01 mol L^{-1} $CaCl_2$ for approximately 2 d before displacement experiments started. The same solution was also used as a background solution. A thin layer of coarse quartz sand was placed on top of the columns to protect the bare soil surface from the impact of the irrigation water. Six soil columns were irrigated at a constant flow rate of about 0.19 cm h−1. An additional experiment was performed using a second undisturbed column containing Soil K to which manure was applied. In this case, the same amount of irrigated water per hour was applied at a higher flow rate for 5 min, followed by 55 min of redistribution.

All soil column experiments were run with software-controlled equipment. Irrigation of the soil columns started a few days before the leaching experiments. The irrigation rate was recorded by weighing the storage bottle of the irrigation solution. Suction was applied at the bottom of the soil columns. Suctions within the range of 4 to 41 mbar were chosen separately for each soil column to establish a constant pressure head (water content) in the soil columns for a given flow rate. This meant that gravity was the primary factor driving water flow. The suctions inside of the columns were followed using two tensiometers installed 2.5 and 7.5 cm below the soil columns' surfaces. Fifteen milliliters of the outflow was collected in test tubes for each sample. Water lost due to evaporation, which was approximately 2.19×10^{-6} L h^{-1}, was included in calculations of the solute concentrations to correct the measured concentrations for evaporation losses.

Evaporation losses were determined by weighing two water-filled tubes at regular time steps.

Before and after the SDZ-transport experiments, we used Cl^- as a non-reactive tracer to characterize the physical transport mechanisms in the soil columns. For this purpose, pulses of 0.05 mol L^{-1} $CaCl_2$ solution were applied to the columns for 1 h (corresponding pore volumes are listed in Table 4.3. The Cl^- concentration in the outflow samples was measured using an electrical conductivity sensor included in the experimental setup. The correlation between electrical conductivity and Cl^- concentration was determined by establishing a calibration curve using samples of known Cl^- concentration.

For determining the BTCs of SDZ and its transformation products, either 15.07 g of pig manure containing ^{14}C-SDZ or 15.07 g of a 0.01 mol L^{-1} $CaCl_2$ solution with the same amount of SDZ was incorporated into the top 1 cm of the soil columns. Manure or the SDZ solution was first mixed with the air-dried soil of the particular soil type and then added to the top of the soil columns from which the original soil had been removed.

When the leaching experiments were finished, the soil columns were cut into slices of 0.5 or 1 cm thickness to measure ^{14}C concentrations in the column profiles by combusting aliquots of each slice in an oxidizer (Robox 192, Zinsser Analytik GmbH, Frankfurt, Germany), following the approach described in Unold et al. (2009). This method allows ^{14}C concentrations in soils to be measured without applying any extraction procedures, which were reported to have low efficiencies and variations between fresh (<71%) and aged (<46%) SDZ residues (Förster et al., 2009). Thus only the total amount of radioactivity was measured in the soil. For each slice, three 0.5-g replicates of ovendried (105°C), ground, and homogenized soil were combusted in an oxidizer. After combustion, the evolving gas was washed into a scintillation cocktail (Oxysolve C-400, Zinsser Analytics, Frankfurt, Germany), in which the labeled CO_2 was trapped and then analyzed by liquid scintillation counting (LSC). Blanks were run before and after the samples to check for background and cross-contamination. The efficiency of the combustion process (>95%) was ascertained by combusting samples spiked with a known amount of the model compound ^{14}C-anilazine prior to and after analyzing the samples.

All experiments were performed in a laboratory without sunlight to prevent photodegradation. Samples were exposed only briefly to artificial light during sample collection and preparation. Biodegradation was not impeded. Samples were stored in a refrigerator until measurements were conducted within approximately 2 or 3 wk. We

assumed that concentrations of the transformation products did not change during this time due to the low temperature environment.

The content of total organic C (TOC) in selected samples was measured using a TOC 5050A analyzer (Shimazdu, Duisburg, Germany). Samples for this purpose were frozen before TOC measurements.

4.3.2 Analysis of sulfadiazine and transformation products

The pig manure containing ^{14}C-labeled sulfonamides used in our studies was obtained from a feeding experiment conducted at Bayer AG Monheim where ^{14}C-SDZ with single labeling of the pyrimidine ring and ^{12}C-SDZ were administered to pigs in a ratio of 1:19. The specific radioactivity of SDZ in manure was 0.44 MBq mg^{-1}. After dosing, manure was collected, mixed, and stored at 4°C in darkness. The total ^{14}C concentration of the manure was 270 mg L^{-1} in mass equivalents of SDZ. Carbon-14-SDZ was provided by Bayer HealthCare AG (Wuppertal, Germany) as a powder with a purity of 99% and a specific radioactivity of 8.88 MBq mg^{-1}. The application solution for the experiments without manure was prepared by adding appropriate amounts of ^{14}C- and ^{12}C-SDZ (Sigma Aldrich, Germany) to a 0.01 mol L^{-1} $CaCl_2$ solution. Since the pH value of the manure was approximately 8, the SDZ application solutions were buffered to this pH value by adding low amounts of 0.01 mol L^{-1} NaOH. Since the added amounts of Na were very low, its presence should not have substantially affected the results.

The method of Lamshöft et al. (2007) was used to determine the transformation products in the manure. Briefly, 4 cm^3 of McIlvaine buffer (1 mol L^{-1} citric acid/1 mol L^{-1} Na_2HPO_4, 18.15 cm^3/81.85 cm^3; adjusted to pH 7) was added to centrifuging vials containing 1 g of homogenized manure. The extracts were shaken for 30 s with a vortex mixer, treated for 15 min in an ultrasonic bath, and centrifuged for 0.5 h (514 × g) in an Allegra 6 KR centrifuge (Beckmann Coulter, Palo Alto, CA). This procedure produced clear supernatants, which were transferred into high performance liquid chromatography (HPLC) vials and analyzed with radio HPLC (LB 509 detector, Berthold Technologies, Bad Wildbad, Germany). Our HPLC system included a reversed-phase column (Phenomenex Synergi Fusion RP 80, 250 by 4.6 mm), which was eluted with a mixture of water (490 cm^3) and methanol (10 cm^3), buffered with 0.5 cm^3 of a 25% H_3PO_4 solution. The injection volume was 0.25 cm^3 for each sample. A gradient with an increased amount of methanol was used for peak separation, starting with 100% water for 6 min. The methanol fraction

increased linearly to 27% during the first 23 min, then to 37% within the next 3 min, and to 47% during the following 2 min. The methanol part reached its maximum of 57% after 30 min. Sulfadiazine, N-Ac-SDZ, and 4-OH-SDZ could be detected using this HPLC method. The substances were identified according to their retention times compared with standards of SDZ and N-Ac-SDZ. The retention time of 4-OH-SDZ was known from previous experiments. Retention times of SDZ, N-Ac-SDZ, and 4-OH-SDZ were approximately 16.70, 20.18, and 15.60 min. The detection limit of the radio HPLC was about 3 μg L^{-1} mass equivalents of SDZ. For two manure extractions that we conducted, 7.6 and 8.3% of the radioactivity could not be assigned to a peak, probably due to sorption onto organic material.

Sulfadiazine and its main transformation products in the outflow samples were also separated using radio HPLC. Using the measurement protocol described above, four peaks could be distinguished in the chromatograms. In addition to SDZ and the two main transformation products, we also detected 4-[2-iminopyrimidine-1(2H)-yl]-aniline with a known retention time from previous experiments of approximately 6.2 min. The same measurement technique applied in previous experiments (Unold et al., 2009a) was also used here to detect SDZ and its transformation products in samples with concentrations below the detection limit of the HPLC radio detector. Outflow from the HPLC was collected during the retention times of SDZ and its transformation products, as well as within these time frames, for background correction. Solutes in three replicate samples were quantified with LSC using a counting time of 15 min, for which the samples were mixed with 10 cm^3 of the scintillation cocktail (Insta-Gel Plus, Canberra Packard GmbH, Dreieich, Germany). The detection limit of the LSC detector was 0.4 Bq, which corresponds to 0.045 ng mass equivalents of SDZ dissolved in an aliquot of the outflow sample. Non-zero concentrations were assigned to a solute when the measured radioactivity was >1.2 Bq, which was three times the detection limit of LSC. Otherwise its contribution was set to zero. Using this method, the transformation products could be quantified with the help of the specific radioactivity of ^{14}C down to a concentration of 0.5 μg L^{-1} mass equivalents of SDZ in the outflow samples. A background correction of the HPLC measurements was done and the method was validated by measuring a calibration curve. Triplicate measurements of total radioactivity in the samples were performed with LSC after mixing an aliquot of 0.5 cm^3 with 10 cm^3 of the scintillation cocktail. Selected samples were filtered (Centricon 10, Millipore, Billerica, MA) and total ^{14}C was measured before and after filtration. Since there

was no difference in the measurements, we concluded that solutes in the outflow samples were not attached to colloidal particles.

4.3.3 Theory of solute transport

The steady-state transport experiments on unsaturated repacked and undisturbed soil columns were analyzed as one- dimensional transport problems, assuming constant water contents and fluxes throughout the soil columns. Solute transport is commonly described using the convection–dispersion equation (CDE), which for conservative, non-reacting tracers during steady state flow conditions can be expressed as

$$\frac{\partial C}{\partial t} = -v\frac{\partial C}{\partial z} + D\frac{\partial^2 C}{\partial z^2} \quad , \tag{4.1}$$

where t is time [T], v is the average pore-water velocity [L T^{-1}], C is the solute concentration in the liquid phase [M L^{-3}], D is the dispersion coefficient [L^2 T^{-1}], and z is depth [L]. The parameters v and D for the Cl^- BTCs were estimated using a nonlinear parameter estimation procedure based on the Levenberg–Marquardt algorithm. We used the CXTFIT code (Toride et al., 1999), which analytically solves the CDE for appropriate boundary conditions. The estimated transport parameters (i.e., v and D) and the experimentally determined Darcian flux, q [L T^{-1}], were then used to evaluate the volumetric water content, $\theta = q/v$ [L^3 L^{-3}], and the longitudinal dispersivity, $\lambda = D/v$. These parameters were assumed to fully characterize the physical transport process and were fixed in subsequent transport simulations of reactive SDZ and its transformation products using a modified version 4.03 of HYDRUS-1D (Šimůnek et al., 2008).

Based on a previous study with SDZ BTCs (Unold et al., 2009a), a model concept with one reversible and one irreversible kinetic sorption site was used to analyze the BTCs of SDZ and its transformation products. The model concept (Figure 4.1) for the experiments was developed to account for all known processes. We included the transformation of N-Ac-SDZ into SDZ according to information from the literature (Berger et al., 1986). The irreversible sorption site was omitted for N-Ac-SDZ according to Förster et al. (2009), who found no significant sequestration of the N-Ac-SDZ metabolite in soils. Covalent coupling to organic material as described by Bialk and Pedersen (2008) is also unlikely for N-Ac-SDZ since the free aniline moiety is not available. A transformation from SDZ into 4-OH-SDZ was included in the model according to our experimental results using SDZ solutions.

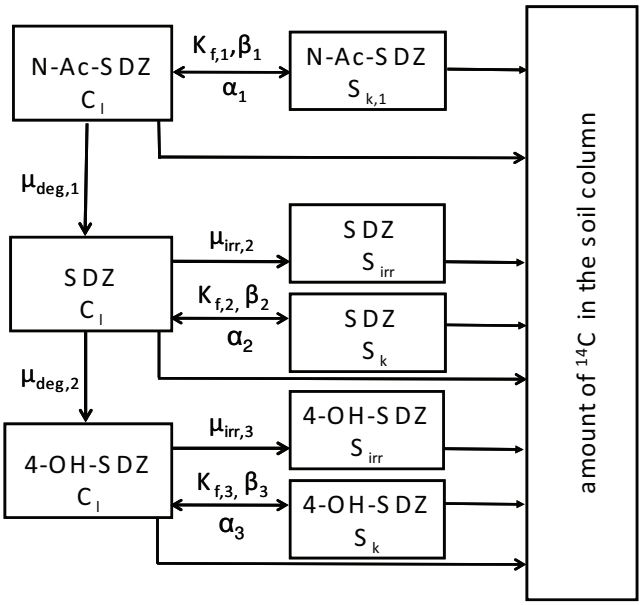

Figure 4.1. The conceptual model for the transport of SDZ and its transformation products in the experiments with manure.

Using the above model concept, the transport equation for each solute with the transformation chain can now be written as

$$\frac{\partial C_k}{\partial t} + \frac{\rho}{\theta}\frac{\partial S_{k,k}}{\partial t} = -\mathrm{v}\frac{\partial C_k}{\partial z} + D\frac{\partial^2 C_k}{\partial z^2} - \mu_{irr,k}C_k - \mu_{\mathrm{deg},k}C_k + \mu_{\mathrm{deg},k-1}C_{k-1} \qquad (4.2)$$

k=1,2,3 ,

where ρ is the soil bulk density [M L^{-3}], $S_{k,k}$ is the sorbed solute concentration at the kinetic sorption site [M M^{-1}], the subscript k indicates the kth solute, μ_{irr} [T^{-1}] is a first-order coefficient that is used to mimic irreversible sorption (Baek et al., 2003), and $\mu_{deg,k}$ [T^{-1}] is a first-order rate constant that accounts for the degradation of the kth solute into the solute k+1. The sorbed concentration at the sorption sites of the fully kinetic model was calculated as

$$\frac{\partial S_{k,k}}{\partial t} = \alpha_k (K_{f,k} C_k^{\beta_k} - S_{k,k}) \qquad (4.3)$$

,

where $K_{f,k}$ [$M^{1-\beta}_{solute}L^{3\beta}M^{-1}_{soil}$] is the Freundlich coefficient, β_k [-] is the Freundlich exponent and α_k [T^{-1}] is a first-order sorption rate coefficient.

While a flux-type boundary condition with zero concentration for all compounds was used as the upper boundary condition, the lower boundary condition was a zero-concentration gradient in the numerical solutions. Liquid-phase initial concentrations of SDZ and its transformation products in the uppermost centimeter of the soil profile were calculated using the initial total mass of solutes (Table 4.4) and water contents of the particular soil columns. In the experiments with the SDZ solution, all of the mass was initially contributed to SDZ since no transformation products were present in the input solution. For the fully kinetic model, all solid-phase concentrations were initially set to zero. While BTCs were available for each particular solute, only total ^{14}C measurements (i.e., the sum of all three solutes in both the liquid and the solid phases) were available for the various solutes in the soil columns at the end of the experiments. The HYDRUS-1D code was therefore modified to add the sorbed (both reversible and irreversible) and liquid concentrations of all three solutes in a particular degradation chain. Concentrations of the transformation products were lower than those of SDZ. To obtain adequate fits for all BTCs during the simultaneous fitting process, the data points of N-Ac-SDZ, 4-OH-SDZ, and the total concentration profile were weighed relative to SDZ according to

$$w = \frac{n_{BTC_{\deg},Profile}}{n_{SDZ}} \frac{\sum_{i=1}^{n_{SDZ}} C_{i,SDZ}}{\sum_{i=1}^{n_{BTC_{\deg},Profile}} C_{i,BTC_{\deg},Profile}} \quad , \tag{4.4}$$

where n accounts for the number of data points of the BTCs or concentration profiles of SDZ and its transformation products (BTC_{deg}), and C_i are measured concentrations at the i^{th} time for a particular BTC expressed in mass equivalents of SDZ per volume of solution (or per volume of soil for the concentration profile).

The goodness of fit for particular solutes and BTCs was expressed using the mean absolute error:

$$MAE = \frac{1}{n} \Sigma \mid f_i - y_i \mid \quad , \tag{4.5}$$

where n is the number of data points on a particular BTC, and where f_i and y_i are predicted and measured values, respectively.

Except for several BTCs of N-Ac-SDZ and 4-OH-SDZ, most BTCs showed extensive tailing on a logarithmic scale, a phenomenon that was also observed in two previous studies (Wehrhan et al., 2007; Unold et al., 2009a). In these two studies, the numerical models were fitted to logarithmically transformed outflow ^{14}C concentrations to better capture the long tailing. Fitting of logarithmically transformed data had the advantage of adding additional weight to, and thus properly describing, low concentration values, while at the same time decreasing the weight on, and hence probably describing less well, the concentration of the peaks. A disadvantage of fitting log-transformed data is that the model may also capture less well the overall leached mass. Therefore in this study the observed data were fitted without the logarithmic transformation.

4.4 Results and Discussion

4.4.1 Chloride breakthrough curves

Chloride BTCs (Figure 4.2) were measured on soil columns before and after the incorporation of pig manure or the SDZ stock solution (except for the repacked column of Soil K treated with the SDZ solution, KrepSOL, for which only the "before" BTC was measured).

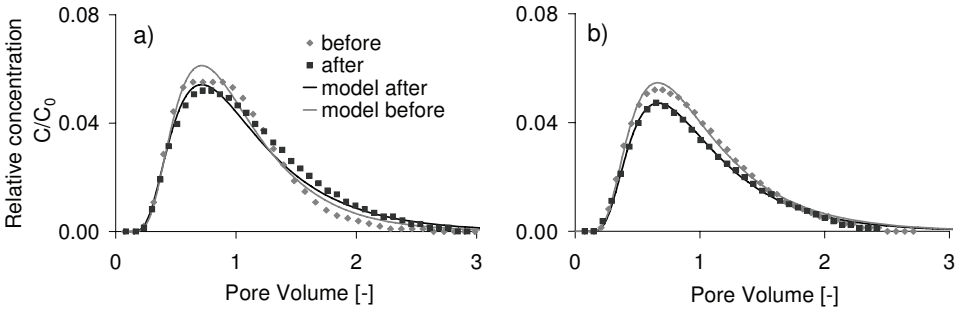

Figure 4.2. Selected Cl^- breakthrough curves for soil columns KundMAN (a) and MundMAN (b) measured on soil columns before and after incorporating pig manure.

Time is expressed in Figure 4.2 as dimensionless pore volumes, i.e., the time needed to replace all the water in the soil column. Although most measured Cl^- BTCs were very similar before and after the SDZ experiments, some BTCs differed slightly. There was no visible trend in Cl^- BTCs that would indicate that incorporation of manure or the stock solution affected the soil structure. Transport parameters obtained by fitting the Cl^- BTCs

after the incorporation of manure were used to model the BTCs of SDZ and its transformation products, except for soil column KrepSOL, for which the "after" BTC was not available. Fitted transport parameters for the Cl^- BTCs are summarized in Table 4.3.

Table 4.3: Transport parameters for the conservative tracer Cl^-: *v* is pore-water velocity, *D* is dispersion coefficient, R^2 is a measure of the relative magnitude of the total sum of squares associated with the fitted equation, ρ is bulk density, λ is dispersivity and θ is water content.

soil column[a]	*v* [cm h^{-1}]	*D* [cm^2 h^{-1}]	Pore Volume	R^2	λ [cm]	θ [cm^3 cm^{-3}]
KrepMAN	0.56 (±0.02) [b]	0.41 (±0.04)	17.9	0.97	0.74	0.32
KrepSOL	0.78 (±0.03)	0.42 (±0.10)	12.7	0.94	0.54	0.25
KundMAN	0.54 (±0.01)	0.85 (±0.04)	16.4	0.99	1.57	0.37
$KundMAN_i$	0.53 (±0.01)	0.45 (±0.02)	18.7	0.99	0.84	0.34
MrepMAN	0.44 (±0.01)	0.25 (±0.02)	22.7	0.99	0.57	0.43
MrepSOL	0.54 (±0.01	0.29 (±0.02)	18.5	0.99	0.54	0.36
MundMAN	0.46 (±0.01)	0.71 (±0.02)	21.7	0.99	1.54	0.42

[a] The first letter represents soil type (either K or M), columns were either repacked (rep) or undisturbed (und), and either manure (MAN) or a stock solution (SOL) was incorporated into the column; subscript i denotes intermittent infiltration.
[b] Values in parentheses indicate 95% confidence intervals.

The dispersivity of two of the three undisturbed soil columns was higher than those of the repacked soil columns, indicating more heterogeneity in the original soil material. Since Cl– BTCs from both repacked and undisturbed soil columns could be described well using the CDE for conservative tracers, we concluded that physical non-equilibrium processes, such as preferential flow, did not influence solute transport in our columns. The Cl– BTC for the soil column subject to transient water fl ow (i.e., intermittent irrigation) could also be described well using the CDE. Intermittent irrigation was used to generate higher water contents and higher fluxes to induce macropore flow, which apparently did not happen.

4.4.2 ^{14}C breakthrough curves and concentration profiles

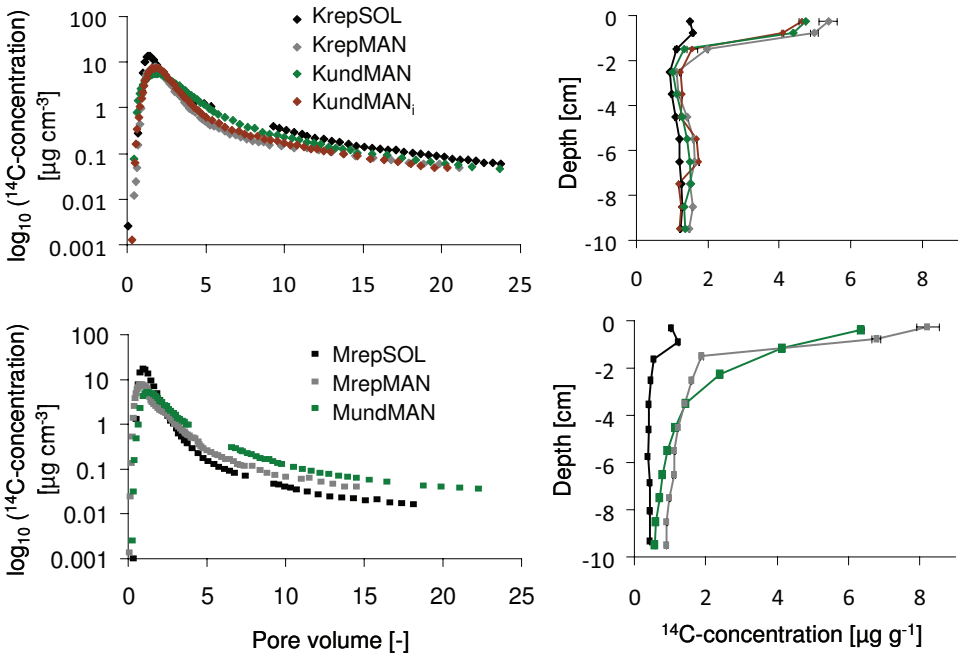

Figure 4.3. ^{14}C BTCs for a) soil K and c) soil M, as well as distributions of ^{14}C in the soil column profiles for b) soil K and d) soil M. ^{14}C concentrations are given in mass equivalents of SDZ.

Figure 4.3 presents ^{14}C BTCs and profiles in the soil columns for all column experiments. The amounts of ^{14}C that were eluted or that remained in the soil columns, as well as the sums of both, are summarized in Table 4.4. Solute mass recoveries were, in most cases, between 95 and 105%. Although the manure was stirred before its application, the applied radioactivity in the experiments with manure may differ due to in-homogeneities in the substrate. This explains why some mass recoveries are >100%. Recovery rates for the experiments with the SDZ solution were <100%. The missing amount can be assigned to the profile data, since mass errors in BTCs are less likely because more data points were available and more precise experimental techniques had been used. Peaks in the ^{14}C BTCs for the loamy sand (Soil K) appeared after approximately 1.3 pore volumes, which was about 0.6 pore volumes later than in the silt loam (Soil M). There are several factors indicating more extensive sorption in Soil M. Due to the larger

clay content of Soil M, a larger specific surface area of the mineral phase can be expected, which is also reflected in the cation exchange capacity. Additionally, the fraction of TOC was higher in this soil. One possible explanation for the faster observed transport is the amphoteric character of SDZ, which causes a pH-dependent sorption of sulfonamides (Kurwadkar et al., 2007; Gao and Pedersen, 2005). The average pH value in the outflow samples from Soil M was higher than from Soil K, as was shown for the repacked soil columns with manure (Table 4.1). This leads to the presence of relatively more of the less sorbing anionic SDZ species in Soil M (89%) than in Soil K (68%). Calculations of the species distribution were done according to Schwarzenbach et al. (2003). Another factor that may cause the difference in apparent transport velocities between the soils is the kinetic component of SDZ sorption. All BTCs were characterized by a fast initial increase in concentration at the beginning and extended tailing after the peak concentration was reached. In general, the peak height was influenced by the dispersivity of the soil columns. Undisturbed soil columns of both soils with manure added (KundMAN and MundMAN) with dispersivities of around 1.5 cm had about 2 μg cm^{-3} lower peak concentrations than the repacked soil columns (7.75 μg cm^{-3}), with dispersivities ranging from 0.54 to 0.84 cm. Similar ^{14}C peak concentrations were observed for the undisturbed soil column with intermittent irrigation and the repacked soil column with constant irrigation (Soil K), indicating that a similar dispersivity was more important than the modality of irrigation. Of the two columns receiving the SDZ solution, the ^{14}C peak in Soil K (13.8 μg cm^{-3}) was lower than the corresponding ^{14}C peak of Soil M (17.4 μg cm^{-3}), although both had similar dispersivities. While Soil K showed similar amounts of ^{14}C (71%) eluted from both the undisturbed and repacked columns with manure, the amounts were different for the repacked (75%) and undisturbed (62%) soil columns of the silt loam (Table 4.4). Compared with the experiments with the SDZ solution, lower ^{14}C peaks and slightly lower eluted amounts of ^{14}C were observed for the soil columns spiked with manure. These lower eluted amounts in the experiments with manure can be explained using the ^{14}C-concentration profiles. Although the highest ^{14}C concentrations were found in the first centimeter of all soil columns, these surface layer concentrations were much higher for the columns with manure. We hypothesize that this accumulation of ^{14}C in the uppermost centimeter of the soil columns with manure was caused by the sorption of SDZ and its transformation products to colloidal particles in the manure. These particles then may have been unable to move through the soil because of straining in small pores. This assumption was supported

by the fact that, during the HPLC measurements of the manure extracts, approximately 8% of the radioactivity could not be related to a peak, probably due to adsorption to organic material. Filtration of manure particles dependent on the pore size distribution of the porous medium was shown by Bradford et al. (2006). They determined concentration profiles of manure particles in sandy soil columns and similarly found that most manure particles were retained in the uppermost layer.

Table 4.4: Mass fractions of ^{14}C in the breakthrough curves (BTCs) and the soil profile and mass fractions (in %) of the parent compound sulfadiazine (SDZ) and the transformation products in the BTCs.

Column[a]	Radio-activity in BTC [%]	Radio-activity in the soil profile [%]	Total mass recovery [%]	SDZ [%]	Acetyl-SDZ [%]	OH-SDZ [%]	4-[2-iminopyri-midine-1(2H)-yl]-aniline [%]
Manure1				67.7 [b]	14.9 [b]	17.4 [b]	n.d. [c]
Manure2 [d]				82.4 [b]	8.7 [b]	8.8 [b]	n.d.
KrepMAN	70.3	32.3	102.6	76.0	9.7	17.3	n.d.
KrepSOL	76.0	19.0	95.0	75.9	n.d.	7.8	16.1
KundMAN	70.9	30.5	101.4	78.0	9.9	15.2	n.d.
$KundMAN_i$	74.2	28.3	102.5	80.7	8.9	12.5	n.d.
MrepMAN	75.3	29.0	104.3	74.0	7.7	18.5	n.d.
MrepSOL	86.0	6.4	92.4	90.0	n.d.	1	12.0
MundMAN[†]	62.0	37.8	99.8	91.0	7.4	4.8	0.9

[a] The first letter represents soil type (either K or M), columns were either repacked (rep) or undisturbed (und), and either manure (MAN) or a stock solution (SOL) was incorporated into the column; subscript i denotes intermittent infiltration.
[b] The amount of ^{14}C which could not be associated with a peak was distributed among SDZ and the transformation products
[c] n.d. indicates that the transformation product could not be detected
[d] Manure 2 was applied to soil column MundMAN

The presence of manure may also influence sorption behavior in other ways. Sukul et al. (2008a) found in batch experiments an increased sorption of SDZ onto soils of different origins when manure was present. Kreuzig and Höltge (2005) also found in batch experiments a higher tendency of SDZ to form nonextractable residues in the presence of manure with 7-d-old SDZ. In their lysimeter studies in which an SDZ test slurry was incorporated into undisturbed profiles, Kreuzig and Höltge (2005) observed similar concentration profiles as in our soil columns. Distinct differences were observed in the ^{14}C concentration profiles between the sand and loam columns. The observed amount of ^{14}C in

the first centimeter of the loam soil (Soil M) was higher than in the sand soil (Soil K). There are two explanations for this phenomenon. On the one hand, this finding corresponds with the results of Schmidt et al. (2008), who studied the formation of nonextractable residues of manure-based ^{14}C-SDZ to the same two soils. For short contact times, the nonextractable part was higher in a silt loam (Soil M) (69%) than in a loamy sand (Soil K) (54%). On the other hand, smaller pore sizes could have led to enhanced filtration in this soil. The ^{14}C concentrations gradually decreased with depth in the experiments with manure on Soil M. The ^{14}C concentrations in the soil profiles were more or less constant below the first centimeter in the experiments with Soil K and in the repacked column of Soil M treated with the SDZ solution (MrepSOL), although in the Soil K columns with manure a slight increase in concentrations was observed below a depth of about 4 cm.

4.4.3 Breakthrough curves of SDZ and its transformation products

Both experimental and simulated BTCs of SDZ and its transformation products 4-OH-SDZ, *N*-Ac-SDZ, and 4-[2-iminopyrimidine-1(2*H*)-yl]-aniline are presented in Figures 4.4 and 4.5. Although no transformation products were present in the input solution of the experiments with the SDZ solution (KrepSOL and MrepSOL), both 4-OH-SDZ and 4-[2-iminopyrimidine-1(2*H*)-yl]-aniline were detected in the outflow from these columns (Figure 4.4). Mass fractions of particular transformation products for all soil columns are listed in Table 4.4. For the experiments with the SDZ solution, the mass fraction of SDZ was largest compared with its transformation products in all soil columns. The 4-[2-iminopyrimidine-1(2*H*)-yl]-aniline was the main transformation product, followed by 4-OH-SDZ, which provided only a minor contribution. The transformation from SDZ into 4-[2-iminopyrimidine-1(2*H*)-yl]-aniline and 4-OH-SDZ was higher in Soil K than in Soil M. The 4-[2-iminopyrimidine-1(2*H*)-yl]-aniline was detected in the outflow of the columns with the SDZ solution and also in the manure experiment on the undisturbed Soil M (MundMAN), but at very low concentrations. Sukul et al. (2008b) identified this compound to be the major photoproduct of SDZ, but they observed it also as a product of biodegradation. We can assume that 4-[2-iminopyrimidine-1(2*H*)-yl]-aniline was formed in the soil column, since our experiments were conducted in the dark. So far we have no explanation why we detected this transformation product in the experiments with the SDZ solution and not in the experiments with manure.

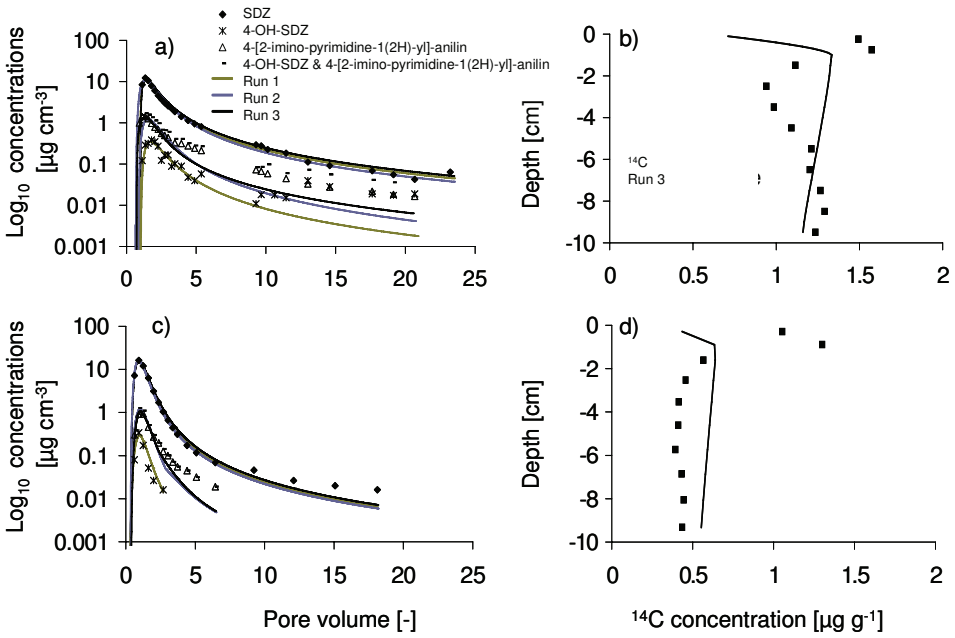

Figure 4.4. Breakthrough curves of sulfadiazine (SDZ) and its transformation products 4-OH-SDZ and 4-[2-iminopyrimidine-1(2*H*)-yl]-aniline, as well as ^{14}C-concentration profiles for the experiments with the SDZ solution for the (a) and (b) KrepSOL experiments and (c) and (d) MrepSOL experiments. Simulations using a model with one reversible kinetic and one irreversible sorption site are also presented. Concentrations are given in mass equivalents of SDZ. Run 1: models were fitted to breakthrough curves (BTCs) of SDZ and 4-OH-SDZ; Run 2: models were fitted to BTCs of SDZ and 4-[2-iminopyrimidine-1(2*H*)-yl]-aniline; Run 3: models were fitted to BTCs of SDZ and the sum of both transformation products as well as to the ^{14}C data in the profile.

In the soil columns with manure (Figure 4.5), SDZ, 4-OH-SDZ, and *N*-Ac-SDZ were detected in the outflow as well as in the manure at the time of application. Mass fractions of the two transformation products in the outflow samples differed with time. While *N*-Ac-SDZ was characterized by a fast dissipation, the mass fraction of 4-OH-SDZ was stable or increased. According to these results, we can expect a constant release of low 4-OH-SDZ concentrations from soils in the long term, similarly as for SDZ. Note that manure incorporated in the undisturbed Soil M column (MundMAN) had lower mass fractions of 4-OH-SDZ and *N*-Ac-SDZ, probably due to advanced aging. The lower fraction of applied transformation products was also reflected in their lower fractions in the column effluents (Table 4.4).

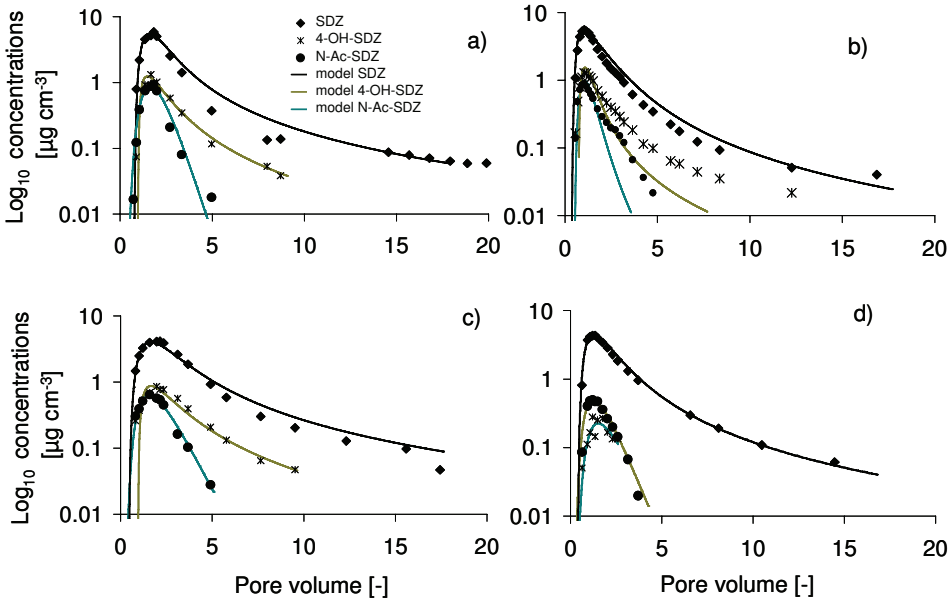

Figure 4.5. Breakthrough curves of sulfadiazine (SDZ), 4-OH-SDZ, and *N*-Ac-SDZ in repacked and undisturbed soil columns of Soils K and M for the experiments with manure, as well as simulations using a model with one reversible kinetic and one irreversible sorption site: (a) KrepMAN, (b) MrepMAN, (c) KundMAN, and (d) MundMAN experiments. Concentrations are given in mass equivalents of SDZ.

4.4.4 BTC of the organic material

Figure 4.6 shows BTCs of ^{14}C concentrations, the electrical conductivity, pH, and the TOC for soil column KundMAN. The TOC reflects the amount of organic substances in the outflow samples. Changes in pH were relatively small, ranging from 6.6 to 7.0. This indicates fast dilution of the slurry, which had a higher pH of 8. The peak of the electrical conductivity appeared a short time before the peak in ^{14}C, probably reflecting the breakthrough of the main anion in the manure (i.e., Cl^-). The peak in TOC also appeared shortly before the peak in ^{14}C, at the same time as the peak in the electrical conductivity. This indicates that the main part of SDZ was not transported together with the dissolved organic material (i.e., facilitated transport).

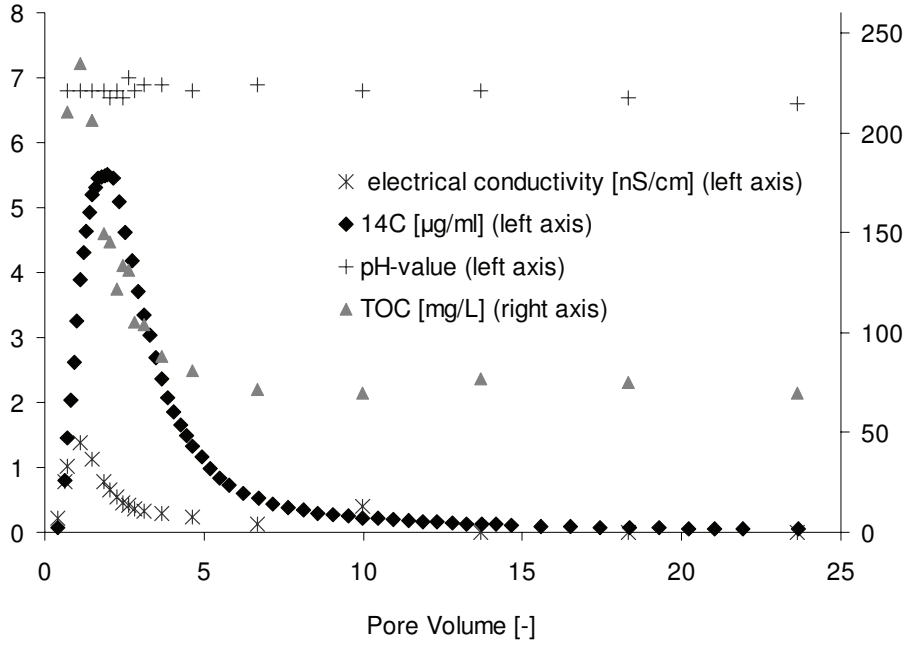

Figure 4.6. Breakthrough curves of ^{14}C, electrical conductivity, and total organic C (TOC) measured in the soil column KundMAN after the manure application.

We could not observe any differences in ^{14}C concentrations between filtered and unfiltered outflow samples. These findings are consistent with observations by Thiele-Bruhn and Aust (2004), who did not find any sulfonamide losses in their batch experiments during solid phase extraction with the supernatants. Solid-phase extraction is supposed to remove the dissolved organic material (pig slurry and soil organic matter) together with the adsorbed substances. We therefore conclude that although transport facilitated by dissolved organic C may not be completely ruled out, this process does not seem to be a major transport mechanism involved in the leaching of SDZ and its transformation products. The outflow TOC concentrations, however, did not reach zero during the experiments (Figure 4.6), thus suggesting a continuous release of organic material. While this supports the hypothesis that the ^{14}C accumulation in the first centimeter of the soil columns is caused by the filtration of organic material, in the long term the release of organic material, possibly together with bound SDZ residues, may still be possible.

4.4.5 Modeling Results

Similarly to Unold et al. (2009a), we selected a transport model with one kinetic reversible and one kinetic irreversible sorption site. Sorption on the reversible site was described assuming a first-order process and Freundlich-type sorption. The conceptual model could describe most curves quite well (see Figures 4.4 and 4.5). The long tailing is characteristic for chemical non-equilibrium processes and nonlinear sorption. The tailing could not be described solely by assuming a fully kinetic process, however. It was also necessary to consider nonlinearity of the sorption process by using low values of the Freundlich exponent, β. Initial estimates of the Freundlich parameters were selected in a way so that the tailing was described well. This was accomplished by choosing a Freundlich exponent <0.44, similar to the findings of the previous studies of Wehrhan et al. (2007) and Unold et al. (2009a). In the experiments of Kurwadkar et al. (2007), a linear sorption isotherm was able to describe the sorption data of sulfonamides for concentrations up to approximately 0.5 mg L^{-1}. Concentrations of both the applied solution and the manure were much higher (272 mg L^{-1}) in our study. Because of the much wider concentration range in our study, we can assume strong nonlinear sorption behavior.

4.4.5.1 Experiments with the SDZ solution

The modeling process for each experiment with the SDZ solution was split into three parts, since it was not possible with HYDRUS-1D to simultaneously fit degradation from SDZ into 4-OH-SDZ and 4-[2-iminopyrimidine-1(2H)-yl]-aniline. In the first run, the BTCs of SDZ and 4-OH-SDZ were fitted without considering the profile data. In the second model run, the same was done for 4-[2-iminopyrimidine-1(2H)-yl]-aniline. The profile data were not included in these optimization runs since degradation into a particular transformation product was compensated by an increase in irreversible SDZ sorption. Irreversible sorption of the transformation products was fixed to zero since the rate of their formation (degradation of SDZ) would have otherwise been influenced by this process. In the third run, concentrations of the two transformation products were summed up and the resulting BTC was fitted together with the BTC of SDZ and the ^{14}C concentration profile data. The degradation coefficient in this case refers to the sum of 4-OH-SDZ and 4-[2-iminopyrimidine-1(2H)-yl]-aniline degradation. For all transformation products that showed very low concentrations in the SDZ-solution experiments, we fixed the kinetic

sorption rate coefficient, α, at the very high value of 10 h^{-1}, thus assuming that sorption was basically an equilibrium process. This was done to reduce the number of optimized parameters and to increase the reliability of the optimized sorption parameters, which had in some cases large confidence intervals. Values of the Freundlich exponents for SDZ and its transformation products were closely correlated with the K_f values and therefore were fixed in optimization model runs to values that were needed to describe the tailing of the BTCs. The model could describe the BTCs of SDZ and 4-OH-SDZ reasonably well, except for the observed increase in the 4-OH-SDZ concentration after 10 pore volumes. There is a clear difference between the two soils in terms of the Freundlich sorption coefficients for SDZ (Table 4.5). While the Freundlich sorption coefficients for the silt loam are lower than for the loamy sand, the Freundlich exponents are in a similar range. This indicates a lower sorption capacity for the silt loam and reflects the earlier breakthrough in this soil. On the other hand, the lower kinetic sorption rate reflects the slightly faster transport in Soil M.

Optimized Freundlich parameters for 4-OH-SDZ in the loamy sand produced an isotherm with a much lower sorption capacity than for SDZ. No sorption parameters were fitted for this transformation product for the silt loam because of very low observed concentrations. Sorption capacities for 4-[2-iminopyrimidine-1(2H)-yl]-aniline were in a similar range in both soils and for Soil K the sorption capacity for 4-[2-iminopyrimidine-1(2H)-yl]-aniline was lower than for 4-OH-SDZ. Breakthrough curve tailing of 4-[2-iminopyrimidine-1(2H)-yl]-aniline in both soils could not be described with the model, although the Freundlich exponent was in a range low enough to describe the tailing of SDZ and 4-OH-SDZ in the experiments with manure.

In the first model run to optimize the BTC parameters of 4-OH-SDZ and SDZ, the profile data were considerably overestimated for both soils since the amount of SDZ that degraded to form 4-[2-iminopyrimidine-1(2H)-yl]-aniline was added to irreversible sorption. While the same tendency was observed for Soil K for the model run that optimized the BTC parameters of SDZ and 4-[2-iminopyrimidine-1(2H)-yl]-aniline, this run described the profile data best for Soil M. The reason is that the effect of 4-OH-SDZ formation on irreversible sorption was negligible. Since the third model run included the profile data (Figure 4.4), this run was expected to provide the best fits. While this was true for Soil K, we overestimated data points in deeper layers of soil M. Increased irreversible sorption to reduce the misfits between observed and simulated values in the top layer was the reason for this overestimation. This effect was smaller for Soil K, where the difference

between concentrations in the top and deeper soil layers was smaller. Average concentrations in the soil profiles were captured reasonably well by the model, although the sorption process was probably not correctly understood. This became obvious from the opposite trends between the data and the model in the uppermost layers.

Compared with previous experiments with SDZ solutions (Unold et al., 2009a), optimized values of the kinetic sorption rate coefficient, α, were higher, indicating that kinetic sorption was faster when SDZ was incorporated directly into the soil. In several cases, sorption was even close to equilibrium. Therefore, some BTCs could be fitted reasonably well by assuming equilibrium reversible sorption, but in such cases the initial increase in the BTCs was predicted less well.

4.4.5.2 Experiments with manure

For each experiment with manure, the BTCs of SDZ and its transformation products were fitted simultaneously together with the concentration profile data below the uppermost 1 cm. Concentrations in the top 1 cm were significantly higher than in the rest of the soil profile. We hypothesized that the high sorbed concentrations in the uppermost soil column layers were the result of interactions between the organic material of the slurry and the soil structure. We did not attempt to model these processes. Therefore, the two uppermost data points in the profiles were not included in the objective function and hence we did not expect that the high sorbed concentrations in the top of the soil columns would be reproduced by the model. The Freundlich exponents for SDZ were fixed to values optimized to experimental data with the SDZ solution to avoid large parameter correlations with the Freundlich distribution coefficients. The kinetic sorption rate coefficients for the transformation products were again fixed to 10 h^{-1} to decrease the number of parameters and to increase parameter reliability. Since most BTCs of *N*-Ac-SDZ did not show much tailing, its Freundlich exponent was fixed to one, thus assuming linear sorption in all soil columns except for the repacked Soil M column treated with manure (MrepMAN). In preliminary model runs, the tailing of 4-OH-SDZ concentrations was not captured well since it was described by only a few data points. Therefore, we increased the weights on the tailing concentrations compared with the data points in the peak according to Eq. [4.4]. For Soil K, the Freundlich exponent was fitted for the repacked soil column with the manure application and fixed for the undisturbed soil columns. For Soil M, this parameter was

Table 4.5: Fitting parameters for the breakthrough curves (BTCs) of sulfadiazine (SDZ), 4-OH-SDZ, and 4-[2-imino-pyrimidine-1(2*H*)-yl]-aniline for the experiments with the SDZ solution (SOL) in repacked columns (rep) of Soils K and M. Run 1: parameters were fitted to the BTC data of SDZ and 4-OH-SDZ; Run 2: parameters were fitted to the BTC data of SDZ and 4-[2-imino-pyrimidine-1(2*H*)-yl]-aniline; Run 3: parameters were fitted to the BTC data of SDZ, the ^{14}C-profi le data, and the sum of the BTCs of both transformation products.

Parameter[a]		KrepSol Run 1	KrepSol Run 2	KrepSol Run 3	MrepSOL Run 1	MrepSOL Run 2	MrepSOL Run 3
K_{f1} [$\mu g^{1-\beta} cm^{3\beta} g^{-1}$]	SDZ	1.18 (±0.03)	1.20 (±0.04)	1.29 (±0.07)	0.52(±0.03)	0.55 (±0.04)	0.50 (±0.1)
β_1 [-]	SDZ	0.38[c]	0.38[b]	0.38[b]	0.44[c]	0.44[b]	0.44[b]
μ_{irr1} [h^{-1}]	SDZ	0.035 (±0.004)	0.026 (±0.002)	0.018 (±0.003)	0.010 (±0.002)	0.0044 (±0.002)	0.006 (±0.001)
μ_{deg1} [h^{-1}]	SDZ	0.0036 (±0.0002)	0.012 (±0.0006)	0.011 (±0.001)	0.0016(±0.0001)	0.0061 (±0.0002)	0.0076 (±0.002)
α_1 [h^{-1}]	SDZ	10[b]	10[b]	0.74 (±0.3)	0.50 (±0.09)	0.43 (±0.07)	0.55 (±0.4)
MAE		0.13	0.16	0.23	0.028	0.086	0.078
		4-OH-SDZ	**4-[2-imino-pyrimidine-1(2H)-yl]-anilin**	**Sum of both transformation products**	**4-OH-SDZ**	**4-[2-imino-pyrimidine-1(2H)-yl]-anilin**	**Sum of both transformation products**
K_{f2} [$\mu g^{1-\beta} cm^{3\beta} g^{-1}$]	4-OH-SDZ /4-[2-imino-pyrimidine-1(2H)-yl]-aniline/ Sum of both	0.098 (±0.008)	0.044 (±0.03)	0.12 (±0.003)	0[a]	0.052 (±0.009)	0.36 (±0.05)
β_2 [-]	4-OH-SDZ /4-[2-imino-pyrimidine-1(2H)-yl]-aniline/ Sum of both	0.53[c]	0.27[c]	0.50[c]	0[a]	0.72[c]	0.72[c]
μ_{irr2} [h^{-1}]	4-OH-SDZ /4-[2-imino-pyrimidine-1(2H)-yl]-aniline/ Sum of both	0[b]	0[b]	0[b]	0[a]	0[b]	0[b]
α_2 [h^{-1}]	4-OH-SDZ /4-[2-imino-pyrimidine-1(2H)-yl]-aniline/ Sum of both	10[b]	10[b]	10[b]	0[b]	10[b]	10[b]
MAE		0.023	0.09	0.12	0.035	0.036	0.032
$MAE_{profile}$		0.79	0.35	0.21	0.51	0.19	0.25
Eluted [%]		59.4	65.0	72.3	75.4	80.9	0.77
R^2		1	0.99	0.98	0.99	1	0.98

[a] K_{fj}, Freundlich coefficient for solute *j*; β_j, Freundlich exponent for solute *j*; μ_{irrj}, irreversible sorption rate for solute *j*; μ_{degj}, transformation rate of solute *j*; αj, kinetic sorption rate of solute *j*; MAE, mean absolute error; Eluted, mass eluted out of the soil column.
[b] Parameter was fixed
[c] Parameter was fixed at a value determined in a previous model run

fitted for each soil column separately, since no extended tailing for the 4-OH-SDZ BTC was observed for the undisturbed column treated with manure (MundMAN).

The relatively low transformation rates from SDZ into 4-OH-SDZ as estimated from the experimental data with the SDZ solution were used to model the experiments with manure. A possible transformation reaction from 4-OH-SDZ into another product was not included in the model, since no additional product was detected in the outflow samples. The model with optimized parameters produced reasonable descriptions of the transport of SDZ and its two transformation products for the experiments with manure. Four examples are presented in Figure 4.5. Similarly as for the experiments with the SDZ solution, the SDZ sorption capacity for the experiments with manure was lower for Soil M than for Soil K, but the difference was smaller. The same tendency in *K*f values as for SDZ was found for *N*-Ac-SDZ, and partly also for 4-OH-SDZ, for which the soil column MrepMAN had a similar Freundlich coefficient as the soil column KrepMAN. For 4-OH-SDZ, fitted Freundlich exponents were similar as for SDZ but the Freundlich coefficients were lower, indicating a lower sorption capacity for 4-OH-SDZ. On the other hand, the irreversible sorption rate was higher for 4-OH-SDZ and thus the overall sorption may be similar. Since linear sorption was found for *N*-Ac-SDZ in most soil columns, the sorption capacity was lower than for SDZ only when the concentration was <8 μg cm^{-3}. In our experiments, both higher and lower concentrations were present. Fitted Freundlich coefficients for SDZ in the experiments with manure were higher than for the experiments with the SDZ solution for both soils, reflecting the slightly higher sorbed amounts in the experiments with manure. For Soil K, the kinetic effect was more distinct for the experiments with manure than for the experiments with the SDZ solution (Table 4.6). There was no clear difference in the kinetic sorption rates α in the experiments with manure between the two soils. The ^{14}C-concentration profiles were described quite well in the deeper soil layers below the depth of application, where they reached more or less constant values (Figure 4.7). Simulations for cases where no profile data were included in the objective function led to similar results (data not shown).

Table 4.6: Fitting parameters for the breakthrough curves (BTCs) of sulfadiazine (SDZ), 4-OH-SDZ, and *N*-Ac-SDZ for the experiments with manure (MAN) on columns of Soil K or M that were either repacked (rep) or undisturbed (und); subscript i denotes intermittent infiltration.

Parameter[a]		KrepMAN	KundMAN	KundMANi	MrepMAN	MundMAN
K_{f1} [$\mu g^{1-\beta} cm^{3\beta} g^{-1}$]	N-Ac-SDZ	0.30 (± 0.02)	0.37 (± 0.03)	0.35 (± 0.05)	0.16 (± 0.02)	0.25 (± 0.02)
β_1 [-]		1 [b]	1 [b]	1 [b]	0.70[c]	1 [b]
μ_{deg1} [h^{-1}]		0.063 (± 0.006)	0.067 (± 0.007)	0.053 (± 0.008)	0.054 (± 0.008)	0.040 (0.005)
α_1 [h^{-1}]		10 [b]	10 [b]	10 [b]	10 [b]	10 [b]
MAE		0.05	0.03	0.05	0.09	0.02
K_{f2} [$\mu g^{1-\beta} cm^{3\beta} g^{-1}$]	SDZ	1.49 (± 0.05)	1.58 (± 0.1)	1.53 (± 0.1)	1.18 (± 0.1)	1.03 (± 0.06)
β_1 [-]		0.38 [b]	0.38 [b]	0.38 [b]	0.44 [b]	0.44 [b]
μ_{irr1} [h^{-1}]		0.012 (± 0.002)	0.0054 (± 0.002)	0.0061 (± 0.002)	0.0078 (± 0.003)	0.017 (± 0.004)
μ_{deg1} [h^{-1}]		0.0036 [b]	0.0036 [b]	0.0036 [b]	0.0016 [a]	0.0016 [b]
α_2 [h^{-1}]		0.57 (± 0.07)	0.36 (± 0.1)	0.68 (± 0.2)	0.13 (± 0.02)	0.51 (± 0.2)
MAE		0.19	0.15	0.31	0.33	0.13
K_{f1} [$\mu g^{1-\beta} cm^{3\beta} g^{-1}$]	4-OH-SDZ	0.39 (± 0.04)	0.52 (± 0.06)	0.50 (± 0.007)	0.19 (± 0.04)	0.41 (± 0.04)
β_1 [-]		0.44[c]	0.44 [b]	0.44 [b]	0.41[c]	1[c]
μ_{irr1} [h^{-1}]		0.040 (± 0.005)	0.035 (± 0.007)	0.033 (± 0.007)	0.036 (± 0.006)	0.090 (± 0.009)
α_3 [h^{-1}]		10 [b]	10 [b]	10 [b]	10 [b]	10 [b]
MAE		0.07	0.09	0.09	0.13	0.03
MAE profile		0.84	0.73	0.78	1.43	1.30
R^2		0.98	0.97	0.97	0.95	0.99
Eluted [%]		72.3	75.1	74.2	75.3	63.7

[a] K_{fj}, Freundlich coefficient for solute *j*; β_j, Freundlich exponent for solute *j*; μ_{irrj}, irreversible sorption rate for solute *j*; μ_{degj}, transformation rate of solute *j*; αj, kinetic sorptio rate of solute *j*; MAE, mean absolute error; Eluted, mass eluted out of the soil column.
[b] Parameter was fixed
[c] Parameter was fixed at a value determined in a previous model run

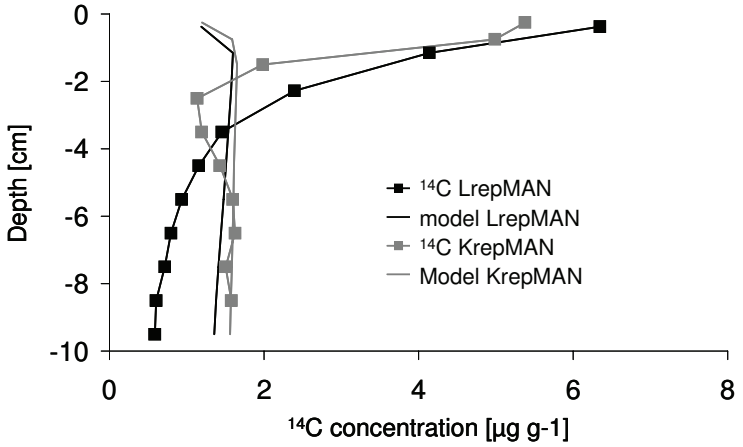

Figure 4.7. Carbon-14 distributions in soil columns KrepMAN and MrepMAN and simulations using a model with one reversible and one irreversible kinetic sorption site. The ^{14}C concentrations are given in mass equivalents of sulfadiazine.

Eluted solute masses were described quite well with the numerical model, which over- or underestimated the maxima by only about 5%. Since the mass in the uppermost layer of the soil columns of the experiments with manure was not included in the optimization, the model compensated for this missing mass by slightly overestimating concentrations below the 1-cm depth or by predicting higher eluted masses (KundMAN and KundMANi). Because of the complex nature of the invoked transport model, it was difficult to find unique solutions; however, the BTCs could not be described with parameter combinations out of the range of the fitted ones. Optimized parameters for the Freundlich isotherm characterize the sorption equilibrium state and thus can only be compared with sorption parameters from batch experiments determined when equilibrium is reached. This was the case for the batch experiments of Kurwadkar et al. (2007) and Sukul et al. (2008a). In both studies, the Freundlich exponents for sulfonamides were higher than in our study. In the study of Sukul et al. (2008a), they were even >1. An explanation for the lower exponents fitted to our transport experiments is that a kinetic process leading to extended tailing may partly mask strong sorption nonlinearity. To compare our results with the results reported in these two studies, we calculated the sorption capacity for a liquid

concentration of 1 μg cm^{-3} and compared it with the highest and lowest reported values. The Freundlich sorption capacities in the batch studies were higher than in our study, probably because in batch sorption experiments the process of irreversible sorption is not considered separately.

4.5 Conclusions

The application of pig manure containing SDZ and its transformation products to soil columns led to an accumulation of total ^{14}C in the uppermost soil layers and resulted in lower peak values of the ^{14}C BTCs compared with experiments with a pure SDZ solution. For the assumed experimental conditions, SDZ as well as its transformation products showed a high potential for leaching. Co-transport with dissolved organic matter did not seem to be a major transport mechanism for the solutes. The conceptual model with degradation and one kinetic and one irreversible sorption site provided a good description for most BTCs of SDZ and its transformation products 4-[2-iminopyrimidine-1(2*H*)-yl]-aniline, *N*-Ac-SDZ, and 4-OH-SDZ. The ^{14}C concentrations remaining in the soil columns could not be predicted correctly for the experiments with the SDZ solution, which suggests a sorption process that is not well understood. Transport parameters fitted to BTCs of individual species (SDZ and its transformation products) revealed a lower sorption capacity for the transformation products than for SDZ in the low concentration ranges. The *N*-Ac-SDZ was rapidly transformed and did not show any patterns useful for characterizing SDZ transport, such as an extended tailing of the BTCs or irreversible sorption. The transport behavior of 4-OH-SDZ seemed to be similar to that of SDZ. The model also revealed a higher sorption capacity for SDZ in the presence of manure.

5 Final Remarks

5.1 General discussion

The transport and transformation of SDZ in two agricultural soils was studied using soil column experiments and numerical studies. While the experiments presented in chapters 2 and 3 deal with the characteristic transport behavior of SDZ applied as a solution via irrigation, the transport of SDZ and its transformation products in presence of manure was investigated in chapter four. Analysis of the experimental data shows that a single column experiment with specific boundary and application conditions is not sufficient to understand the complex sorption behavior of SDZ. With the help of various experiments differing in input concentration, flow conditions and mode of application, some important factors which contribute to the overall understanding of the fate of SDZ in soils have been identified.

The modeling of the experimental results showed that sorption behavior of SDZ was time and concentration dependent requiring different modeling concepts. The term "concentration" in this case refers to the outflow concentration which was mainly governed by flow rate, the applied concentration or mass and the investigated soil. So in the experiments with higher SDZ (outflow) concentrations (chapter 2 and 4) an isotherm-based model using one reversible kinetic sorption site with Freundlich sorption and one irreversible sorption site could describe the experiments quite well, whereas for the experiments with lower outflow concentrations (chapter 3) the attachment detachment approach with an additional parameter was needed, especially for the description of the BTC tailings. For the experiments of chapter 4, where the applied (and outflow) concentrations where highest, even a two site model with one sorption site in equilibrium could describe the experiments reasonably well.

Figure 5.1 presents the measured ^{14}C data of the BTC of soil K (chapter 2) described with a two-site two rates (2S2R) Freundlich model together with various predictions of this BTC using the fitted parameters of models used to describe different experiments. First, predictions were made with parameters fitted to the corresponding experiment in soil M with the same model. Second, the parameters of the attachment/detachment models fitted to experiments conducted in undisturbed soil columns with lower flow rates and different modes of application (chapter 3) were used for the description. Finally, the parameters of

the two-site two rates (2S2R) Freundlich model which were fitted to an experiment where a SDZ solution was incorporated in a repacked soil column of soil K (chapter 4) were used for prediction. The curves show that most models fit the occurrence of the peak concentration well, whereas the height of the peak and the absolute values of the tailing were not captured. Only one model predicted the peak maximum too late. This model described the data of an experiment in which the SDZ-solution was incorporated into the uppermost centimeter of the soil and showed a remarkably higher Freundlich coefficient compared to the experiments for which the SDZ-solution was applied via the irrigation head. One possible explanation for this phenomenon may be the influence of contact time on sorption. During the time in which the SDZ-solution was blended into the uppermost centimeter and irrigation was started (about 5 to 10 minutes) first sorption processes could have taken place.

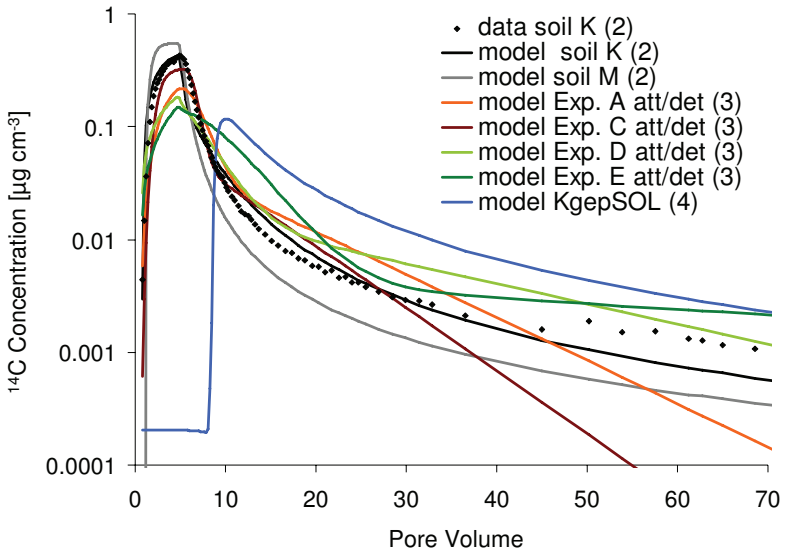

Figure 5.1. BTC data measured and modeled for the saturated soil column experiment with soil K (chapter 2) together with the model fitted to the corresponding experiment with soil M (chapter 2), selected models fitted to the experiments with undisturbed soil columns (chapter 3) and the model fitted to the experiment where a SDZ solution was blended in a repacked soil column of soil K (chapter 4). The chapter to which the respective models belong to is given in parentheses.

In conclusion it can be stated that the experiments on transport of SDZ using different application conditions reveal the presence of identical mechanisms characterizing

SDZ transport, although fitted sorption parameters and rates for the various experiments are different. Important factors influencing SDZ transport are the flow rate, the applied concentration/mass, the soil properties and also the way of application.

In the following paragraphs several points are discussed in more detail. Additionally, the model is compared with other developed models for the fate of sulfonamides.

5.2 The influence of soil properties

Analysis of the BTCs measured in repacked soil columns of the silty loam and the loamy sand showed a clear difference in total eluted amount of ^{14}C. The amount eluted was larger for the silty loam (soil M) than for the loamy sand (soil K). This suggests that sulfadiazine is being sorbed to a lesser extent in the M soil which is also supported by the modeling results. At the same time the sorbed amount in the uppermost cm of the soil column profile were higher for soil M. The transport experiments which were conducted with manure application showed comparable results. This means that on the one hand transport in the silty loam soil is faster. This may be due to the higher pH value connected with a higher part of the anionic species. On the other hand the process which led to the accumulation of ^{14}C in the uppermost soil layers (chapter 2) seems to be stronger for soil M. The empirical model approaches showed that the prediction of the soil concentration profile is mainly governed by the irreversible sorption process. According to the defined fractions by Förster et al. (2009) and Zarfl (2008) this fraction could be subdivided in the reversible bound residual fraction and the actual bound amount of substance. Either both or one of this processes seems to be more intense in the loamy soil which may be caused by a more diverse pore structure, a higher mineral surface area or the higher amount of soil organic matter. While the more diverse pore structure would provide more space for sequestration process, the organic substance is a partner for covalent binding.

A comparison with data from Förster et al. (2009) provides a hint that the pore structure plays a role in the different results for the soils. In incubation experiments with SDZ amended manure made with the same soils (sieved to 2 mm) the influence of the soil type on the fate of SDZ was considered to be low. This was confirmed in the modeling of the data and in almost equal apparent K_d values (Zarfl 2008) for the two soils. In the batch

techniques the influence of different pore structures is supposed to be low, whereas it may lead to a higher contact area in transport experiments.

Based on experiments with disturbed soil columns of soil M and K (chapter 2), which correspond to one scenario in the work of Wehrhan et al. (2007), the two soils used in this thesis can be also compared to a silty loam soil from Greifensee (Wehrhan et al., 2007). These authors found that the leached amounts were lower under similar boundary conditions as used in chapter 2. The silty loam used in the study of Wehrhan et al. (2007) had higher clay and organic carbon contents, whereas the pH-vale was with 6.1 was close to the pH values of the investigated soils. The difference in eluted amounts shows that clay and organic carbon content influence SDZ transport. This may also cause the different reaction as the same amount of SDZ is applied in a higher concentration (chapter 3): While in chapter 3 an increase of the eluted amount in soil K was observed, the eluted amount decreased strongly in the experiments of Wehrhan et al. (2007). This may be explained with a higher sorption capacity in the soil from Greifensee. The role of organic carbon on sorption is also shown in the sorption experiments of Sukul et al. (2008a). In one of their five experiments the content of organic carbon was more than two times higher compared to the other soils connected with a lower pH value. In this soil the determined sorption coefficients were remarkably higher than in the other soils. But the order of decreasing sorption does not follow only one parameter. The second highest sorption was found in a soil with high clay content but a relatively low content of organic carbon and a high pH-value. Also transformation processes depend on the soil properties. Transformation was higher in the loamy sand than in silty loam soil. Since these transformation processes are not yet fully understood no explanation can be given at this stage.

5.3 Description of profile data

The description of the vertical ^{14}C-distribution in the various soil columns was also one aim of this thesis. Therefore, two empirical model approaches were applied to describe the concentration profiles. While the description could be improved with the applied models, the governing process could not be identified. This lack of fitting the SDZ concentration profiles was also raised in the study of Wehrhan et al. (2007).

In experiments run with undisturbed soil columns at a lower flow rate different patterns for the ^{14}C-concentration profiles were found (chapter 3). There, the ^{14}C-concentration decreased also within the first centimeters, but the differences in concentrations were less pronounced and the concentration profiles were generally more curved. One reason for the different patterns may be the usage of undisturbed and unsaturated soil columns, meaning that the probability for ^{14}C to reach areas with lower flow velocities and be subject to subsequent binding processes may be higher. Another impact factor may the pH value of the input solutions. In the experiments of Wehrhan et al. (2007) and Unold et al. (2009a) the SDZ application solution (in $CaCl_2$) was directly applied onto soil, whereas in the experiments in chapter 4 the pH-value of the application solution was buffered to the pH-value of the background $CaCl_2$ solution (~5.6). Indeed the specific effect of the change in pH values is unknown.

In almost all transport experiments with soil K an increase in resident concentrations within the soil column profiles was observed but not in the experiments with soil M. One possible explanation could be the development of a strong sorbing transformation product. As experiments of chapter 2 and 3 revealed, transformation was higher in soil K. In future experiments this could be possibly checked using extraction procedures of the soil after finishing the leaching experiments.

5.4 Transport behavior of the transformation products

For experiments with SDZ-solution a transformation from SDZ into An-SDZ and 4-OH-SDZ was shown for both soils. The parts of transformation products in the outflow of the soil columns were different (13.8-38.3%) throughout the various experiments and seem to be dependent on concentration and soil properties.

The transport of the main transformation products present in pig manure (N-Ac-SDZ and 4-OH-SDZ) was studied using the experiments with manure application. Transport parameters fitted to the BTCs of individual species (SDZ and its transformation products) using a conceptual model with one kinetic and one irreversible sorption site as well as a degradation chain from N-Ac-SDZ to SDZ and from SDZ to 4-OH-SDZ revealed a lower sorption capacity for the transformation products than for SDZ in low concentration ranges. In the case of 4-OH-SDZ the lower sorption capacity could be confirmed with the experiments with SDZ-solution. The transport behavior of 4-OH-SDZ seems to be similar

as for SDZ having BTCs with an extended tailing. The same was true for An-SDZ for which lower sorption capacities than for 4-OH-SDZ were found. N-Ac-SDZ on the other hand was rapidly transformed and did not show patterns which proved to be characteristic for SDZ-transport, like an extended tailing of the BTCs or irreversible sorption. This was a hint that not only the irreversible sorption of SDZ but also reversible processes characteristic for the sorption and transport behavior of SDZ are mainly dominated by the NH_2-moiety of SDZ. This hypothesis is supported by the description of aniline sorption by Kosson & Byrne (1995) who described a process occurring in two steps: First a very rapid process occurs which was attributed to ionic binding on cation exchange sites. Then covalent bonds with soil organic matter are developed.

5.5 Comparison of the transport model for SDZ and its main transformation products with other existing models

In chapter 4 a model was developed that comprises the simultaneous transport of SDZ and its main metabolites in pig manure including transformation processes and different sorption properties for the three solutes. Based on the sorption experiments and following sequential extraction steps of Förster et al. (2009) a similar model was developed by Zarfl (2008) where comparable pig manure was applied to the same two soils. This model includes three compartments for SDZ: One compartment, called the available fraction, comprises the SDZ and metabolite fractions that could be extracted using $CaCl_2$ and methanol as solvents. These parts represent the amounts of solutes present in solution as well as sorbed amounts that were not yet subject to sequestration. The second compartment, the residual fraction, contains the amount of solutes that was sequestered by reversible processes and could be extracted with a harsher extraction method (acetonitrile-water, microwave). The third fraction is the irreversibly sorbed amount that was defined as not extractable with the applied methods.

For the description of the available fraction instantaneous equilibrium sorption is considered implicitly by Zarfl et al. (2008). This compartment includes the dissolved and kinetically sorbed amounts of SDZ in the transport model used in chapter 4. There the three compartments (dissolved, reversibly sorbed and irreversibly sorbed) are based on the results of the modeling process. The assumption of equilibrium sorption of Zarfl et al. (2008) supports the finding of a very fast kinetic rate coefficient for reversible kinetic sorption

compared to a previous study (chapter 2), even if sorption is considered as non-linear Freundlich sorption there. The irreversibly sorbed amount in the transport model comprised both the residual and the irreversibly sorbed amount of the sorption model.
As is described by Zarfl (2008), the structure of the sorption model and transport models can also be compared to the models with 3 sorption sites used by Wehrhan et al. (2007) and in the experiments presented in chapter 3.

The residual fraction, defined by Förster et al. (2009) as the amount of SDZ which can be extracted with a water acetonitrile mixture and subsequent microwave extraction, possibly provides the amount of SDZ which is eluted from the soil columns in the transport experiments step by step. This part may become visible in the long tailing of SDZ BTCs (Wehrhan et al., 2007, chapter 2 & 3) and in the observed desorption in batch experiments (Wehrhan et al., 2009). However, soil columns where only eluted with $CaCl_2$, and it is not clear how much of the residual fraction can thus be extracted. Furthermore the BTC tailings may also be partly attributed to the non-linear sorption behavior of SDZ. Therefore, the respective sites in the sorption and transport models can not be related one to one.

In general the comparison of the models reveals that the fraction which provides a reversibly bound but not easily extractable part of SDZ seems to be very important to describe the sorption and transport of SDZ. This is supported by the fact that a three sorption site model was needed to properly describe the observed BTCs showing a pronounced tailing. In transport experiments the quantification of this fraction using extraction methods could possibly be helpful.

5.6 General Conclusions

Flow rate, applied concentration, application conditions, pig manure as well as the soil properties affect SDZ transport. The concentration dependent sorption behavior of SDZ led to different appropriate model concepts. A two-site isotherm based model including one reversible kinetic sorption site was able to describe the experiments conducted at higher concentrations, whereas a three site attachment-detachment model was needed to describe the experiments with a lower concentration range. However, both models had to capture the BTC tailings which are caused either by the non-linear sorption behavior of SDZ or by kinetic processes.

Modeling revealed a higher mobility for all transformation products than for the parent compound SDZ. While the shapes of the BTCs for An-SDZ and 4-OH-SDZ are similar to the BTCs of SDZ, the BTC of N-Ac-SDZ does not show the extended tailing which hints on an influence of the aniline-moiety on the long term reversible sorption of SDZ.

The prediction of one BTC using the parameters from other BTCs reveals that the overall shape and in most cases also the peak maximum or arrival can be predicted correctly. This shows that the same sorption mechanisms occur. However, peak heights and tailings could not be captured which may be caused by i) an inappropriate model concept to describe the transport, or ii) unknown influence factors on transport.

In conclusion it can be stated that the experiments helped to understand the transport behavior of SDZ, but that the processes which govern SDZ sorption in detail are still not sufficiently understood.

5.7 Outlook

For the future prediction of SDZ transport, the processes that govern the sorption mechanisms need to be understood better. Applying extraction procedures to the soil after the leaching experiments could clarify whether the sorbed amount of ^{14}C is present as SDZ or in the form of transformation products. Fractionation of the soil and identification of the soil organic matter can help to identify the most important sorption sites for SDZ during transport. To be able to study the transport of SDZ without the interference of transformation processes transport experiments in sterilized soil could be helpful. Also the kind of application seems to be important, since higher Freundlich coefficients were observed in the experiments where SDZ was blended into the soil columns. For the prediction of SDZ transport in the field, also the influence of transient flow conditions as well as multiple application times has to be determined.

6 References

Baek, D.S., Kim, S.B. and D.J. Kim. 2003. Irreversible sorption of benzene in sandy aquifer materials. Hydrological Processes 17 (6), 1239-1251

Batt, A., S. Kim, I.B. Bruce and D.S. Aga. 2006. Determination of antibiotics within various wastewater treatment plants and the impact of their discharges on surrounding surface waters. Abstracts of Papers American. Chemical Society, 231, 151-ENVR

Berger, K., Petersen, B. and H.B. Pfaue. 1986. Persistenz von Gülle-Arzneistoffen in der Nahrungskette. Archiv für Lebensmittelchemie. 37, 99-102

Bergmann, A., R. Fohrmann and A. Hembrock-Heger. 2008. Bewertung der Umweltrelevanz von Arzneistoffen. Umweltwissenschaften und Schadstoff-Forschung, 20, 197-298

Bialk, H.M., Hedmann, C., Castillo, A. and J. Pedersen. 2007. Laccase-Mediated Michael Addition of 15N-Sulfapyridine to a Model Humic Constituent. Environmental Science and Technology, 41 (10), 3593-3600

Bialk, H.M. and J.A. Pedersen. 2008. NMR investigation of enzymatic coupling of sulfonamide antimicrobials with humic substances. Environmental Science and Technology, 42, 106-112

Blackwell, P., P. Kay and A.B.A. Boxall. 2007. The dissipation and transport of veterinary antibiotics in a sandy loam soil. Chemosphere, 67, 292-299

Boreen, A., 2005. Triplet-sensitized photodegradation of sulfa drugs containing six-membered heterocyclic groups: Identification of an SO2 extrusion photoproduct. Environmental Science & Technology, 39 (10), 3630-3638

Boxall, A.B.A., Blackwell, P., Cavallo, R., Kay, P. and J. Tolls. 2002. The sorption and transport of a sulphonamide antibiotic in soil systems. Toxicology Letters, 131 (1-2), 19-2

Boxall, A.B.A. 2004. The environmental side effects of medication - How are human and veterinary medicines in soils and water bodies affecting human and environmental health? Embo Reports, 5, 1110-1116

Bradford, S.A., Yates, S.R., Bettahar, M. and J. Šimůnek. 2002. Physical factors affecting the transport and fate of colloids in saturated porous media. Water Resources Research, 38 (12), doi: 10.1029/2002WR001340

Bradford, S., Y.F. Tadassa and Y. Pachepsky. 2006. Transport of Giardia and Manure Suspensions in Saturated Porous Media. Journal of Environmental Quality, 35, 749-757

Braida, W.J., J.C. White, F.J. Ferrandino and J.J. Pignatello. 2001. Effect of solute concentration on sorption of polyaromatic hydrocarbons in soil: Uptake rates. Environmental Science and Technology, 35, 2765-2772

Brusseau, M.L. and P.S.C. Rao. 1989. Sorption Nonideality during Organic Contaminant Transport in Porous-Media. Critical Reviews in Environmental Control, 19 (1), 33-99

Brusseau, M.L. 1992. Nonequilibrium Transport of Organic-Chemicals - the Impact of Pore-Water Velocity. Journal of Contaminant Hydrology, 9, 353-368

Burkhardt, M., C. Stamm, C. Waul, H. Singer and S. Muller. 2005. Surface runoff and transport of sulfonamide antibiotics and tracers on manured grassland. Journal of Environmental Quality, 34, 1363-1371

Burkhardt, M. and C. Stamm. 2007. Depth distribution of sulfonamide antibiotics in pore water of an undisturbed loamy grassland soil. Journal of Environmental Quality, 36, 588-596

Casey, F.X.M., H. Hakk, J. Šimůnek and G.L. Larsen. 2004. Fate and transport of testosterone in agricultural soils. Environmental Science and Technology, 38, 790-798

Casey, F.X.M., G.L. Larsen, H. Hakk and J. Šimůnek. 2003. Fate and transport of 17 beta-estradiol in soil-water systems. Environmental Science and Technology, 37, 2400-2409

Casey, F.X.M. and J. Šimůnek. 2001. Inverse analyses of transport of chlorinated hydrocarbons subject to sequential transformation reactions. Journal of Environmental Quality, 30, 1354-1360

Casey, F.X.M., J. Šimůnek, J. Lee, G.L. Larsen and H. Hakk. 2005. Sorption, mobility, and transformation of estrogenic hormones in natural soil. Journal of Environmental Quality, 34, 1372-1379

Christian, T., Schneider, R.J., Farber, H.A., Skutlarek, D., Meyer, M.T. and H.E. Goldbach. 2003. Determination of antibiotic residues in manure, soil, and surface waters. Acta Hydrochimica Et Hydrobiologica, 31 (1), 36-44

References

Das, B.S., L.S. Lee, P.S.C. Rao and R.P. Hultgren. 2004. Sorption and degradation of steroid hormones in soils during transport: Column studies and model evaluation. Environmental Science and Technology, 38, 1460-1470

Davis, J.G., Truman, C.C., Kim, S.C., Ascough, J.C. and K. Carlson. 2006. Antibiotic transport via runoff and soil loss. Journal of Environmental Quality, 35 (6), 2250-2260

Deng, J.C., X. Jiang, X.X. Zhang, W.P. Hu and J.W. Crawford. 2008. Continuous time random walk model better describes the tailing of atrazine transport in soil. Chemosphere, 71, 2150-2157

de Jonge, L., C. Kjaergaard and P. Moldrup. 2004. Colloids and colloid-faciliated transport of contaminants in soils: An introduction. Vadose Zone Journal, 3, 321-325

Diaz-Cruz, M. and D. Barcelo. 2006. Determination of antimicrobial residues and metabolites in the aquatic environment by liquid chromatography tandem mass spectrometry. Analalytical and Bioanalytical Chemistry, 386, 973-985

Doherty, J., 2002. PEST: Model-independent parameter estimation v4. Watermark Numerical Modeling.

Dolliver, H., Kumar, K. and S. Gupta. 2007. Sulfamethazine uptake by plants from manure-amended soil. Journal of Environmental Quality, 36 (4), 1224-1230

Drillia, P., Stamatelatou, K. and G. Lyberatos. 2005. Fate and mobility of pharmaceuticals in solid matrices. Chemosphere, 60 (8), 1034-1044

Fan, Z.S., Casey, F.X.M., Hakk, H. and G.L. Larsen. 2007. Discerning and modeling the fate and transport of testosterone in undisturbed soil. Journal of Environmental Quality, 36 (3), 864-873

Focazio, M.J., D.W. Kolpin, K.K. Barnes, E.T. Furlong, M.T. Meyer, S.D. Zaugg, L.B. Barber, and M.E. Thurman. 2008. A national reconaissance for pharmaceuticals and other organic wastewater contaminants in the United States - II) Untreated drinking water resources. Science of the total Environment, 402, 201-216

Förster, M., Laabs, V., Lamshöft, M., Pütz, T. and W. Amelung. 2008. Analysis of aged sulfadiazine residues in soils using microwave extraction and liquid chromatography tandem mass spectrometry. Analytical and Bioanalytical Chemistry, 391 (3), 1029-1038

Förster, M., Laabs, V., Lamshöft, M. Groeneweg, J. Zühlke, S, Spiteller M., Krauss, M., Kaupenjohann, M. and W. Amelung. 2009: Sequestration of Manure-Applied

Sulfadiazine Residues in Soils. Environmental Science and Technology, 43, 1824-1830

Gao, J.A. and J.A. Pedersen. 2005. Adsorption of sulfonamide antimicrobial agents to clay minerals. Environmental Science & Technology, 39 (24), 9509-9516

Hammesfahr, U., Heuer, H., Manzke, B., Smalla, K. and S. Thiele-Bruhn. 2008. Impact of the antibiotic sulfadiazine and pig manure on the microbial community structure in agricultural soils. Soil Biology & Biochemistry. 40 1583-1591

Hamscher, G., Pawelzick, H.T., Hoper, H. and H. Nau. 2005. Different behavior of tetracyclines and sulfonamides in sandy soils after repeated fertilization with liquid manure. Environmental Toxicology and Chemistry, 24 (4), 861-868

Hanson, B.R., J. Šimůnek and J.W. Hopmans. 2006. Evaluation of urea-ammonium-nitrate fertigation with drip irrigation using numerical modeling. Agricultural Water Management, 86, 102-113

Heise, J., S. Höltge, S. Schrader and R. Kreuzig. 2006. Chemical and biological characterization of non-extractable residues in soil. Chemosphere, 65, 2352-2357

Hesketh, N., P.C. Brookes and T.M. Addiscott. 2001. Effect of suspended soil material and pig slurry on the facilitated transport of pesticides, phosphate and bromide in sandy soil. European Journal of Soil Science, 52, 287-296

Heuer, H. and K. Smalla. 2007. Manure and sulfadiazine synergistically increased bacterial antibiotic resistance in soil over at least two months. Environmental Microbiology, 9 (3), 657-666

Hilton, M.J. and K.V. Thomas. 2003. Determination of selected human pharmaceutical compounds in effluent and surface water samples by high-performance liquid chromatography-electrospray tandem mass spectrometry. Journal of Chromatography A, 1015, 129-141

Höper, H., Kues, J., Nau, H., and G. Hamscher. 2002. Eintrag und Verbleib von Tierarzneimitteln in Böden. Bodenschutz, 4, 141-148

Jarvis, N.J., K.G. Villholth and B. Ulen. 1999. Modelling particle mobilization and leaching in macroporous soil. European Journal of Soil Science, 50, 621-632

Jørgensen, S.E. and B. Halling-Sørensen. 2000. Drugs in the environment. Chemosphere, 40 (7), 691-699

References

Kahle, M. and C. Stamm. 2007a. Time and pH-dependent sorption of the veterinary antimicrobial sulfathiazole to clay minerals and ferrihydrite. Chemosphere. 68, 1224-1231

Kahle, M. and C. Stamm. 2007b. Sorption of the veterinary antimicrobial sulfathiazole to organic materials of different origin. Environmental Science & Technology, 41 (1), 132-138

Kan, A.T., Fu, G., Hunter, M., Chen, W., Ward, C.H. and M.B. Tomson. 1998. Irreversible sorption of neutral hydrocarbons to sediments: Experimental observations and model predictions. Environmental Science & Technology. 32 (7), 892-902

Kay, P., Blackwell, P.A. and A.B.A. Boxall. 2004. Fate of veterinary antibiotics in a macroporous tile drained clay soil. Environmental Toxicology and Chemistry, 23 (5), 1136-1144

Kay, P., Blackwell, P.A. and A.B.A. Boxall. 2005a. Column studies to investigate the fate of veterinary antibiotics in clay soils following slurry application to agricultural land. Chemosphere, 60 (4), 497-507

Kay, P., P.A. Blackwell and A.B.A. Boxall. 2005b. A lysimeter experiment to investigate the leaching of veterinary antibiotics through a clay soil and comparison with field data. Environmental Pollution, 134, 333-341

Kemper, N., 2008. Veterinary antibiotics in the aquatic and terrestrial environment. Ecological indicators, 8 (1), 1-13

Kim, S.B., H.C. Ha, N.C. Choi and D.J. Kim. 2006. Influence of flow rate and organic carbon content on benzene transport in a sandy soil. Hydrological Processes, 20, 4307-4316

Kools, S.A.E., Moltmann, J.F., and T. Knacker. 2008. Estimating the use of veterinary medicines in the European union. Regulatory Toxicology and Pharmacology, 50, 59-65

Kosson, D.S. and S.V. Byrne. 1995. Interactions of Aniline with Soil and Groundwater at an Industrial Spill site. Environmental Health Perspectives, 103, 00-00 (Suppl 5)

Kotzerke, A., Sharma, S., Schauss, K., Heuer, H., Thiele-Bruhn, S., Smalla, K., Wilke, B-M. and M. Schloter. 2008. Alterations in soil microbial activity and N-transformation processes due to sulfadiazine loads in pig-manure. Environmental Pollution. 153, 315-322

Kretzschmar, R. 1994. Filter Efficiency of 3 Saprolites for natural Clay and Iron-Oxide Colloids. Environmental Science and Technology, 28, 1907-1915

Kreuzig, R., Kullmer, C., Matthies, B., Höltge, S. and H. Dieckmann. 2003. Fate and behaviour of pharmaceutical residues in soils. Fresenius Environmental Bulletin, 12 (6), 550-558

Kreuzig, R. and S. Höltge. 2005. Investigations on the fate of sulfadiazine in manured soil: Laboratory experiments and test plot studies. Environmental Toxicology and Chemistry, 24 (4), 771-776

Kreuzig, R., S. Holtge, J. Brunotte, N. Berenzen, J. Wogram and R. Schulz. 2005. Test-plot studies on runoff of sulfonamides from manured soils after sprinkler irrigation. Environmental Toxicology and Chemistry, 24, 777-781

Kurwadkar, S.T., Adams, C.D., Meyer, M.T. and D.W. Kolpin. 2007. Effects of sorbate speciation on sorption of selected sulfonamides in three loamy soils. Journal of Agricultural and Food Chemistry, 55 (4), 1370-1376

Lamshöft, M., Sukul, P., Zühle, S. and M. Spiteller. 2007. Metabolism of ^{14}C-labelled and non-labelled sulfadiazine after administration to pigs. Analytical and Bioanalytical Chemistry, 388 (8), 1733-1745

Löscher, W., Ungemach, R. and R. Kroker. 1994.Grundlagen der Pharmakotherapie bei Haus- und Nutztieren-2., neubearbeitete und erweiterte Auflage, mit 13 Abbildungen und 80 Tabellen. Paul Parey

Loftin, K.A., C.D. Adams, M.T. Meyer and R. Surampalli. 2008. Effects of ionic strength, temperature, and pH on degradation of selected antibiotics. Journal of Environental Quality, 37, 378-386

Managaki, S., A. Murata, H. Takada, B.C. Tuyen and N.H. Chiem. 2007. Distribution of macrolides, sulfonamides, and trimethoprim in tropical waters: Ubiquitous occurrence of veterinary antibiotics in the Mekong Delta. Environmental Science and Technology, 41, 8004-8010

McGechan, M.B. and D.R. Lewis. 2002. Transport of particulate and colloid-sorbed contaminants through soil, part 1: General principles. Biosystems Engineering, 83, 255-273

Martinez-Carballo E., G.-B.C., Scharf S., and O. Gans. 2007. Environmental monitoring study of selected veterinary antibiotics in animal manure and soils in Austria. Environmental Pollution, 148, 570-579

References

Mazel, D. and J. Davies. 1998. Antibiotic resistance - The big picture. Resolving the Antibiotic Paradox, 456, 1-6

Nobel Lectures. 1965. Physiology or Medicine 1922-1941. Elsevier Publishing Company. Amsterdam

Nouws, J.F.M., Mevius, D., Vree, T.B. and M. Degen. 1989. Pharmacokinetics and Renal Clearance of Sulfadimidine, Sulfamerazine and Sulfadiazine and Their N4-Acetyl and Hydroxy Metabolites in Pigs. Veterinary Quarterly, 11 (2), 78-86

Pailler, J.-Y., Krein, A., Pfister, L., Hoffmann, L., and C. Guignard. 2009. Solid phase extraction coupled to liquid chromatography-tandem mass spectrometry analysis of sulfonamides, tetracyclines, analgesics and hormones in surface water and wastewater in Luxembourg. Science of the total Environment. 407, 4736-4743

Pang, L. and J. Šimůnek. 2006. Evaluation of bacteria-facilitated cadmium transport in gravel columns using the HYDRUS colloid-facilitated solute transport model. Water Resources Research, 42, W12S10

Papiernik, S.K., S.R. Yates, W.C. Koskinen and B. Barber. 2007. Processes affecting the dissipation of the herbicide isoxaflutole and its diketonitrile metabolite in agricultural soils under field conditions. Journal of .Agricultural and Food Chemistry, 55, 8630-8639

Park, JH., YC. Feng, SY Cho, TC Voice and SA Boyd. 2004. Sorbed atrazine shifts into non-desorbable sites of soil organic matter during aging. Water Research, 18, 3881-3892

Pignatello, J.J. and B.S. Xing. 1996. Mechanisms of slow sorption of organic chemicals to natural particles. Environmental Science & Technology, 30 (1), 1-11

Rooklidge, S.J. 2004. Environmental antimicrobial contamination from terraccumulation and diffuse pollution pathways. Science of the Total Environment, 325, 1-13

Sacher, F., Lange, F.T., Brauch, H.-J., and I. Blankenhorn. 2001. Pharmaceuticals in groundwaters - analytical methods and results of a monitoring program in Baden-Würtemberg, Germany. Journal of Chromatograhy A, 938, 199-210

Sakurai, H. and T. Ishimitsu. 1980. Microionization constants of sulphonamides. Talanta, 27, 293-298

Schaerlaekens, J., D. Mallants, J. Šimůnek, M.T. van Genuchten and J. Feyen. 1999. Numerical simulation of transport and sequential biodegradation of chlorinated aliphatic hydrocarbons using CHAIN_2D. Hydrological Processes, 13, 2847-2859

Schmidt, B., J. Ebert, M. Lamshoft, B. Thiede, R. Schumacher-Buffel, R. Ji, P.F.X. Corvini and A. Schaeffer. 2008. Fate in soil of C-14-sulfadiazine residues contained in the manure of young pigs treated with a veterinary antibiotic. Journal of Environmental Science and Health B, 43, 8-20

Schwarzenbach, R.P., Geschwend, P.M. and D.M. Imboden. 2003. Environmental Organic Chemistry (second ed.). John Wiley & Sons. New Jersey.

Šimůnek, J., D. Jacques, M.T. van Genuchten and D. Mallants. 2006. Multicomponent geochemical transport modeling using HYDRUS-1D and HP1. Journal of the American Water Resources Association, 42, 1537-1547

Šimůnek, J., Huang, K. and M.T. Van Genuchten. 1998. The Hydrus code for simulating the movement of water, heat and multiple solutes in variably saturated media. Version 6.0. , U.S. Salinity Laboratory, Agricultural Research Service US Department of Agriculture, Riverside, California, Research Report, vol 144

Šimůnek, J., H. Sejna, M. Saito, M. Sakai and M.T. van Genuchten, 2008. The Hydrus-1D Software Package for Simulating the One-Dimensional Movement of Water, Heat, and Multiple Solutes in Variably-Saturated Media. Version 4.0. Department of Environmental Sciences, University of California Riverside, Riverside, California.

Srivastava, P.; S.M. Sanders, J.H. Dane, Y. Feng, J.Basile and M.I. Barnett. 2009. Fate and Transport of Sulfadimethoxine and Ormetoprim in Two Southeastern Unites States Soils. Vadose Zone Journal, 8, 32-41

Stoob, K., H.P. Singer, S.R. Mueller, R.P. Schwarzenbach and C.H. Stamm. 2007. Dissipation and transport of veterinary sulfonamide antibiotics after manure application to grassland in a small catchment. Environmental Science and Technology, 41, 7349-7355

Sukul, P., M. Lamshöft, S. Zuhlke and M. Spiteller. 2008a. Sorption and desorption of sulfadiazine in soil and soil-manure systems. Chemosphere, 73, 1344-1350

Sukul, P., Lamshöft, M., Zühlke, S. and M. Spiteller. 2008b. Photolysis of C14-sulfadiazine in water and manure. Chemosphere, 71 (4), 717-725

Tamtam, F., Mercier, F., Le Bot, B., Eurin, J., Dinh, Quoc T., Clement, M. and M. Chevreuil. 2008. Occurrence and fate of antibiotics in the Seine River in various hydrological conditions. Science of the total environment. 393 84-95

Thiele-Bruhn,S. 2003. Pharmaceutical antibiotic compounds in soils – a review. Journal of Plant Nutrition and Soil Science, 166, 145-167

References

Thiele-Bruhn, S. and M.O. Aust. 2004. Effects of pig slurry on the sorption of sulfonamide antibiotics in soil. Archives of Environmental Contamination and Toxicology, 47, 31-39

Thiele-Bruhn, S., Seibicke, T., Schulten, H.R. and P. Leinweber. 2004. Sorption of sulfonamide pharmaceutical antibiotics on whole soils and particle-size fractions. Journal of Environmental Quality, 33 (4), 1331-1342

Toride, T., F.J. Leij and M.T. van Genuchten. 1999. The CXTFIT code for estimating transport parameters from laboratory or field tracer experiments. Version 2.1. US Salinity Laboratory, Agricultural Research Service US Department of Agriculture, Riverside, California, Research Report, vol 137.

Turku, I., Sainio, T. and E. Paatero. 2007. Thermodynamics of tetracycline adsorption on silica. Environmental Chemistry Letters 5 (4), 225-228.

Unold, M., R. Kasteel, J. Groeneweg and H. Vereecken. 2009a. Transport and transformation of sulfadiazine in soil columns packed with a silt loam and a loamy sand. Journal of Contaminant Hydrology, 103, 38-47

Unold, M., J. Šimůnek, R. Kasteel, J. Groeneweg and H. Vereecken. 2009b. Transport of manure-based applied sulfadiazine and its main transformation products in soil columns. Vadose Zone Journal, 8, 677-689

van Genuchten, M.T. 1985. Convective-Dispersive Transport of Solutes involved in sequential 1st-order decay reactions. Computers and Geosciences, 11, 129-147

van Genuchten, M.T. and R.J. Wagenet. 1989. 2-Site 2-Region Models for Pesticide Transport and Degradation - Theoretical Development and Analytical Solutions. Soil Science Society of America Journal, 53, 1303-1310

Wang, Q. 2006. Sulfadimethoxine degradation kinetics in manure as affected by initial concentration, moisture, and temperature. Journal of Environmental Quality, 35, 2162-2169

Wehrhan, A., 2006. Fate of veterinary pharmaceuticals in soil: An experimental and numerical study on the mobility, sorption and transformation of sulfadiazine. Doctoral Thesis. Forschungszentrum Jülich GmbH, Germany

Wehrhan, A., Kasteel, R., Šimůnek, J., Groeneweg, J. and H. Vereecken. 2007. Transport of sulfadiazine in soil columns - Experiments and modelling approaches. Journal of Contaminant Hydrology, 89 (1-2), 107-135

Wehrhan A., T. Streck, J. Groeneweg, H. Vereecken and R. Kasteel. 2009. Long-term sorption and desorption of sulfadiazine in soil - experiments and modelling. Accepted by Journal of Environmental Quality.

Wilson, G.V., Rhoton, F.E. and H.M. Selim. 2004. Modeling the impact of ferrihydrite on adsorption-desorption of soil phosphorus. Soil Science, 169 (4), 271-281

Woolley, J.L. and C.W. Sigel. 1979. Metabolism and Disposition by the Rat of Sulfadiazine-S-35 Alone and in the Presence of Trimethoprim. Drug Metabolism and Disposition, 7 (2), 94-99

Wortmann, C.S. and C.A. Shapiro. 2008. The effects of manure application on soil aggregation. Nutrient Cycling in Agroecosystems, 80, 173-180

Ye, Z.Q., H.S. Weinberg and M.T. Meyer. 2007. Trace analysis of trimethoprim and sulfonamide, macrolide, quinolone, and tetracycline antibiotics in chlorinated drinking water using liquid chromatography electrospray tandem mass spectrometry. Analytical Chemistry, 79, 1135-1144

Zeldowitsch, J., 1934. Über den Mechanismus der katalytischen Oxydation von CO an MnO2. Acta Physicochimica URSS, 1, 364-449

Zhang, X.X., J.W. Crawford and L.M. Young. 2008. Does pore water velocity affect the reaction rates of adsorptive solute transport in soils? Demonstration with pore-scale modelling. Advances in Water Resources, 31,425-437

Zhang, X.X and M. Lv. 2009. The nonlinear adsorptive kinetics of solute transport in soil does not change with pore water velocity: Demonstration with pore scale simulations. Journal of Hydrology, 371, 42-52

Zielezny, Y., Groeneweg, J., Vereecken, H., and W. Tappe. 2006. Impact of sulfadiazine and chlorotetracycline on soil bacterial community structure and respiratory activity. Soil Biology & Biochemistry. 38, 2372-2380

Zarfl, C. 2008: Chemical Fate of Sulfadiazine in Soil: Mechanisms and Modelling Approaches (Dissertation). Shaker Verlag. Aachen. ISBN 978-3-8322-7491-7

7 Appendixes

7.1 Appendix A: Sulfadiazine and its transformation products

For all experiments ^{14}C-SDZ (IUPAC: 4-amino-N-pyrimidin-2-yl-benzenesulfonamide) with a single labeling in the pyrimidine-ring and a specific radioactivity of 8.88 MBq mg^{-1} was used. It was provided by Bayer HealthCare AG (Wuppertal, Germany) as a powder with a purity of 99%. For the experiments with SDZ solution in chapter 4, additionally unlabeled ^{12}C-SDZ (Sigma Aldrich, Germany) was used. The pig manure containing ^{14}C-labeled sulfonamides we used in the manure experiments was obtained from a feeding experiment conducted at Bayer AG Monheim where ^{14}C-SDZ with a single labeling in the pyrimidine-ring and ^{12}C-SDZ were administered to pigs in a ratio of 1:19. The specific radioactivity of SDZ in the manure was 0.44 MBq mg^{-1}. After dosing, manure was collected, mixed and stored at 4°C in the dark. The specific radioactivity of the fresh manure was 0.12 MBq g^{-1}. Selected physicochemical properties are listed in Table A.1. Figure A.1 presents the chemical structures of SDZ and the relevant transformation products.

Table A.1: Physico-chemical properties of SDZ according to the supplier of the non-labeled SDZ, Sigma Aldrich, Taufkirchen, Germany.

Molecular Formula	$C_{10}H_{10}N_4O_2S$
Molar weight	250.28 g mol^{-1}
Water solubility	13 to 77 mg L^{-1}
pK_{a1}, pK_{a2}	1.57±0.1/6.50± 0.3
Octanol/water distribution coefficient	0.76
Henry's Law constant	1.58 x 10^{-5} Pa m^3 mol^{-1}

In the SDZ solution or in the pig manure the following transformation products were present:

1. N-Ac-SDZ (N^4-acetyl-N^1-2-pyrimidinylsulfanilamide) Fig A.1 b)
2. 4-OH-SDZ (N^1-2-(4-Hydroxypyrimidinyl)sulfanilamide) Fig A.1 c)
3. 4-(2-iminopyrimidin-1(2H)-yl)aniline Fig A.1 d)

Chemical detection and quantification of SDZ and the transformation products was done by High Performance Liquid Chromatography (HPLC) combined with radioactivity measurement. A detailed description of the analytical procedure is given in Appendix D.

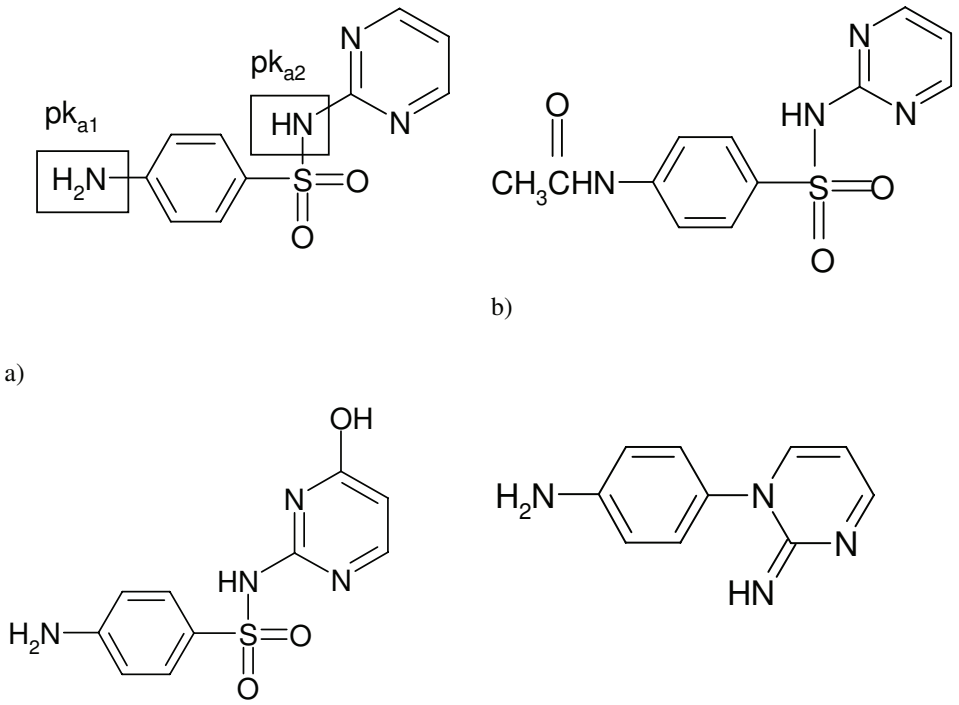

a) b)

c) d)

Fig A.1 Chemical structure of SDZ a) and its transformation products N-Ac-SDZ b), 4-OH-SDZ c) and 4-[2-imino-pyrimidine-1(2H)-yl]-aniline d)

Sorption of SDZ is pH-dependent. The parts of the different SDZ-spezies in dependence on the pH-value are given in Figure A.2.

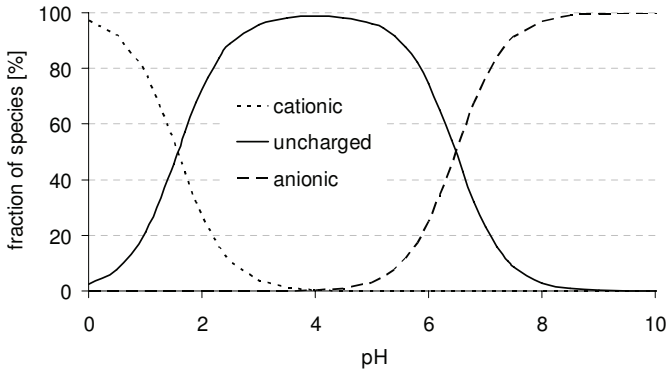

Figure A.2. Species distribution of SDZ in dependence of the pH-value (changed according to Zarfl et al. 2008)

Appendix A

Both acidity constants differ in literature, the variations for pK_{a1} are higher than for pk_{a2}. Therefore the species distribution of SDZ is also dependent on the chosen pK_a-value. Figure A.2 shows the species distribution for pK_{a1} = 1.57 and pKa 2= 6.48 which were provided by the producer of the ^{12}C-SDZ. The calculation of Zarfl et al. 2008, where a pK_{a1} value of 2.48 was used, was adapted to these pK_a-values while the species distribution was calculated according to Schwarzenbach et al. (2003):

cationic species:

$$\alpha_{SH_2^+} = \frac{[SH_2^+]}{[SH_2^+]+[SH]+[S^-]} = \frac{1}{1+\frac{[SH]}{[SH_2^+]}+\frac{[S^-]}{[SH_2^+]}} = \frac{1}{1+\frac{K_{a1}}{[H^+]}+\frac{K_{a1}*K_{a2}}{[H^+]}} = \frac{1}{1+10^{pH-pK_{a1}}+10^{2*pH-pK_{a1}-pK_{a2}}}$$

neutral species:

$$\alpha_{SH} = \frac{1}{1+10^{pK_{a1}-pH}+10^{pH-pK_{a2}}}$$

anionic species:

$$\alpha_{S^-} = \frac{1}{1+10^{pK_{a1}+pK_{a2}-2pH}+10^{pK_{a2}-pH}}$$

7.2 Appendix B: Soil Properties

The undisturbed soil columns and soil samples for the repacked soil columns were taken in two agricultural fields with two representative soil types for Northrhine-Westpfalia, Germany. One sampling site was near Kaldenkirchen (administrative district Viersen). The soil was classified as a loamy sand according to FAO guidelines. The second sampling site was located near Jülich-Merzenhausen (administrative district Düren) and the soil was classified as silty loam. Soil samples were taken in October 2006 in Kaldenkirchen and March 2007 in Merzenhausen. Undisturbed soil columns were covered and stored at 4 C in the dark until usage. Possible earthworms in the soil columns could have destroyed the soil structure and were therefore removed by drying the soil columns for about 48 h at 45 C in a drying oven.

For all undisturbed soil columns used X-ray images were taken in order to get information on the structure inside the soil columns.

Table B.1: Selected physical and chemical properties of the Kaldenkirchen soil (K) and the Merzenhausen soil (M).

	Unit	Soil K	Soil M
Clay (<0.002 mm)[a]	[% mass]	4.9	15.4
Silt (0.002-0.064 mm)[a]	[% mass]	26.7	78.7
Sand (0.064-2.000 mm)[a]	[% mass]	68.5	5.9
pH (0.01 M $CaCl_2$)[b]		6.8	7.4
C_{org} [a,c]	[% mass]	1.07	1.24
CEC[d]	[$cmol_c kg^{-1}$]	7.8	11.4

[a] data were measured at the "Institut für Nutzpflanzenwissenschaften und Ressourcenschutz" at the University of Bonn

[b] average pH-values in the soil column effluents for soil columns with manure

[c] C_{org} is the total organic matter content

[d] Data for CEC were taken from Förster et al. (2008) who performed experiments with the same soils.

7.3 Appendix C: Experimental Setup

Figure C.1 shows the experimental setup which was used for the unsaturated soil column experiments of chapters three and four. The setup was built by members of the Agrosphere Institute within the Research Centre Jülich and controlled with a LabView based software. The solution for irrigating the soil columns was pumped out of a storage bottle with the help of a peristaltic pump (REGLO Digital MS-2/12, ISMATEC Laboratoriumstechnik GmbH, Wertheim-Mondfeld, Germany). The storage bottle was placed on a balance (Kern DS 8K0 1, Gottl. Kern & Sohn GmbH, Balingen-Frommern, Germany) in order to record the irrigation rate regularly. At the bottom of the soil columns suction was applied with the help of a peristaltic pump and a pressure regulation system. The suction was chosen separately for each soil column to establish a constant pressure head (water content) in the soil columns at the given flow rate. This means that water flow was driven only by gravity. The suction inside of the columns was controlled using two tensiometers (T5, UMS GmbH, München, Germany) installed 2.5 and 7.5 cm below the soil column surface. Suctions ranged from 4 to 45 mbar for different soil columns. The outflow from the soil columns was first collected in a buffer vessel. When approximately 15 cm^3 were collected, an electric circuit with two water level sensors was closed. Thereupon a magnetic valve to the cell where the electrical conductivity was measured and recorded automatically, opened and the outflow flew into this cell. For the SDZ-transport experiments the samples were collected in a test tube in the fraction sampler after the measurement of the electrical conductivity.

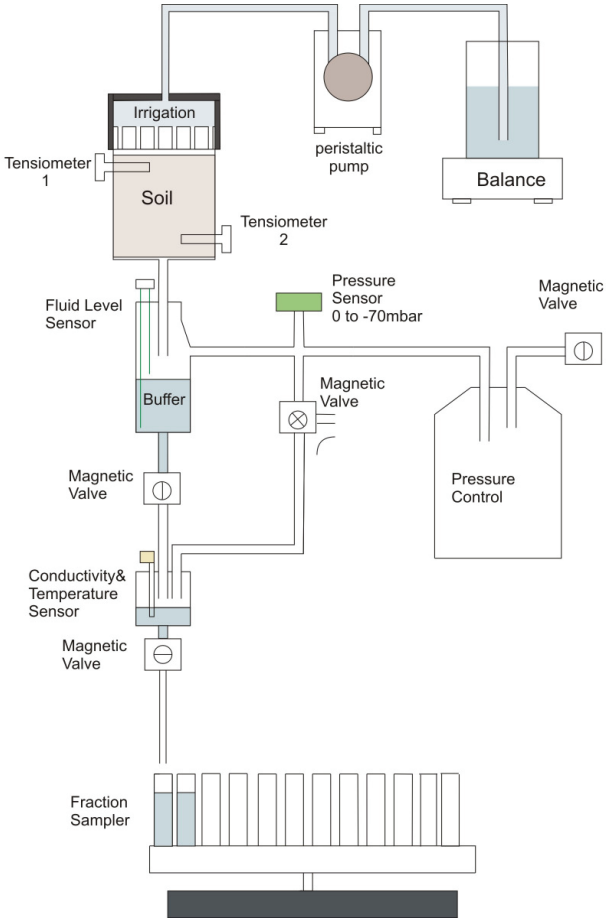

Figure C.1. Experimental setup used for the experiments in chapters 3 & 4

7.4 Appendix D: Analysis of ^{14}C and the transformation products in liquid samples

The total ^{14}C in the outflow samples was determined using radioactivity measurements with Liquid Scintillation Counting (LSC). Therefore three aliquots of each sample were mixed with 10 mL of the scintillation cocktail Instagel and subsequently the radioactivity was measured using Liquid Scintillation Counting with a detection limit of 0.4 Bq. The Concentration of ^{14}C in mass equivalents of SDZ in the samples could be dedicated by dividing the specific radioactivity of SDZ [Bq mg^{-1}], provided by the supplier BayerHealthCare, by the measured radioactivity. Background correction of LSC measurements was done by the additional measurement of a blank. The total ^{14}C-concentration is a lumped measurement for SDZ and the transformation products.

SDZ and the main transformation products were separated by the use of Radio-HPLC. The HPLC-system included an reversed-phase column (Phenomenex Synergi Fusion RP 80, 250 mm x 4.6 mm) which was eluted with a mixture of water (490 mL) and methanol (10 mL), buffered with 0.5 mL of a 25% phosphoric acid solution. The injection volume was 0.25 mL for each sample.

A gradient with an increased amount of methanol was used for peak separation, starting with 100% water for 6 minutes. The methanol fraction increased linearly to 27% till minute 23, then to 37% in the next three minutes and to 47% in the following two minutes. The methanol part reached its maximum with 57% after 30 minutes. With this protocol, we were able to distinguish four peaks in the chromatograms, of which three were identified as SDZ, 4-hydroxy-SDZ (N1-2-(4-hydroxypyrimidinyl)-benzenesulfanilamide) and 4-(2-iminopyrimidin-1(2H)-yl)aniline. The latter one was identified by the Institute of Environmental Research at the University of Dortmund, Germany. Using the HPLC the detection limit for SDZ and its transformation products is about 3 µg L^{-1} mass equivalents of SDZ. For the transformation products this concentration was only found in the samples with the highest ^{14}C-concentrations. In order to detect SDZ and the transformation products also in samples at lower concentrations, we changed the measurement procedure. The outflow of the HPLC was collected according to the retention times of SDZ and the transformation products, and also in-between these time frames. The radioactivity in the collected samples was measured with LSC as described above. We used a standard for sulfadiazine to fix the retention time for the SDZ-peak. No standards were available for 4-

hydroxy-SDZ, 4-(2-iminopyrimidin-1(2H)-yl)aniline and an additional unknown product, which was only detected in soil M. Therefore, these compounds were identified by setting their retention times in relation to the retention time of the known peaks. The correction of the background radioactivity was performed by collecting the outflow of the HPLC-column at the beginning and the end of each HPLC-run and subtracting the averaged background radioactivity from the radioactivity in the peaks. In some samples collected outside of the retention times of the peaks, the radioactivity was higher than the background signal, but this radioactivity could not be associated to an own peak. Additionally, the sum of radioactivity in the collected outflow varied between 95% and 105% of the total radioactivity measured in aliquots of the respective samples. Therefore, we performed the following correction to compare the peak Concentration (C_i) of compound *i*, with the total measured ^{14}C-concentration ($^{14}C_{total}$) in an aliquot of the respective sample:

$$C_i = \frac{(RA_{i_{uncorrected}} - RA_{background})}{\Sigma RA_{j_{corrected}}} * {}^{14}C_{total}$$

where $RA_{i,\text{uncorrected}}$ is the radioactivity in the peak before subtracting the background radioactivity $RA_{background}$ and $RA_{jcorrected}$ is the background corrected radioactivity of compound j in the respective sample. With this procedure, the sum of the transformation products adds up to 100% radioactivity. A transformation product was quantified, when the measured radioactivity was higher than 1.2 Bq, which is three times the detection limit of the LSC. Otherwise its contribution was set to zero. With this method the transformation products could be identified down to a concentration of 0.5 µg L^{-1} mass equivalents of SDZ. The method was validated by determining the correlation between the total radioactivity in one diluted outflow sample of each soil and the radioactivity measured in the peaks of this sample (see Figure 2.2). The obtained correlations for SDZ, 4-(2-iminopyrimidin-1(2H)-yl)aniline and 4-hydroxy-SDZ were good ($R^2 > 0.97$). In Figure D.1 examples of Chromatograms are shown:

Appendix D

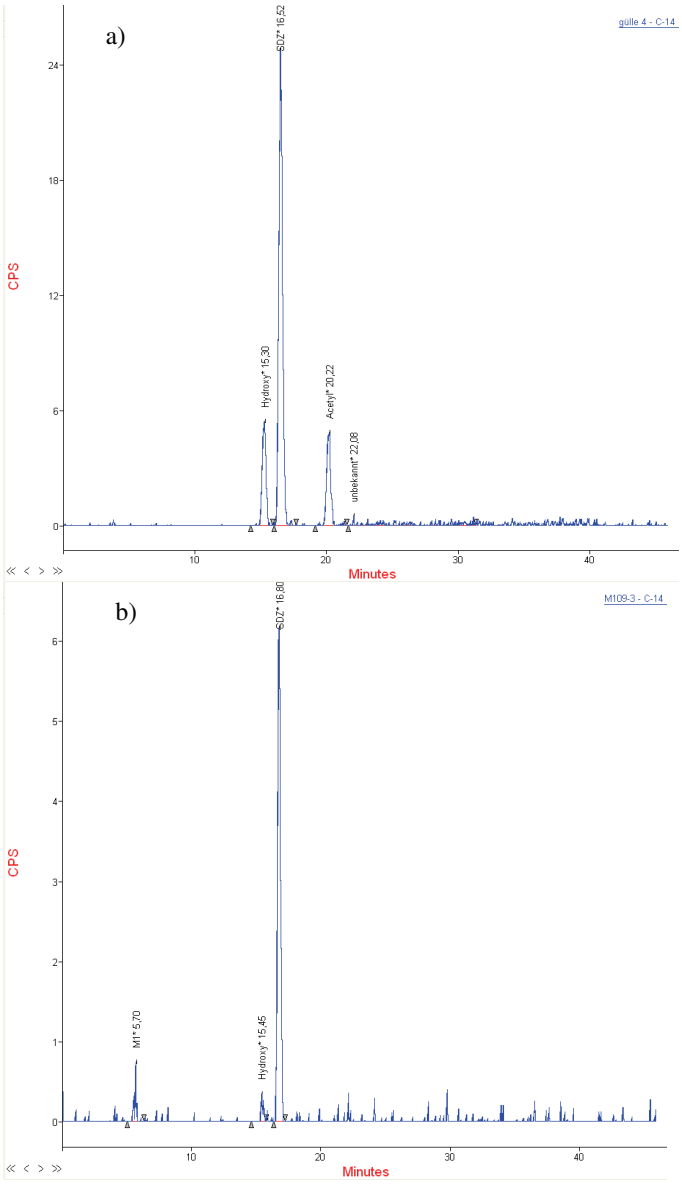

Figure D.1. Example Chromatograms measured in liquid samples with the application of a) manure (chapter 4: KundMAN) and b) a SDZ solution (chapter 2, soil K).

7.5 Appendix E: Chemicals and Instruments

E.1: Chemicals

Acetonitrile	Merck KGaA, Darmstadt, Germany
$CaCl_2$	Merck KGaA, Darmstadt, Germany
liquid scintillation cocktail	Instant Scint-Gel Plus, Canberra Packard GmbH, Dreieich, Germany
Citronensäure-Monhydrat p.A	KFM, Laborchemie Handels GmbH, Lohmar
di-Natriumhydrogencarbonat – Dodecahydrat p.A.	Merck KGaA, Darmstadt, Germany
HCl	Merck KGaA, Darmstadt, Germany
liquid scintillation cocktail	Oxysolve C – 400, Zinnser Analytics, Germany
Methanol (HPLC)	Economy Grade, LGC-Promochem, Wesel, Germany
NaOH	Merck KGaA, Darmstadt, Germany
Phosphoric acid (25%)	Grussing Diagnostika, Filsum, Germany
^{12}C-SDZ	Sigma Aldrich, Taufkirchen, Germany
^{14}C-SDZ	Bayer HealthCare, Wuppertal, Germany

E.2 Instruments

analytical balance	BP211D, Sartorius, Göttingen, Germany
balance	XP5003S/DR, Mettler Toledo GmbH, Gießen, Germany
biological oxidizer	Robox 192, Zinnsser Analytik GmbH, Frankfurt, Germany
centrifuge	Allegra 6KR, Beckmann Coulter, Palo Alto, US
pH-meter	MP 230, Mettler Toledo, Giessen, Germany
planetary ball mill	PM 400, Retsch, Haan, Germany
Liquid Scintillation Counter	2500 TR, Packard Bioscience GmbH, Dreieich, Germany

Appendix E

E.3 Experimental setup

needles (irrigation head)	Sterican Insulin G30X ½, B.Braun Melsungen AG, Melsungen, Germany
glass filter	Vitrapor Glasfilter (Por. 4, B = 80 mm) ROBU Glasfiltergeräte GmbH, Hattert, Germany
conductivity meter	Cond 340i, WTW GmbH, Weilheim, Germany
fraction collector	Fraktionssammler Modell III, Firma Köhler technische Produkte, Neulußheim, Germany
peristaltic pump (suction)	520 DU, Watson-Marlow GmbH, Rommerskirchen, Germany
peristaltic pumps (irrigation)	REGLO Digital MS-2/12, ISMATEC Laboratoriumstechnik GmbH, Wertheim-Mondfeld, Germany
tubes	SC0303 ID mm 0.25, SC0307 ID mm 0.76, Ismaprene, ISMATEC Laboratoriumstechnik GmbH, Wertheim-Mondfeld, Germany
pressure sensors	CTEM7N0706P0, Sensortechnics GmbH, Puchheim, Germany
tensiometers	T5, UMS GmbH, München, Germany
tubes	TU0425 BU, TU0805 BU, TU0805 B, SMC Pneumatik GmbH, Egelsbach, Germany

E.4 HPLC

HPLC – Column	Phenomenex Synergi Fusion RP 80, 4µ grain size, 250 mm x 4.6 mm, Phenomenex Ltd. Aschaffenburg, Germany
pump	PU 1580, Jasco, Gross. Umstadt, Germany
autosampler	Gina 50, Gynkotek, Germering, Germany
column oven	ST585, Gynkotek, Germering, Germany
radio detector	LB508-C, YG-150U4D, Berthold, Bad Wildbad, Germany

1. **Einsatz von multispektralen Satellitenbilddaten in der Wasserhaushalts- und Stoffstrommodellierung – dargestellt am Beispiel des Rureinzugsgebietes**
   von C. Montzka (2008), XX, 238 Seiten
   ISBN: 978-3-89336-508-1

2. **Ozone Production in the Atmosphere Simulation Chamber SAPHIR**
   by C. A. Richter (2008), XIV, 147 pages
   ISBN: 978-3-89336-513-5

3. **Entwicklung neuer Schutz- und Kontaktierungsschichten für Hochtemperatur-Brennstoffzellen**
   von T. Kiefer (2008), 138 Seiten
   ISBN: 978-3-89336-514-2

4. **Optimierung der Reflektivität keramischer Wärmedämmschichten aus Yttrium-teilstabilisiertem Zirkoniumdioxid für den Einsatz auf metallischen Komponenten in Gasturbinen**
   von A. Stuke (2008), X, 201 Seiten
   ISBN: 978-3-89336-515-9

5. **Lichtstreuende Oberflächen, Schichten und Schichtsysteme zur Verbesserung der Lichteinkopplung in Silizium-Dünnschichtsolarzellen**
   von M. Berginski (2008), XV, 171 Seiten
   ISBN: 978-3-89336-516-6

6. **Politikszenarien für den Klimaschutz IV – Szenarien bis 2030**
   hrsg.von P. Markewitz, F. Chr. Matthes (2008), 376 Seiten
   ISBN 978-3-89336-518-0

7. **Untersuchungen zum Verschmutzungsverhalten rheinischer Braunkohlen in Kohledampferzeugern**
   von A. Schlüter (2008), 164 Seiten
   ISBN 978-3-89336-524-1

8. **Inorganic Microporous Membranes for Gas Separation in Fossil Fuel Power Plants**
   by G. van der Donk (2008), VI, 120 pages
   ISBN: 978-3-89336-525-8

9. **Sinterung von Zirkoniumdioxid-Elektrolyten im Mehrlagenverbund der oxidkeramischen Brennstoffzelle (SOFC)**
   von R. Mücke (2008), VI, 165 Seiten
   ISBN: 978-3-89336-529-6

10. **Safety Considerations on Liquid Hydrogen**
    by K. Verfondern (2008), VIII, 167 pages
    ISBN: 978-3-89336-530-2

11. **Kerosinreformierung für Luftfahrtanwendungen**
von R. C. Samsun (2008), VII, 218 Seiten
ISBN: 978-3-89336-531-9

12. **Der 4. Deutsche Wasserstoff Congress 2008 – Tagungsband**
hrsg. von D. Stolten, B. Emonts, Th. Grube (2008), 269 Seiten
ISBN: 978-3-89336-533-3

13. **Organic matter in Late Devonian sediments as an indicator for environmental changes**
by M. Kloppisch (2008), XII, 188 pages
ISBN: 978-3-89336-534-0

14. **Entschwefelung von Mitteldestillaten für die Anwendung in mobilen Brennstoffzellen-Systemen**
von J. Latz (2008), XII, 215 Seiten
ISBN: 978-3-89336-535-7

15. **RED-IMPACT**
Impact of Partitioning, Transmutation and Waste Reduction Technologies on the Final Nuclear Waste Disposal
SYNTHESIS REPORT
ed. by W. von Lensa, R. Nabbi, M. Rossbach (2008), 178 pages
ISBN 978-3-89336-538-8

16. **Ferritic Steel Interconnectors and their Interactions with Ni Base Anodes in Solid Oxide Fuel Cells (SOFC)**
by J. H. Froitzheim (2008), 169 pages
ISBN: 978-3-89336-540-1

17. **Integrated Modelling of Nutrients in Selected River Basins of Turkey**
Results of a bilateral German-Turkish Research Project
project coord. M. Karpuzcu, F. Wendland (2008), XVI, 183 pages
ISBN: 978-3-89336-541-8

18. **Isotopengeochemische Studien zur klimatischen Ausprägung der Jüngeren Dryas in terrestrischen Archiven Eurasiens**
von J. Parplies (2008), XI, 155 Seiten, Anh.
ISBN: 978-3-89336-542-5

19. **Untersuchungen zur Klimavariabilität auf dem Tibetischen Plateau - Ein Beitrag auf der Basis stabiler Kohlenstoff- und Sauerstoffisotope in Jahrringen von Bäumen waldgrenznaher Standorte**
von J. Griessinger (2008), XIII, 172 Seiten
ISBN: 978-3-89336-544-9

20. **Neutron-Irradiation + Helium Hardening & Embrittlement Modeling of 9%Cr-Steels in an Engineering Perspective (HELENA)**
by R. Chaouadi (2008), VIII, 139 pages
ISBN: 978-3-89336-545-6

21. **in Bearbeitung**

22. **Verbundvorhaben APAWAGS (AOEV und Wassergenerierung) – Teilprojekt: Brennstoffreformierung – Schlussbericht**
von R. Peters, R. C. Samsun, J. Pasel, Z. Porš, D. Stolten (2008), VI, 106 Seiten
ISBN: 978-3-89336-547-0

23. **FREEVAL**
Evaluation of a Fire Radiative Power Product derived from Meteosat 8/9 and Identification of Operational User Needs
Final Report
project coord. M. Schultz, M. Wooster (2008), 139 pages
ISBN: 978-3-89336-549-4

24. **Untersuchungen zum Alkaliverhalten unter Oxycoal-Bedingungen**
von C. Weber (2008), VII, 143, XII Seiten
ISBN: 978-3-89336-551-7

25. **Grundlegende Untersuchungen zur Freisetzung von Spurstoffen, Heißgaschemie, Korrosionsbeständigkeit keramischer Werkstoffe und Alkalirückhaltung in der Druckkohlenstaubfeuerung**
von M. Müller (2008), 207 Seiten
ISBN: 978-3-89336-552-4

26. **Analytik von ozoninduzierten phenolischen Sekundärmetaboliten in *Nicotiana tabacum* L. cv Bel W3 mittels LC-MS**
von I. Koch (2008), III, V, 153 Seiten
ISBN 978-3-89336-553-1

27. **IEF-3 Report 2009. Grundlagenforschung für die Anwendung**
(2009), ca. 230 Seiten
ISBN: 978-3-89336-554-8

28. **Influence of Composition and Processing in the Oxidation Behavior of MCrAlY-Coatings for TBC Applications**
by J. Toscano (2009), 168 pages
ISBN: 978-3-89336-556-2

29. **Modellgestützte Analyse signifikanter Phosphorbelastungen in hessischen Oberflächengewässern aus diffusen und punktuellen Quellen**
von B. Tetzlaff (2009), 149 Seiten
ISBN: 978-3-89336-557-9

30. **Nickelreaktivlot / Oxidkeramik – Fügungen als elektrisch isolierende Dichtungskonzepte für Hochtemperatur-Brennstoffzellen-Stacks**
von S. Zügner (2009), 136 Seiten
ISBN: 978-3-89336-558-6

31. **Langzeitbeobachtung der Dosisbelastung der Bevölkerung in radioaktiv kontaminierten Gebieten Weißrusslands – Korma-Studie**
von H. Dederichs, J. Pillath, B. Heuel-Fabianek, P. Hill, R. Lennartz (2009), Getr. Pag.
ISBN: 978-3-89336-532-3

32. **Herstellung von Hochtemperatur-Brennstoffzellen über physikalische Gasphasenabscheidung**
von N. Jordán Escalona (2009), 148 Seiten
ISBN: 978-3-89336-532-3

33. **Real-time Digital Control of Plasma Position and Shape on the TEXTOR Tokamak**
by M. Mitri (2009), IV, 128 pages
ISBN: 978-3-89336-567-8

34. **Freisetzung und Einbindung von Alkalimetallverbindungen in kohlebefeuerten Kombikraftwerken**
von M. Müller (2009), 155 Seiten
ISBN: 978-3-89336-568-5

35. **Kosten von Brennstoffzellensystemen auf Massenbasis in Abhängigkeit von der Absatzmenge**
von J. Werhahn (2009), 242 Seiten
ISBN: 978-3-89336-569-2

36. **Einfluss von Reoxidationszyklen auf die Betriebsfestigkeit von anodengestützten Festoxid-Brennstoffzellen**
von M. Ettler (2009), 138 Seiten
ISBN: 978-3-89336-570-8

37. **Großflächige Plasmaabscheidung von mikrokristallinem Silizium für mikromorphe Dünnschichtsolarmodule**
von T. Kilper (2009), XVII, 154 Seiten
ISBN: 978-3-89336-572-2

38. **Generalized detailed balance theory of solar cells**
by T. Kirchartz (2009), IV, 198 pages
ISBN: 978-3-89336-573-9

39. **The Influence of the Dynamic Ergodic Divertor on the Radial Electric Field at the Tokamak TEXTOR**
von J. W. Coenen (2009), xii, 122, XXVI pages
ISBN: 978-3-89336-574-6

40. **Sicherheitstechnik im Wandel Nuklearer Systeme**
von K. Nünighoff (2009), viii, 215 Seiten
ISBN: 978-3-89336-578-4

41. **Pulvermetallurgie hochporöser NiTi-Legierungen für Implanat- und Dämpfungsanwendungen**
von M. Köhl (2009), XVII, 199 Seiten
ISBN: 978-3-89336-580-7

42. **Einfluss der Bondcoatzusammensetzung und Herstellungsparameter auf die Lebensdauer von Wärmedämmschichten bei zyklischer Temperaturbelastung**
von M. Subanovic (2009), 188, VI Seiten
ISBN: 978-3-89336-582-1

43. **Oxygen Permeation and Thermo-Chemical Stability of Oxygen Permeation Membrane Materials for the Oxyfuel Process**
by A. J. Ellett (2009), 176 pages
ISBN: 978-3-89336-581-4

44. **Korrosion von polykristallinem Aluminiumoxid (PCA) durch Metalljodidschmelzen sowie deren Benetzungseigenschaften**
von S. C. Fischer (2009), 148 Seiten
ISBN: 978-3-89336-584-5

45. **IEF-3 Report 2009. Basic Research for Applications**
(2009), 217 Seiten
ISBN: 978-3-89336-585-2

46. **Verbundvorhaben ELBASYS (Elektrische Basissysteme in einem CFK-Rumpf) - Teilprojekt: Brennstoffzellenabgase zur Tankinertisierung - Schlussbericht**
von R. Peters, J. Latz, J. Pasel, R. C. Samsun, D. Stolten
(2009), xi, 202 Seiten
ISBN: 978-3-89336-587-6

47. **Aging of ^{14}C-labeled Atrazine Residues in Soil: Location, Characterization and Biological Accessibility**
by N. D. Jablonowski (2009), IX, 104 pages
ISBN: 978-3-89336-588-3

48. **Entwicklung eines energetischen Sanierungsmodells für den europäischen Wohngebäudesektor unter dem Aspekt der Erstellung von Szenarien für Energie- und CO_2 - Einsparpotenziale bis 2030**
von P. Hansen (2009), XXII, 281 Seiten
ISBN: 978-3-89336-590-6

49. **Reduktion der Chromfreisetzung aus metallischen Interkonnektoren für Hochtemperaturbrennstofzellen durch Schutzschichtsysteme**
von R. Trebbels (2009), iii, 135 Seiten
ISBN: 978-3-89336-591-3

50. **Bruchmechanische Untersuchung von Metall / Keramik-Verbundsystemen für die Anwendung in der Hochtemperaturbrennstoffzelle**
von B. Kuhn (2009), 118 Seiten
ISBN: 978-3-89336-592-0

51. **Wasserstoff-Emissionen und ihre Auswirkungen auf den arktischen Ozonverlust**
Risikoanalyse einer globalen Wasserstoffwirtschaft
von T. Feck (2009), 180 Seiten
ISBN: 978-3-89336-593-7

52. **Development of a new Online Method for Compound Specific Measurements of Organic Aerosols**
by T. Hohaus (2009), 156 pages
ISBN: 978-3-89336-596-8

53. **Entwicklung einer FPGA basierten Ansteuerungselektronik für Justageeinheiten im Michelson Interferometer**
von H. Nöldgen (2009), 121 Seiten
ISBN: 978-3-89336-599-9

54. **Observation – and model – based study of the extratropical UT/LS**
by A. Kunz (2010), xii, 120, xii pages
ISBN: 978-3-89336-603-3

55. **Herstellung polykristalliner Szintillatoren für die Positronen-Emissions-Tomographie (PET)**
von S. K. Karim (2010), VIII, 154 Seiten
ISBN: 978-3-89336-610-1

56. **Kombination eines Gebäudekondensators mit H2-Rekombinatorelementen in Leichwasserreaktoren**
von S. Kelm (2010), vii, 119 Seiten
ISBN: 978-3-89336-611-8

57. **Plant Leaf Motion Estimation Using A 5D Affine Optical Flow Model**
by T. Schuchert (2010), X, 143 pages
ISBN: 978-3-89336-613-2

58. **Tracer-tracer relations as a tool for research on polar ozone loss**
by R. Müller (2010), 116 pages
ISBN: 978-3-89336-614-9

59. **Sorption of polycyclic aromatic hydrocarbon (PAH) to Yangtze River sediments and their components**
by J. Zhang (2010), X, 109 pages
ISBN: 978-3-89336-616-3

60. **Weltweite Innovationen bei der Entwicklung von CCS-Technologien und Möglichkeiten der Nutzung und des Recyclings von CO_2**
Studie im Auftrag des BMWi
von W. Kuckshinrichs et al. (2010), X, 139 Seiten
ISBN: 978-3-89336-617-0

61. **Herstellung und Charakterisierung von sauerstoffionenleitenden Dünnschichtmembranstrukturen**
von M. Betz (2010), XII, 112 Seiten
ISBN: 978-3-89336-618-7

62. **Politikszenarien für den Klimaschutz V – auf dem Weg zum Strukturwandel, Treibhausgas-Emissionsszenarien bis zum Jahr 2030**
hrsg. von P. Hansen, F. Chr. Matthes (2010), 276 Seiten
ISBN: 978-3-89336-619-4

63. **Charakterisierung Biogener Sekundärer Organischer Aerosole mit Statistischen Methoden**
von C. Spindler (2010), iv, 163 Seiten
ISBN: 978-3-89336-622-4

64. **Stabile Algorithmen für die Magnetotomographie an Brennstoffzellen**
von M. Wannert (2010), ix, 119 Seiten
ISBN: 978-3-89336-623-1

65. **Sauerstofftransport und Degradationsverhalten von Hochtemperatur-membranen für CO2-freie Kraftwerke**
von D. Schlehuber (2010), VII, 139 Seiten
ISBN: 978-3-89336-630-9

66. **Entwicklung und Herstellung von foliengegossenen, anodengestützten Festoxidbrennstoffzellen**
von W. Schafbauer (2010), VI, 164 Seiten
ISBN: 978-3-89336-631-6

67. **Disposal strategy of proton irradiated mercury from high power spallation sources**
by S. Chiriki (2010), xiv, 124 pages
ISBN: 978-3-89336-632-3

68. **Oxides with polyatomic anions considered as new electrolyte materials for solid oxide fuel cells (SOFCs)**
by O. H. Bin Hassan (2010), vii, 121 pages
ISBN: 978-3-89336-633-0

69. **Von der Komponente zum Stack: Entwicklung und Auslegung von HT-PEFC-Stacks der 5 kW-Klasse**
von A. Bendzulla (2010), IX, 203 Seiten
ISBN: 978-3-89336-634-7

70. **Satellitengestützte Schwerewellenmessungen in der Atmosphäre und Perspektiven einer zukünftigen ESA Mission (PREMIER)**
von S. Höfer (2010), 81 Seiten
ISBN: 978-3-89336-637-8

71. **Untersuchungen der Verhältnisse stabiler Kohlenstoffisotope in atmosphärisch relevanten VOC in Simulations- und Feldexperimenten**
von H. Spahn (2010), IV, 210 Seiten
ISBN: 978-3-89336-638-5

72. **Entwicklung und Charakterisierung eines metallischen Substrats für nanostrukturierte keramische Gastrennmembranen**
von K. Brands (2010), vii, 137 Seiten
ISBN: 978-3-89336-640-8

73. **Hybridisierung und Regelung eines mobilen Direktmethanol-Brennstoff-zellen-Systems**
von J. Chr. Wilhelm (2010), 220 Seiten
ISBN: 978-3-89336-642-2

74. **Charakterisierung perowskitischer Hochtemperaturmembranen zur Sauerstoffbereitstellung für fossil gefeuerte Kraftwerksprozesse**
von S.A. Möbius (2010) III, 208 Seiten
ISBN: 978-3-89336-643-9

75. **Characterization of natural porous media by NMR and MRI techniques: High and low magnetic field studies for estimation of hydraulic properties**
by L.-R. Stingaciu (2010), 96 pages
ISBN: 978-3-89336-645-3

76. **Hydrological Characterization of a Forest Soil Using Electrical Resistivity Tomography**
by Chr. Oberdörster (2010), XXI, 151 pages
ISBN: 978-3-89336-647-7

77. **Ableitung von atomarem Sauerstoff und Wasserstoff aus Satellitendaten und deren Abhängigkeit vom solaren Zyklus**
von C. Lehmann (2010), 127 Seiten
ISBN: 978-3-89336-649-1

78. **in Bearbeitung**

79. **Ultrafast voltex core dynamics investigated by finite-element micromagnetic simulations**
by S. Gliga (2010), vi, 144 pages
ISBN: 978-3-89336-660-6

80. **Herstellung und Charakterisierung von keramik- und metallgestützten Membranschichten für die CO_2-Abtrennung in fossilen Kraftwerken**
von F. Hauler (2010), XVIII, 178 Seiten
ISBN: 978-3-89336-662-0

81. **Experiments and numerical studies on transport of sulfadiazine in soil columns**
by M. Unold (2010), xvi, 115 pages
ISBN: 978-3-89336-663-7

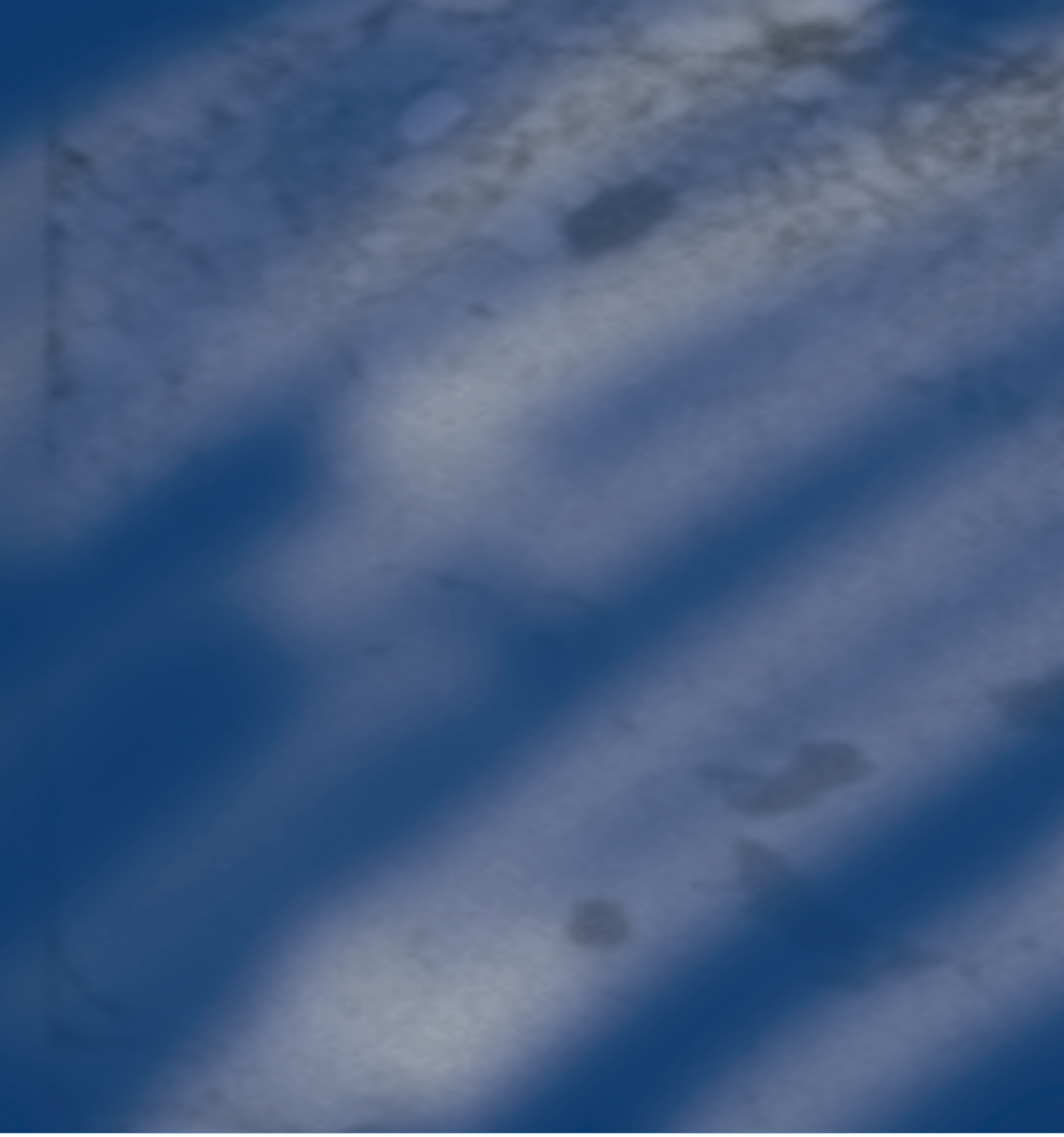

Energie & Umwelt / Energy & Environment
Band / Volume 81
ISBN 978-3-89336-663-7

JÜLICH
FORSCHUNGSZENTRUM